DRIVE
Drought Resilience Improvement in Vineyard Ecosystems

LIFE19 ENV/IT/000035

Report on chemical-physical features and hydraulic properties of selected vineyard soils

Sub-action B2.1 Starting point and road map to selection of most suited resilience practices

Author(s): A. Bosino, M. Bordoni, M. Maerker, P. Torrese, F. Zucca, C. Meisina

31.10.2021

Table of contents

Glossary

DEM: Digital Elevation Model
Sand: percentage of sand
Silt: percentage of silt
Clay: percentage of clay
γ: unit weight
γ_d: dry density
ρ: porosity
e: void index
θ: volumetric water content
S_r: saturation degree
ASTM: American Society for Testing and Materials
USDA: United States Department of Agriculture
WRC: Water Retention Curve
θ_s: saturated water content
θ_r: residual water content
α and n: fitting parameters of WRC equation
Ksat: hydraulic conductivity
R^2: Determination coefficient
MAE: Mean Absolute Error
SiC: Silty Clay
SiCL: Silty Clay Loam
SaC: Sandy Clay
SaCL: Sandy Clay Loam
SiL: Silty Loam
CL: Clay Loam
C: Clay

Summary

List of the figures:

List of the tables:

Introduction

The main objectives of Action B2 “Demonstration in vineyards” are:
- To test the monitoring tool (MT) in demo-vineyards and achieve increased storage and improved use of natural water resources in vineyard with limited or no availability of supplemental water for irrigation. These objectives will be pursued, in each demo vineyard, through comparisons between local practice and a “water resilient management” where more techniques are demonstrated.
- To asses benefits rising from the use of the MT and, through farmers' feedbacks, provide information for improved fine tuning.

In particular, this document aims to describe the Sub-action B2.1 “Starting point and road map to selection of most suited resilience practices” for the six pilot sites.

The deliverable is structured in the following sections:

- Geological and geomorphological settings of the demo farms
- Soil profiles and pedological analysis
- Soil physical features
- Soil hydrological features
- Soil chemical characterization
- Field measurements of hydraulic conductivity
- Installation and verification of the good functioning of integrated weather and hydrological monitoring stations

Geological and geomorphological characterization were done by M. Bordoni and C. Meisina. Geophysical characterization through ERT surveys were performed and analysed by P. Torrese. Geophysical characterization through EMP surveys were performed and analysed by F. Zucca and A. Bosino. Soil profiles were reconstructed and analysed by A. Bosino and M. Maerker. Pedological and chemical analyses were done at CAAR - Laboratori Regionali Analisi Terreni-Produzioni Vegetali e Fitopatologico (Sarzana, Italy) and were analyzed by A. Bosino and M. Maerker. Physical and hydrological analyses were done at Laboratory of Engineering Geology of the Department of Earth and Environmental Sciences of University of Pavia and were analysed by M. Bordoni and C. Meisina. Field measures of hydraulic conductivity were performed by A. Bosino and M. Bordoni. The installation and verification of the good functioning of integrated weather and hydrological monitoring stations were done by A. Bosino, M. Bordoni, M. Maerker and C. Meisina.
Dr. Giacomo Panza, Phd student at Department of Earth and Environmental Sceinces of University of Pavia, working on similar topics regarding the assessment of the effects of vineyards management on shallow landsliding, contributed to the laboratory tests of the soil physical characterization, the field measures of saturated hydraulic conductivity and the installation of the monitoring stations.

Geological and geomorphological settings of the demo farms

Six demo farms (Fig. 1) were selected as test-sites, in order to represent the different geological, geomorphological and land use features of the territory.
For each test-site, relevant preliminary data were collected to characterize the main geological, geomorphological and hydrological features. In particular, the following data have been acquired:

- Digital Elevation Models (DEMs) at 1 m resolution derived from LIDAR surveys acquired by the Italian Ministry for Environment, Land and Sea in the period 2008-2010 for the preliminary geomorphological characterization;
- Geological maps of the bedrock at 1:50.000 scale (Regione Emilia Romagna, 1996; Meisina et al., 2006; Servizio Geologico d'Italia, 2005, 2014);
- Pedological maps at 1:50.000 scale (Regione Emilia Romagna, 1994; ERSAL, 2001);
- Landslide inventory (Inventario Fenomeni Franosi in Italia – IFFI) at 1:10.000 scale (Ispra, 2018).

Furthermore, geophysical surveys were carried out to characterize the underground of the single demo farms.

Electrical Resistivity Tomography (ERT) profiles were acquired at each test site, for a total of six ERT profiles.
Each profile is 94 m long and was obtained using 48 electrodes spaced at 2 m distance. Each profile was collected using a 306 Wenner-Schlumberger array quadrupoles which ensure high vertical resolution and signal amplitude and 328 dipole-dipole array quadrupoles which provide enhanced lateral resolution. A fully automatic multi-electrode resistivitymeter SYSCAL Jr. Switch-48 by IRIS Instruments was used for data collection.
Data inversion was performed using ERTLab Solver (Release 1.3.1, by GeostudiAstier s.r.l. - Multi-Phase Technologies LLC, http://www.geostudiastier.it/area_en.asp?tag=3d-software-for-electrical-tomography&idCanale=56&sezione=1) based on tetrahedral Finite Element Modelling (FEM).
Tetrahedral discretization was used in both forward and inverse modelling. The foreground region was discretized using a 1 m cell size, i.e., half of the electrode spacing, to give the model higher accuracy. The background region was discretized using an increasing element size towards the outside of the domain, according to the sequence: 1×, 1×, 2×, 4× and 8× the foreground element size.
The forward modelling was performed using mixed boundary conditions (Dirichlet-Neumann) and a tolerance (stop criterion) of 1.0E-7 for a Symmetric Successive Over-Relaxation Conjugate Gradient (SSORCG) iterative solver. Data inversion was based on a least-squares smoothness constrained approach. Noise was appropriately managed using a data-weighting algorithm that allows the variance matrix after each data point iteration that was poorly fitted by the model to be adaptively changed. The inverse modelling was performed using a maximum number of internal inverse Preconditioned Conjugate Gradient (PCG) iterations of 5 and a tolerance (stop criterion) for inverse PCG iterations of 0.001. The amount of roughness from one iteration to the next was controlled to assess maximum layering: a low value of reweight constant (0.1) was set with the objective of generating maximum heterogeneity.
The inverse resistivity models were obtained by merging and jointly inverting datasets from different arrays which can deliver better detectability and imaging and, hence, provide more accurate inverse models and more reliable ERT imaging. Inversion involved the application of homogeneous starting models that set at each node the average measured apparent resistivity value. The final inverse resistivity models were chosen based on the minimum data residual (or misfit error).
ERT models revealed the electrical resistivity pattern of the shallow subsoil. Different resistivity ranges are found:

-a high resistivity shallow layer, which is rather homogenous at Sartori-Creta, Canevino and Borgo Priolo and rather heterogeneous at Vicobarone, Genepreto and Santa Maria della Versa;

-a low resistivity deeper layer.

Evidence of slope instabilities is found at Vicobarone, Canevino, Genepreto, Borgo Priolo and Santa Maria della Versa.

Evidence of pipes and drain pipes is found at Vicobarone and Santa Maria della Versa, respectively.

Evidence of possibly small paleochannels and/or landslide accumulation deposits is found at Genepreto.

Moreover, through a portable GSSI' electromagnetic (EM) induction tool the Electrical Conductivity of the first soil horizons was detected and subsequently correlated to the moisture condition. The test allows to identify the Electric Conductivity of the topsoil (0-20 cm), the subsoil (50-60 cm) and finally the deep soil horizon at (100cm). The collected data were spatialized using SAGAGIS and an inverse distance weighting approach.

Finally, both ERT and EMP models are currently being calibrated and interpreted.

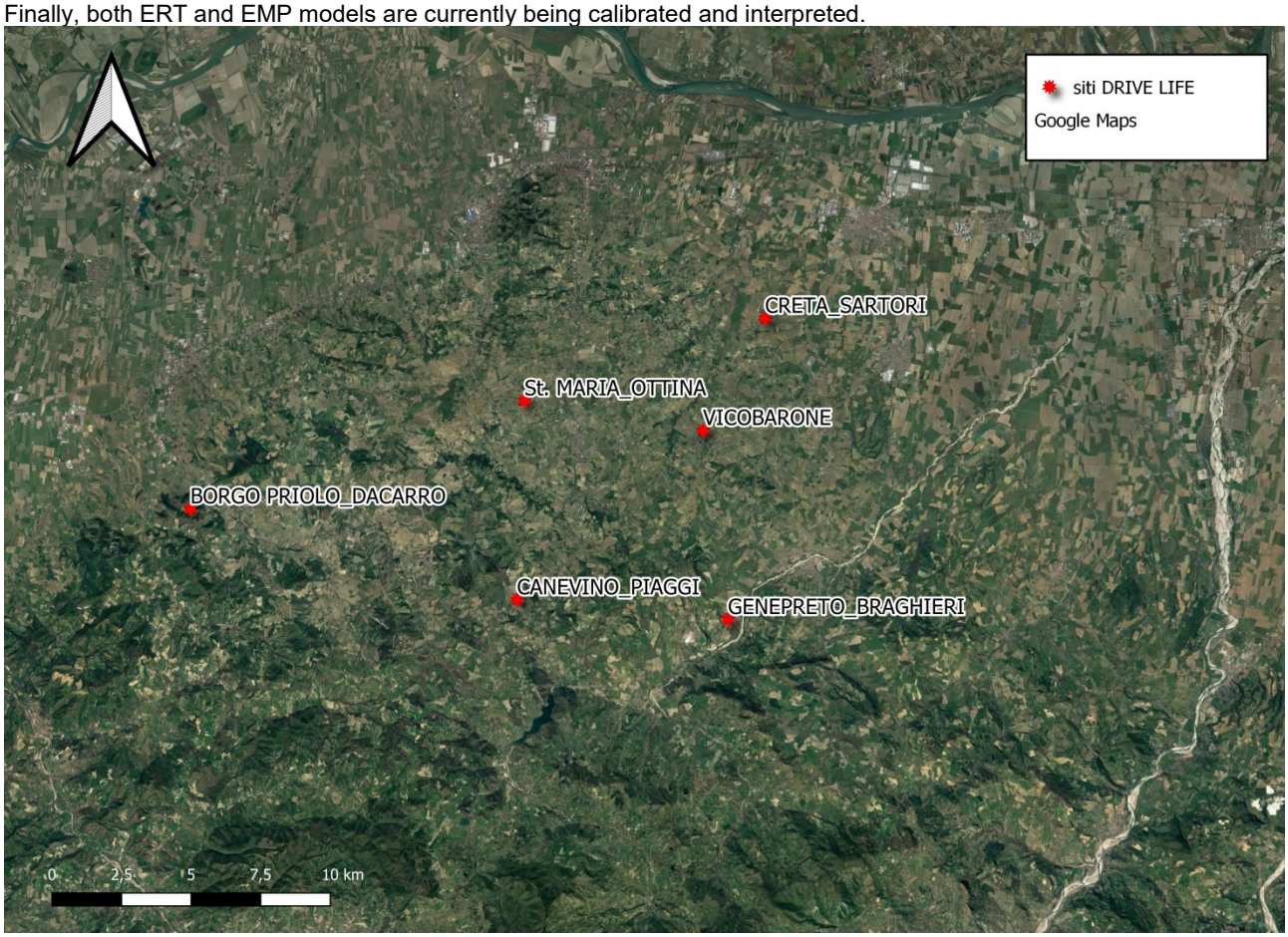

Fig. 1 Map of the demo farms location.

Table 1 Main settings of the demo farms.

Demo farm	Slope angle (°)	Bedrock geology	Soil types (pedological maps at 1:50000 scale)	Soil thickness	Presence of slope instabilities
St. Maria_Ottina-SMV	5-15°	Val Luretta Formation	Calcaric Cambisols	Thin-Medium	No
Vicobarone-VCB	5-15°	Val Luretta Formation	Vertic Cambisols	Very thick	No
Genepreto_Braghieri-GNP	0-20°	Val Luretta Formation	Vertic Cambisols Endoleptic Regosols	Medium-Very thick	Landslide
Creta_Sartori-CRT	0-10°	Agazzano Subsyntem (Alluvial soils)	Silty loams	Very thick	No

Canevino_Piaggi-CNV	10-20°	Varicoloured Clays	Calcaric Cambisols	Thin-Medium	Landslide
Borgopriolo_Dacarro-BPR	5-15°	S. Agata Fossili Marls	-	-	No

Table 2. List of the implemented management practices in demo farms.

Demo farm	Management
SMV	Control
	Green manure High
	Green manure medium
	Green manure low
VCB	Nitrofert
	Control
	Humusfert
	Stratus
GNP	Control
	Nitrofert
	Stratus
CRT	Control
	Rolling
	Swath
CNV	Humusfert
	Control
BPR	Stratus
	Control
	Nitrofert

Santa Maria della Versa (SMV)

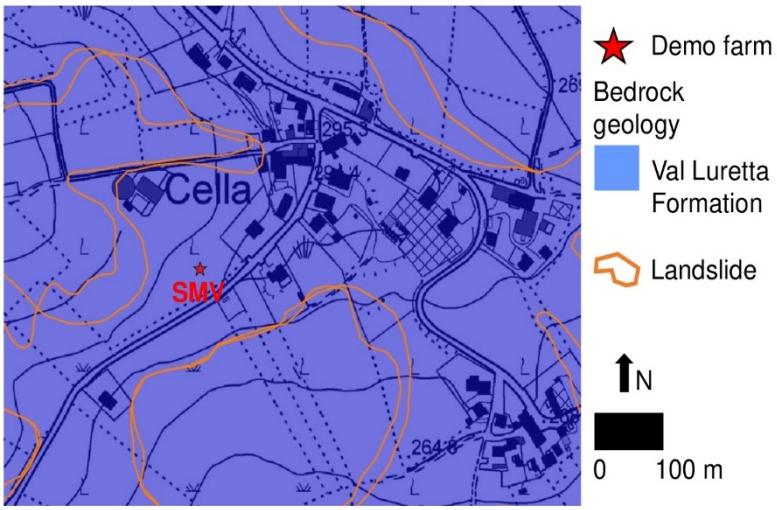

Fig. 2 Main geomorphological attributes and bedrock geology of SMV area.

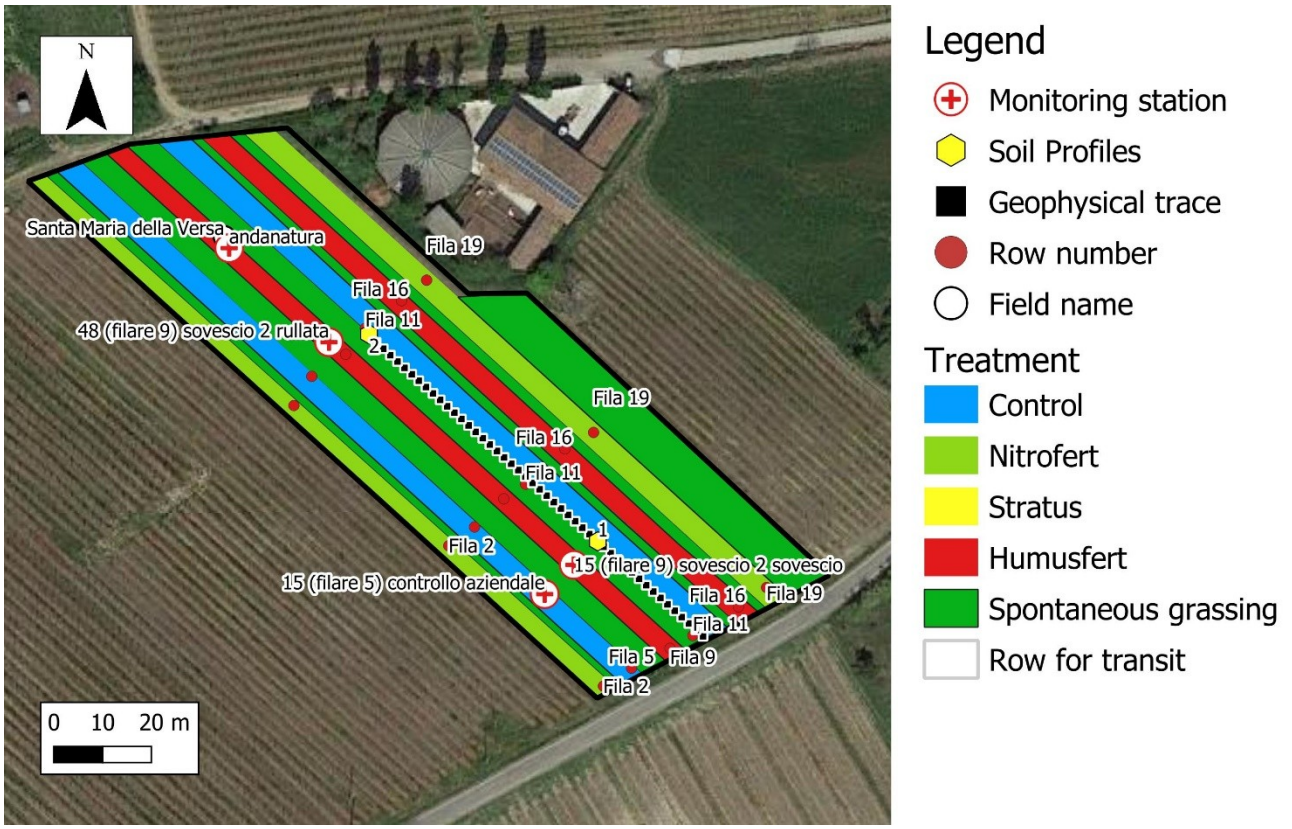

Fig. 3 Map with the different soil management practices, the location of geophysical surveys and pits in SMV area.

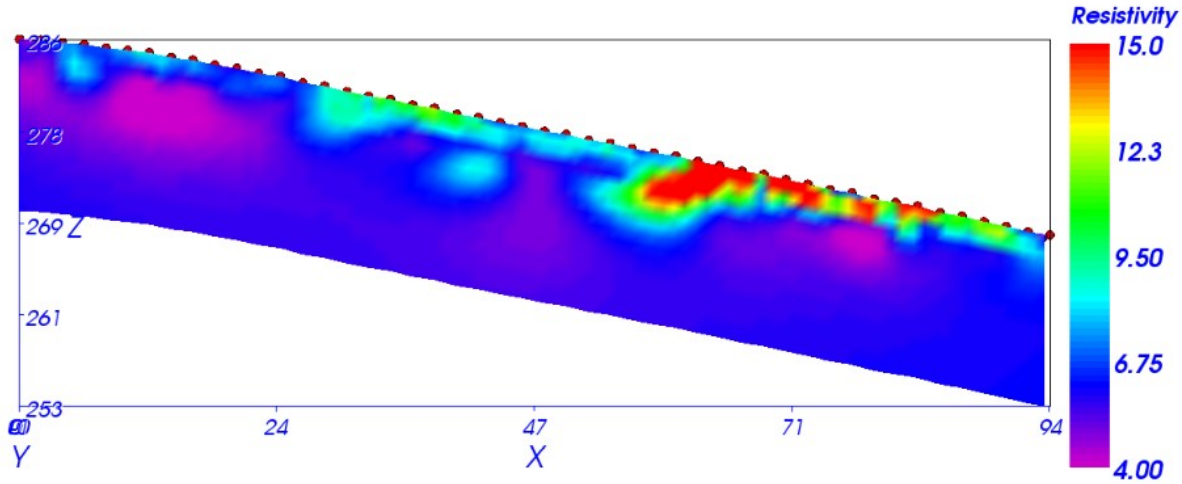

Fig. 4 Geophysical (ERT) surveys of SMV.

Canevino (CNV)

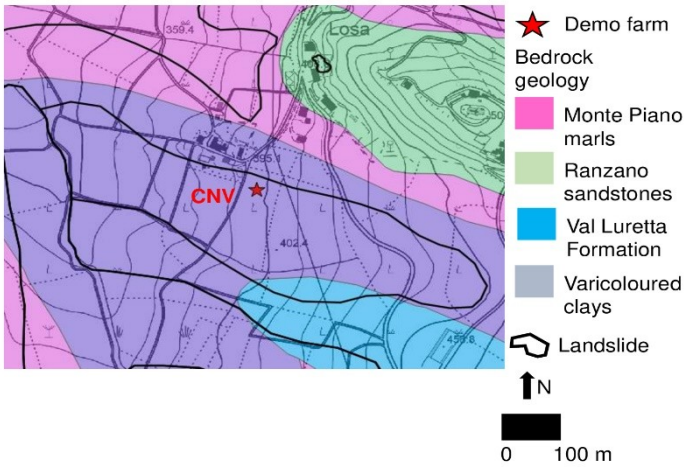

Fig. 5 Main geomorphological attributes and bedrock geology of CNV area.

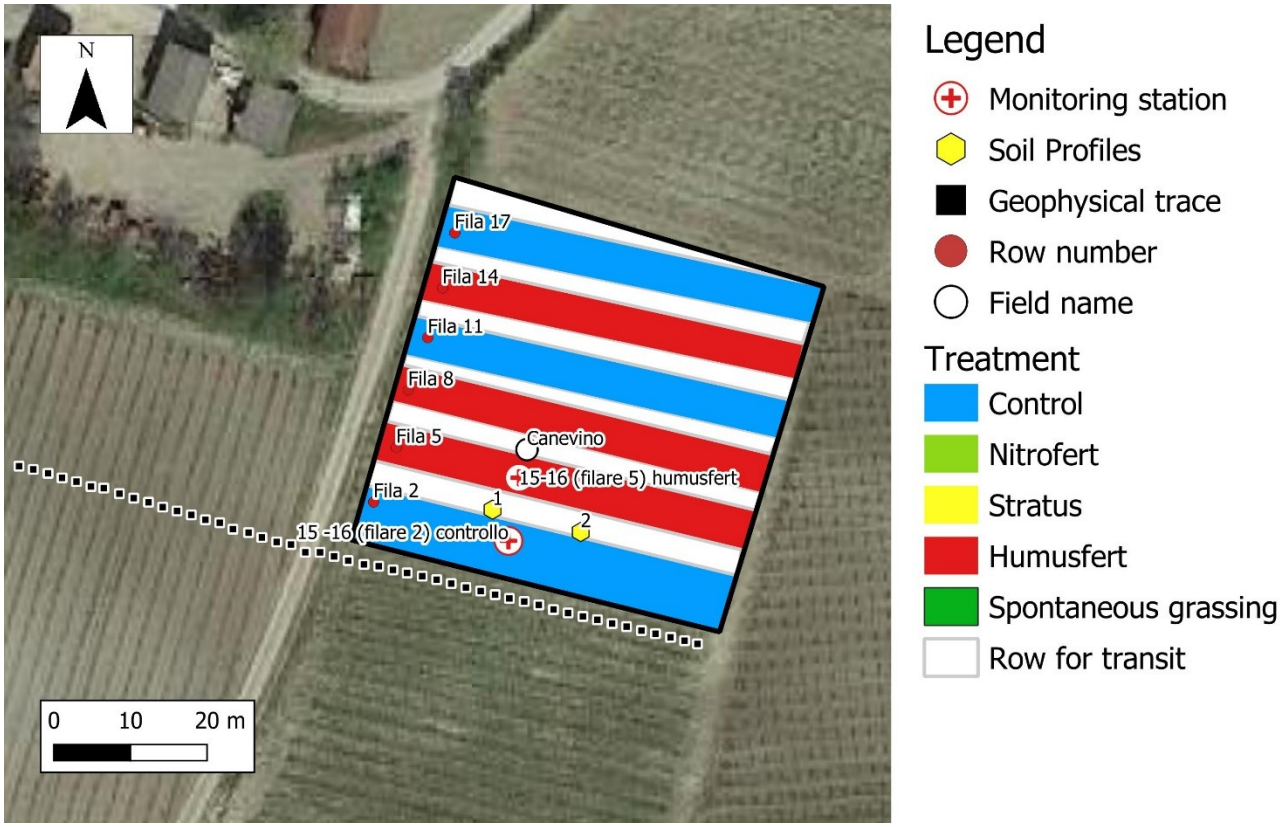

Fig. 6 Map with the different soil management practices, the location of geophysical surveys and pits of CNV area.

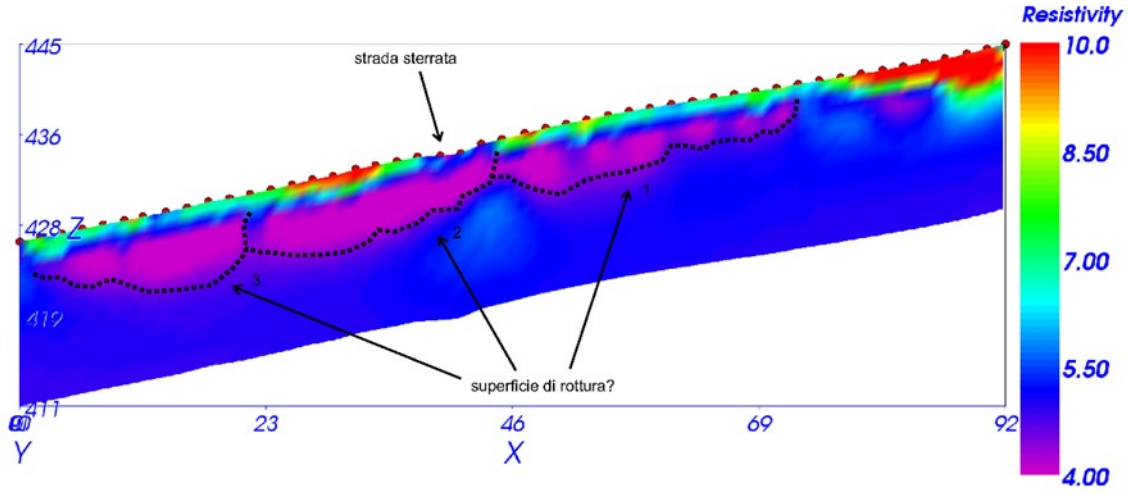

Fig. 7. Geophysical (ERT) surveys of CNV.

Borgo Priolo (BPR)

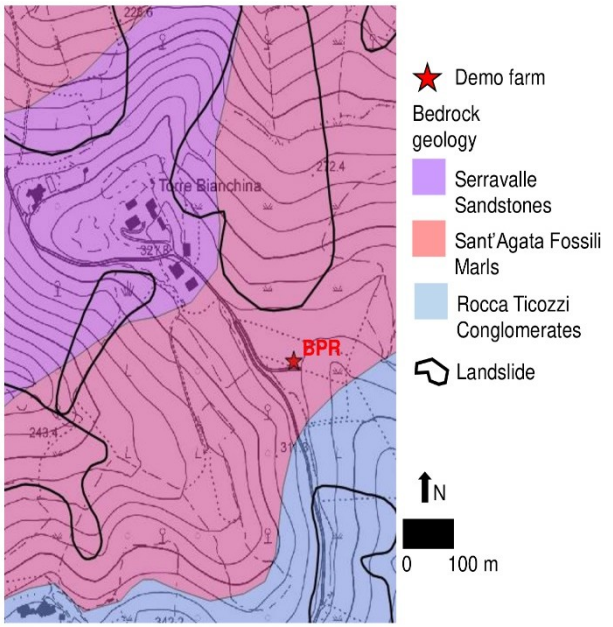

Fig. 8 Main geomorphological attributes and bedrock geology of BPR area.

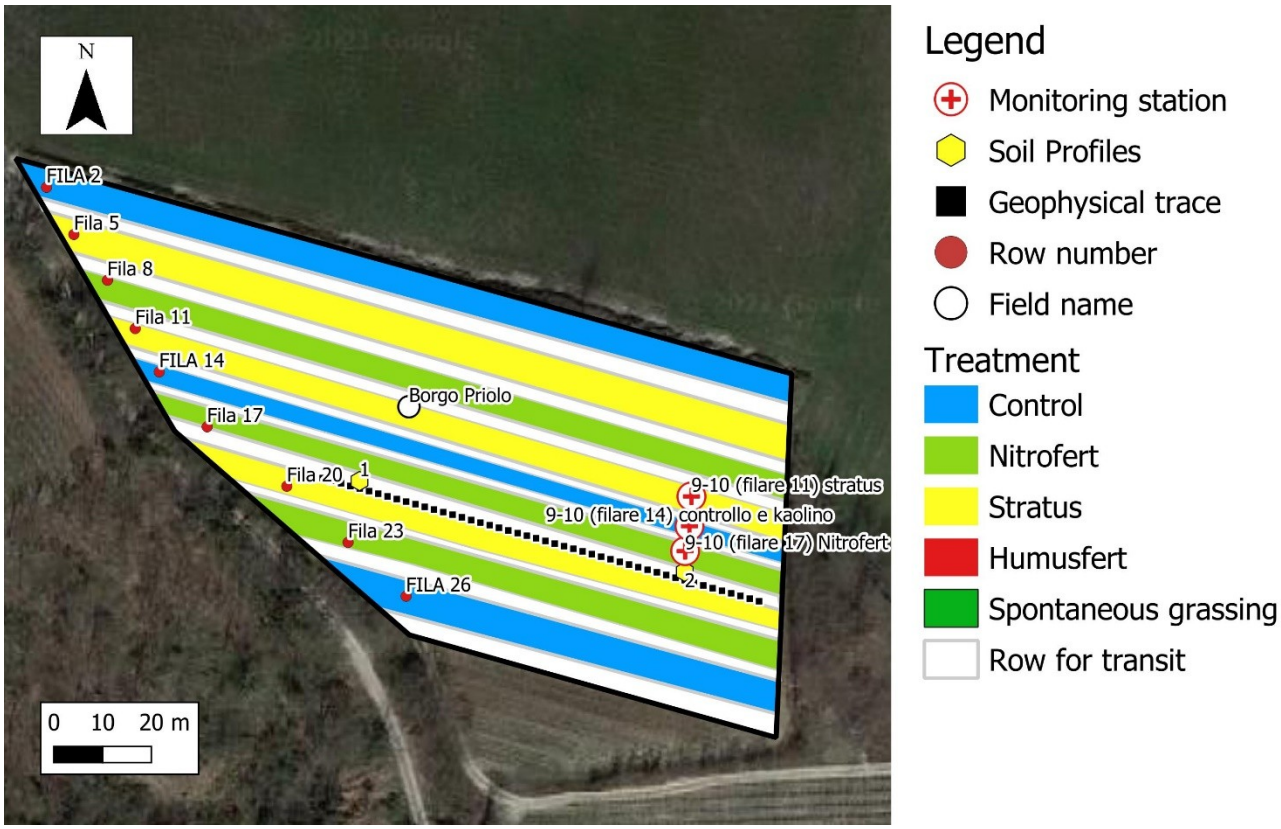

Fig. 9 Map with the different soil management practices, the location of geophysical surveys and pits of BPR area.

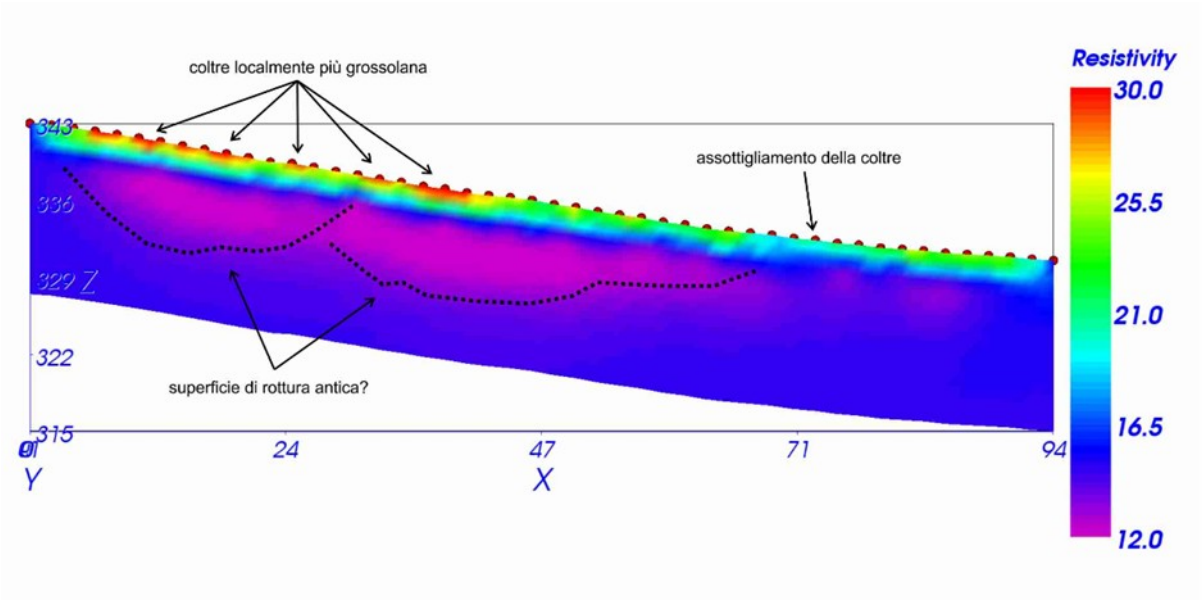

Fig. 10 Geophysical (ERT) surveys of BPR.

Creta (CRT)

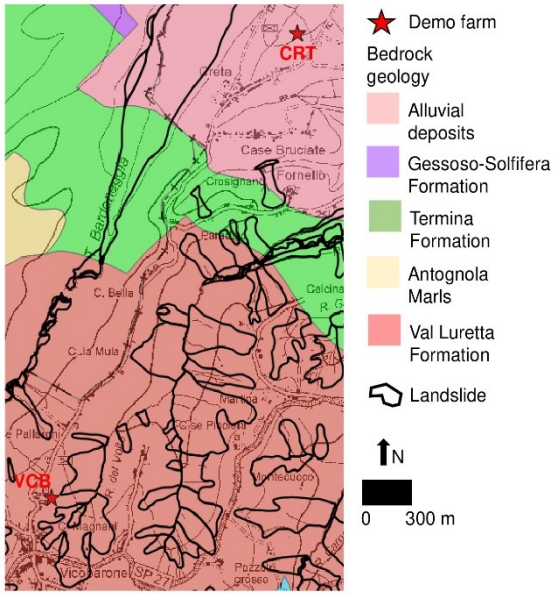

Fig. 11 Main geomorphological attributes and bedrock geology of CRT area.

Fig. 12 Map with the different soil management practices, the location of geophysical surveys and pits of CRT area.

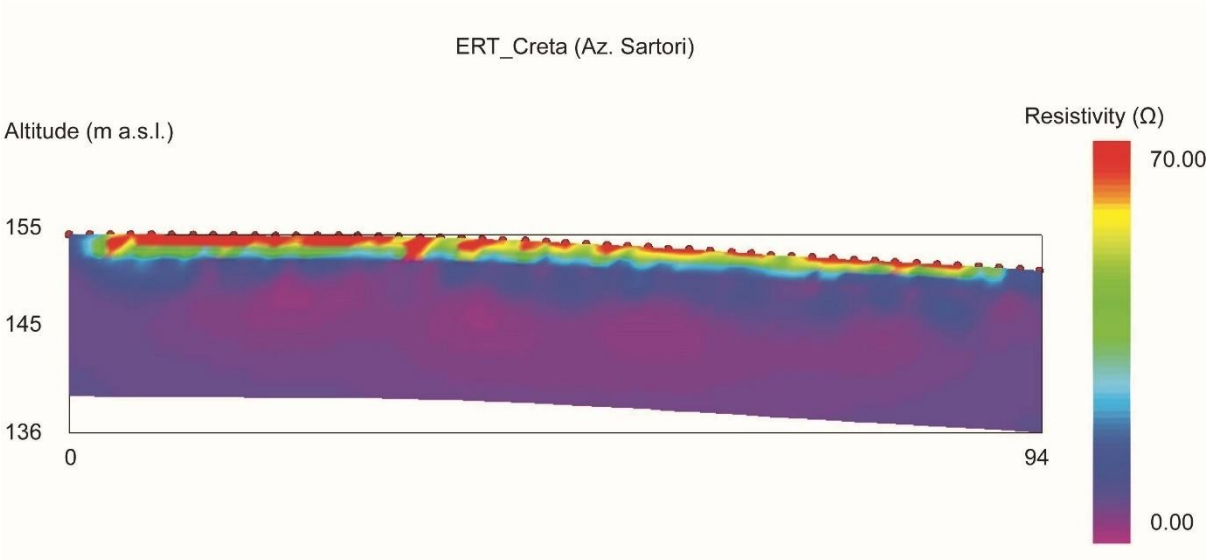

Fig. 13 Geophysical (ERT) surveys of CRT.

Vicobarone (VCB)

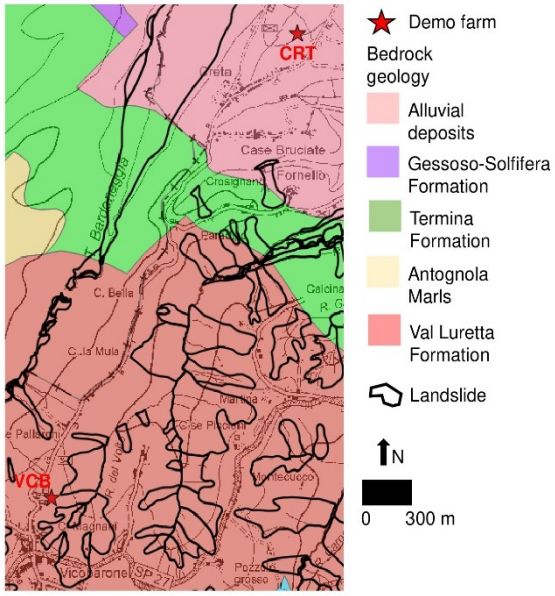

Fig. 14 Main geomorphological attributes and bedrock geology of VCB area.

Fig. 15 Map with the different soil management practices, the location of geophysical surveys and pits of VCB area.

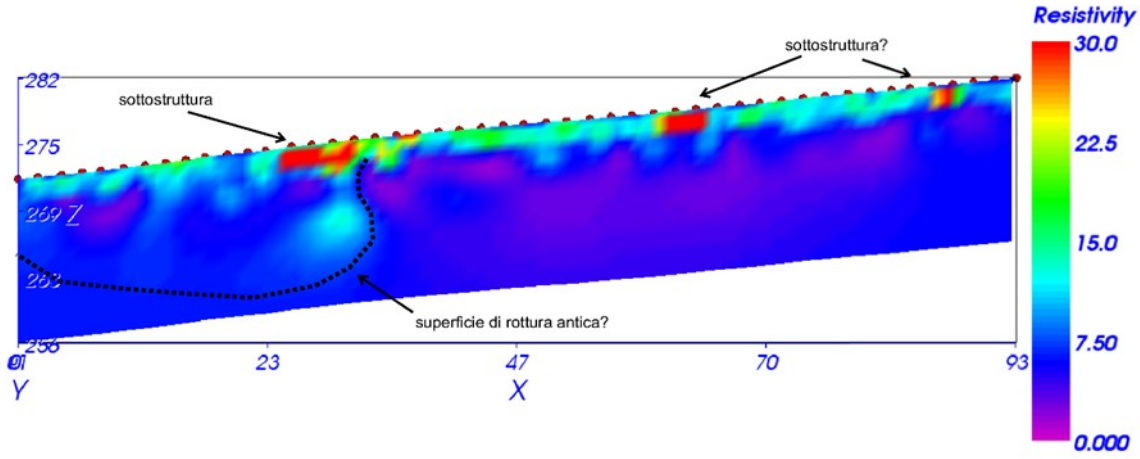

Fig. 16 Geophysical (ERT) surveys of VCB.

Genepreto (GNP)

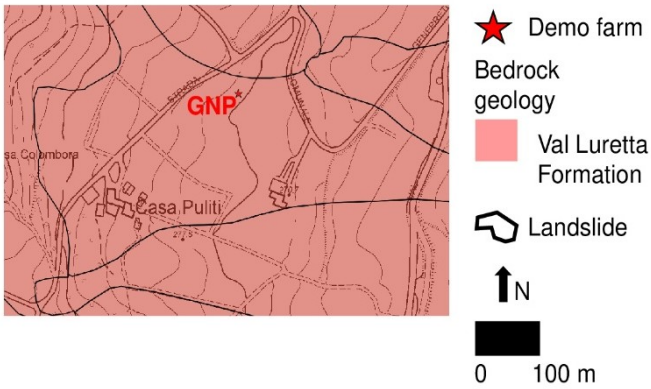

Fig. 17 Main geomorphological attributes and bedrock geology of GNP area.

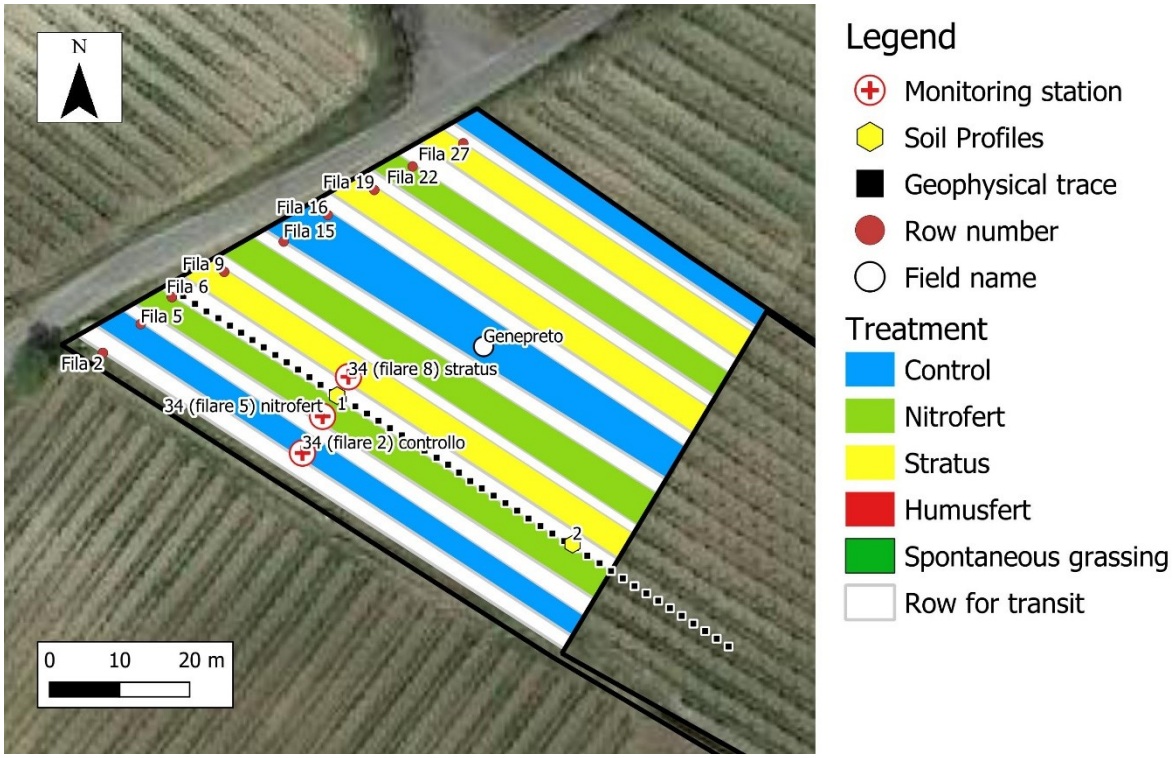

Fig. 18 Map with the different soil management practices, the location of geophysical surveys and pits of GNP area.

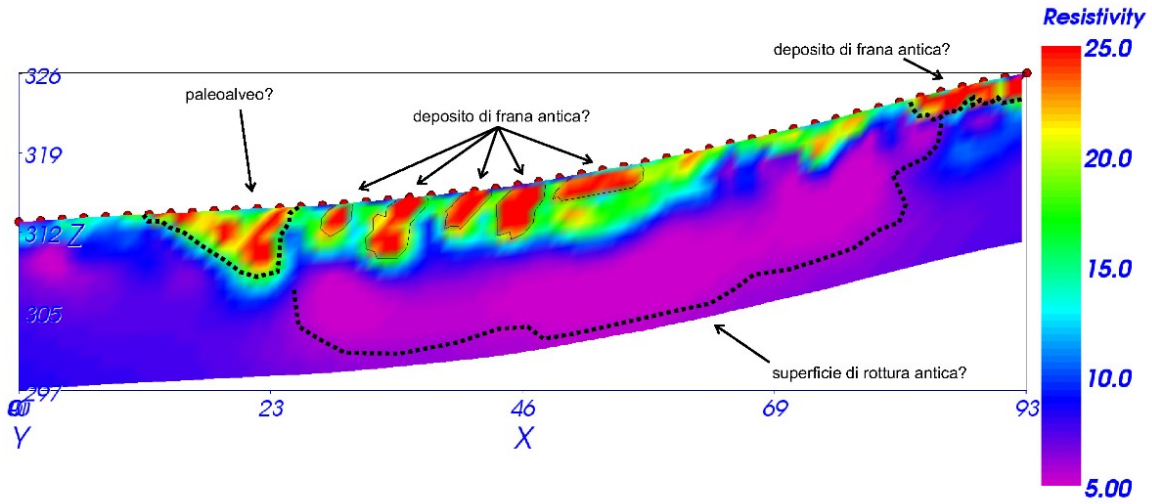

Fig. 19 Geophysical (ERT) surveys of GNP.

Soil profiles and pedological analysis

The soils of each demo farm were characterized from a multidisciplinary point of view. Fig. 20 presents a flow chart illustrating the different field and laboratory analyses carried out.
After the geophysical surveys have been conducted in the first months of 2021, two trench pits were opened in each tested vineyard. These pits were located along the same inter-row, in the upper and the lower parts of the slope to highlight possible differences on soil properties due to the different geomorphological position. The pits were averagely 2 m long and 1.5 m large, with variable depth according to the depth of the weathered bedrock . Generally, the pits were dug up to a depth of 1.5-2 m. These surveys were conducted from April to June 2021.
For each pit the following analysis were carried out:

- Description of the soil profile, with the identification of soil thickness and of the different diagnostic horizons;
- collection of undisturbed samples, for each identified horizon, for the laboratory analysis allowing to derive the following parameters: soil texture (sand, silt and clay percentages); soil chemical properties (pH; organic matter content; cation exchange capacity; carbonate content; active lime content; amount of Na, Ca, K, Mg, P; C/N ratio; electrical conductivity of the soil);
- collection of undisturbed samples, each 10 cm along the soil profile, for the physical laboratory analysis of soil volumetric features (unit weight, dry density, porosity, void index, water content, saturation degree)
- collection of undisturbed soil samples, for the representative soil horizons generally located between 0.2 and 0.7 m from ground level, for the determination of the soil water retention curve.

The general soil characterization was completed with the measure of soil hydraulic conductivity in field, at different depths along the soil profile, in the period between June and July 2021. Soil hydraulic conductivity were measured in different position along the slope where a tested vineyard is located and in correspondence of inter-rows where different management practices are present.

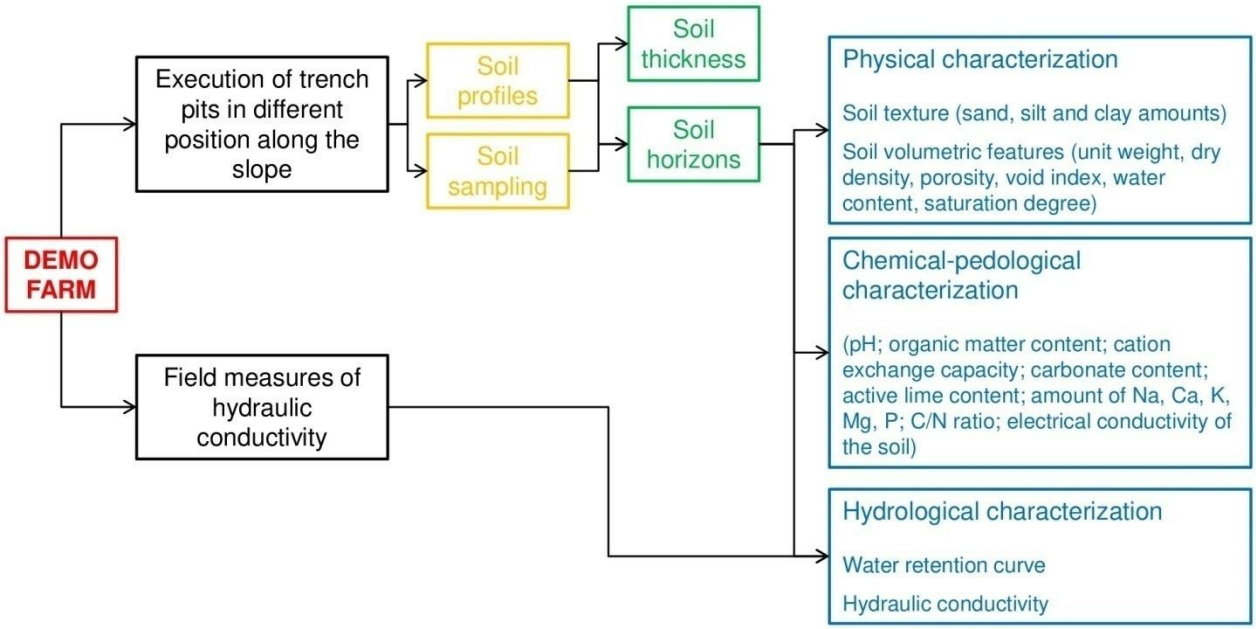

Fig. 20 Flowchart of the methodology of soil characterization.

Fig. 21 Trench pits executed in demo farms (CNV demo farm).

Fig. 22 Description of soil profiles and collection of undisturbed soil samples (SMV demo farm).

Fig. 23 Collection of undisturbed soil samples for soil volumetric characterization (SMV demo farm).

Fig. 24 Field measures of hydraulic conductivity using a constant head permeameter (SMV demo farm).

Soil profiles

In the pedological profiles exposed by soil pits generally a series of prevalently horizontal strata is detectable. These strata can be described and interpreted finally defining specific soil horizons with certain characteristics that in turn allow to attribute particular pedogenetic processes (Fig. 21-25) (Cremashi & Rodolfi 1991, Dazzi 2013, IUSS 2015, Brady & Weil 2002).

The information that we collected during the soil pit description allow already a first description of the soil horizons (Depth, colour, texture, pH, carbonate content, skeleton, concretions, presence and density of roots, etc.). Obviously, these properties were determined for the single soil horizions of the respective soil profiles exposed by the soil pits.

Moreover, several drillings with a Pürckhauer device were conducted that allows to extract a sample of a diameter of ca. 3 cm and a depth of ca 1,5 m (Fig. 25).

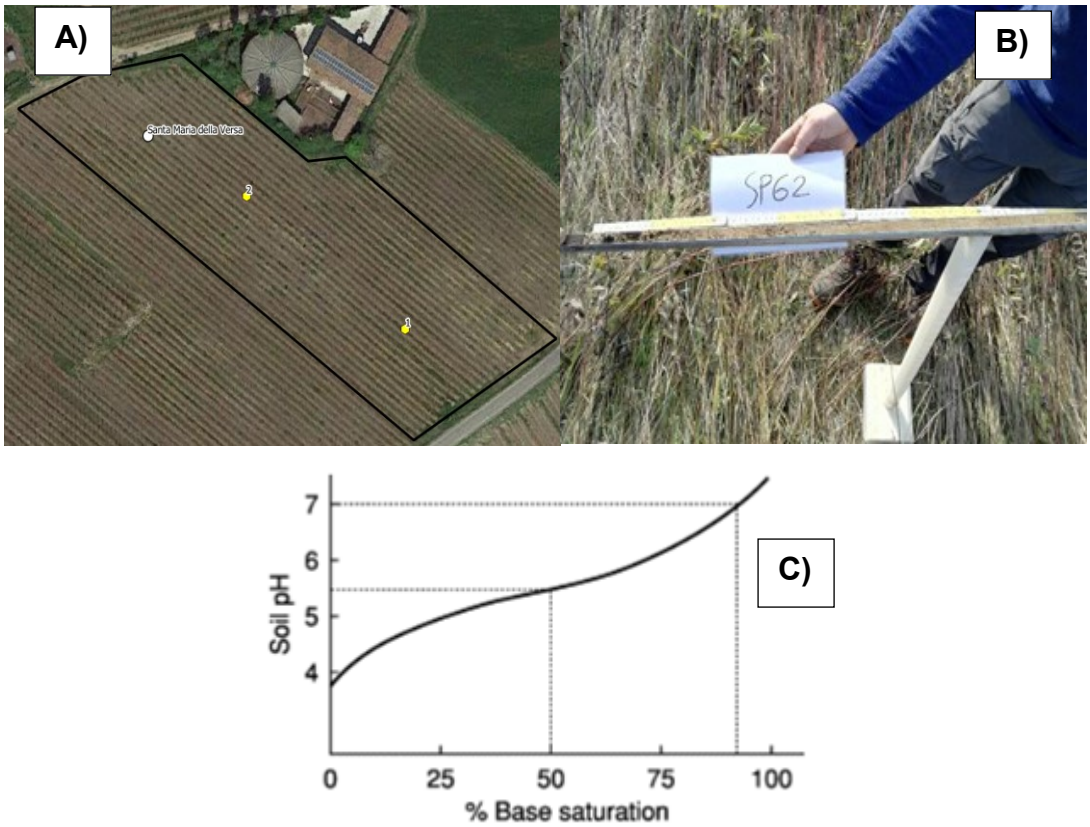

Fig. 25 A) Example of position of the 2 dug profile (Santa Maria della Versa study site); B) Extraction of soil samples using a Pürckhauer device; C) Relation pH-TBS according to Havlin (2005).

All pedological observations and results (Soil pits, Soil sampling with Pürckhauer device) have been georeferenced using coordinated taken with a handheld GPS (Garmin GSP Map 65Ss).
Generally, we took soil samples of the different horizons or in case of not clear horizons every 10 cm up to the bedrock or sedimentary deposits. These samples were analysed in the lab.
In each demonstration vineyard two soil profiles were dug in correspondence of the hydrological monitoring station and at the top/bottom of the respective slopes (e.g fig 25).
The analysis conducted in the laboratory characterize the soil from a physical and chemical point of view and in a quantitative way. In the following the specific methodologies and procedures for the specific analysis are listed:

- Granulometry (sand, silt, clay): following the norm D.M. 13/09/1999 SO n° 185 GU n° 248 21/10/1999 - Met II.6. The samples have been air dried and sieved with a 2mm sieve. Subsequently the fine earth has been analysed using the wet sieving and hydrometer (Stokes) method. The principle is related to the measurement of the volumetric mass of the soil suspension after a specific sedimentation time that finally allows to determine the grain size distribution.
- pH: following norm D.M. 13/09/1999 SO n° 185 GU n° 248 21/10/1999 - Met III.1. The pH was established using potentiometric measurements. Potentiometric pH meters measure the voltage between two electrodes and display the result converted into the corresponding pH value. The measurements were conducted in suspension of water (Aqua dest.) and soil.
- Electric conductivity: following norm D.M. 13/09/1999 SO n° 185 GU n° 248 21/10/1999 - Met IV.1. The measurement is conducted in a soil solution directly measuring the electric conductivity between the electrodes of the device.
- Active carbonates: following norm D.M. 13/09/1999 SO n° 185 GU n° 248 21/10/1999 - Met V.2. The active carbonate content is determined with cold reaction of the fine earth with Ammonium Oxalate.

- Cation Exchange Capacity (C.E.C): following norm D.M. 13/09/1999 SO n° 185 GU n° 248 21/10/1999 - Met XIII.2. The CEC between the soil particle surfaces and the Ammonium ions of the Ammonium Acetate solution is carried out by shaking and leaching. The excess of the Ammonium Acetate solution is eliminated with repeated washing with Ethanol. Subsequently, the absorbed Ammonium is determined by the Kjeldahl distillation directly estimating the sample or an aliquot of the obtained solution leaching NH4 +-soil with a NaCl solution.
- Total N and C/N ratio as well as organic matter: following norm D.M. 13/09/1999 SO n° 185 GU n° 248 21/10/1999 - Met VII.1. The above-mentioned parameters are analysed by elementary analysis. The combustion gasses are passed through a Helium current and a specific catalysator to complete the oxidization process. Then using a copper stratum, the excess oxygen is taken off to reduce the NO to molecular N2. Subsequently the gas mix is separated using gas chromatography and CO_2, N_2, H_2O e SO_2 can be detected by a thermic conductivity detector.
- Assimilable Phosphorus: following norm D.M. 13/09/1999 SO n° 185 GU n° 248 21/10/1999 - Met XV.3. The phosphorous content is determined by Spectro-photo-metrics using the Ascorbic acid method.
- Exchangeable K, Ca, Mg and Na: following norm D.M. 13/09/1999 SO n° 185 GU n° 248 21/10/1999 - Met XIII.5. the content of Ca, Mg, Na and K ions, that have been removed with a Barium Chloride solution with pH 8,2, is determined with flame atom absorption Spectro-photo-meter (AAS).

The CEC describe the total potential of cation exchange taking into account the “acid” cations like Al^+ and H^+ and the “basic” ones like K^+, Na^+, Mg^+ and Ca^+. For the CEC we can use the following table (to classify the CEC values in me/100g (Brady & Weil 2002, Zech et al 2014): Low (CEC of 5-12 me/100 g); Medium (CEC of 12-25 me/100 g); High (CEC of 25-40 me/100 g); Very High (>40 me/100 g).
The total base saturation is given by the following equation:

$$\%TBS = [(Ca^{2+} + Mg^{2+} + K^{+})/CEC] \times 100$$

Since there is a close relation between pH and TBS the function can be used to validate the analysis of the respective parameters. Figure 23b illustrates the relation between TBS – pH.

In the following we describe the obtained results for each soil profile of the demo farms.

Santa Maria della Versa (SMV)

In this study site two soil profiles were dug. One is sited in the upper part (SMV1) and one in the lower parts of the slope (SMV2) .

Fig. 26 a) Location of profiles, b) Soil profile SMV2 and c) soil profile SMV1.

For both SMV1 and SMV2 the finger grain size test resulted very fine (From Clay to Silty clay) with a variable percentage of skeleton (>2mm). The dominant structure of the soil is poly edrical with abundant roots in the first's layers of the soil. Finally, the colour of each horizon was estimated using the Munsell soil color chart. The results are reported in the table below.

Table 3 Summary of parameters detected in the field for SMV1.

Depth [m]	Colour	Texture from field survey	Skeleton [%]	Structure	Roots
0/10	2.5Y4/3	SiC	5% angular pebble gravel	Blocky/Polyehe dral	Yes, abundant mm and cm
10/25	2.5Y5/3	SiC	<5% pebble granule gravel	Blocky/Polyehe dral	Yes, abundant and mm
25/50	2.5Y6/6 E 3/2	SiC	20% angular and rounded	Blocky/Polyehe dral	si, poor, mm and cm

			pebbles		
50/90	2.5Y5/4	SiC	<5 % granule gravel pebble gravel	Blocky/Polyehedral	yes, really poor, mm
90/160	2.5Y5/4 E 6/4	C	10% with marly limestones flankes	Blocky/Polyehedral	yes, really poor, mm

Table 4 Summary of parameters detected in the field for SMV2.

Depth [m]	Colour	Texture from field survey	Skeleton [%]	Structure	Roots
0/10	2.5Y5/4 E 6/4	C	<5%	Blocky/ Polyhedral	yes, mm
10/30	2.5Y4/4 E 5/4	C	10% and angular	Blocky /Polyhedral	yes, mm to cm
35/65	2.5Y6/4	SiC	15% rounded clast of quartzite, and angular marly limestones	Blocky/ Polyhedral	yes, abundant, mm to cm
65/95	2.5Y8/1 e 5/4	C	25 % marly limestone and angular	Blocky/ Polyhedral	yes, really poor, mm
95/120	2.5Y4/7				

Canevino (CNV)

In this study site two soil profiles were dug in the upper part and in the lower part of the slope and called CNV2 and CNV1 respectively.

Fig. 27 a) Location of profiles, b) Soil profile in CNV1 and c) soil profile in CNV2.

For both CNV1 and CNV2 the field grain size analysis show a very fine texture (Silty clay texture) with a variable percentage of skeleton (>2mm). The dominant structure of the soil is polyhedrical with abundant roots in the first's layers of soil. Finally, the colour of each horizon was estimated using the Munsell soil colour chart. The upper mentioned results are reported in the table below.

Table 5 Summary of parameters detected in the field for CNV1.

Depth [m]	Colour	Texture from field survey	Skeleton [%]	Structure	Roots
0/15	2.5Y 5/3 E 5/2	SiC	<2	Blocky/ Polyhedral	Yes, poor and mm
15/80	2.5Y 5/3 con lenti di 5YR 5/4 E 4/4	SiC	<2	Blocky/ Polyhedral	yes, poor and mm and cm
80/130	10y-5GY 10y6/2 E 2Y6/6 (few) e 5YR 5/4 (really few)	SiC	<2	Blocky/ Polyhedral	yes, poor and mm and cm
130/150	10YR4/3 e Gley1-5/N E Gley1-5/10Y E Gley1-4/10 e Gley 2-4/10	SiC	5	Blocky/ Polyhedral	yes, really poor and mm

Table 6 Summary of parameters detected in the field for CNV2.

Depth [m]	Colour	Texture from field survey	Skeleton [%]	Structure	Roots
0/15	2.5Y 5/2	SiC	<2	Blocky/ Polyhedral	Yes, mm
15/35	2.5Y 5/3	SiC	<2	Blocky/ Polyhedral	Yes, mm
35/65	2.5Y 5/2 e 5/3 e 6/2	SiC	<2	Blocky/ Polyhedral	yes, mm and cm abundant
65/90	5YR 5/6 e 6/4 e 5/3	SiC	20	Blocky/ Polyhedral	yes, mm and cm abundant
90/150	5YR 4/3 E 5/6 E 4/4 with few 10Y-5GY 10Y6/2 and 10Y 5/2	/	/	Blocky/ Polyhedral	not presents

Borgo Priolo (BPR)

In this study site two soil profiles were dug in the upper part and in the lower part of the slope and called BPR2 and BPR1 respectively.

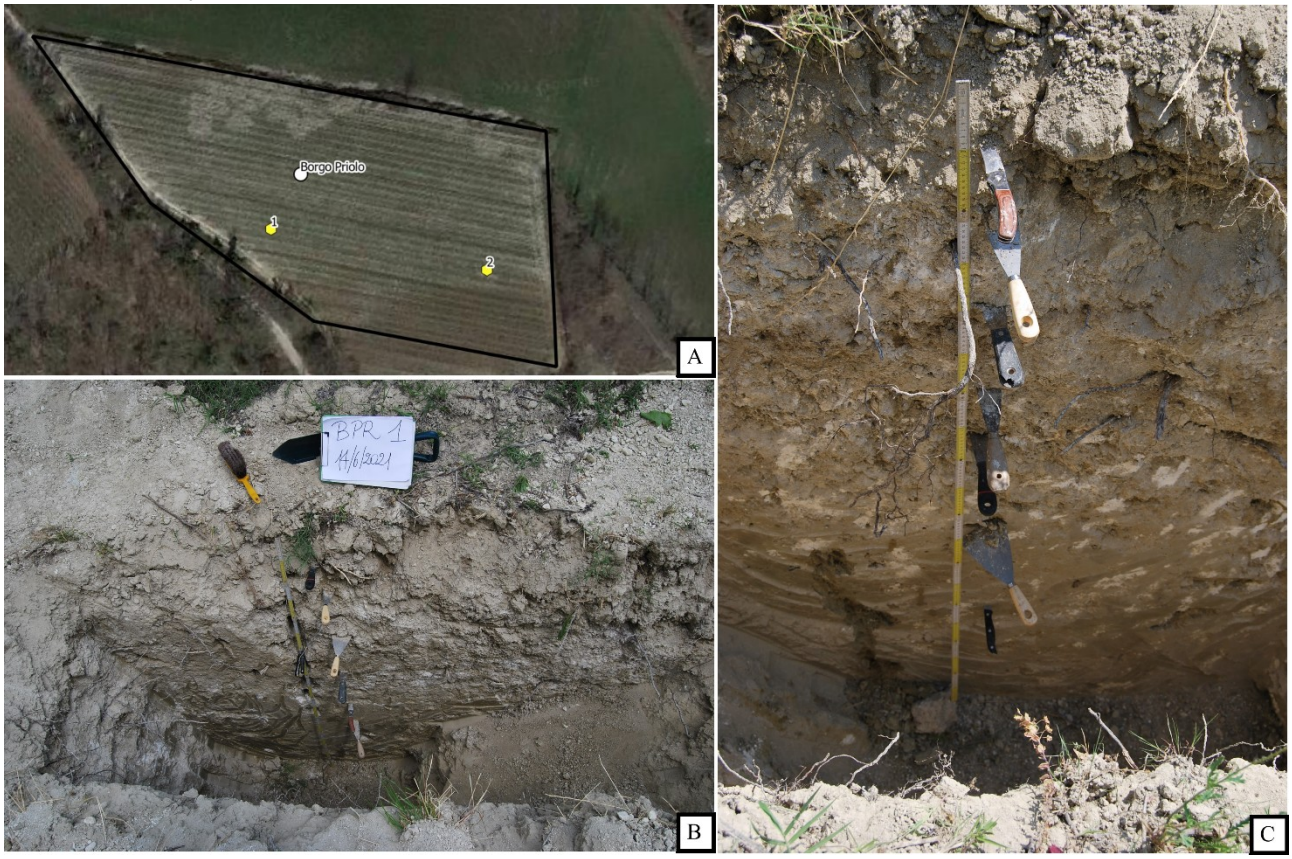

Fig. 28 a) Location of profiles, b) Soil profile in BPR1 and c) soil profile in BPR2.

For both BPR1 and BPR2 the field grain size analysis done in the field resulted fine (From Silty clay to Silty clay loam to Sandy clay loam) with a variable percentage of skeleton (>2mm). The dominant structure of the soil is blocky polyhedrical with abundant roots in the first's layers of soil. Finally, the colour of each horizon was estimated using the Munsell soil colour chart. The results are reported in the table below.

Table 7 Summary of parameters detected in the field for BPR1.

Depth [m]	Colour	Texture from field survey	Skeleton [%]	Structure	Roots
0-17	2.5Y 7/2	SiCL	5	Granular and Polyhedral	yes, poor and mm
17-28	2.5Y 6/2	SiC	<5	Blocky/ Polyhedral	yes, mm
28-50	2.5Y 6/2 E white 7.5YR/19/	SaCL	20	Blocky/ Polyhedral	yes, abundant, mm e cm
50-75	2.5Y 6/3 E 7/1	SaC	15	Blocky/ Polyhedral	yes, abundant, mm e cm

75-110	2.5Y 6/2 E E white 7.5YR/19/	SiC	saprolite	Blocky/ Polyhedral	yes, poor and mm
110-140	2.5Y 6/2 with some 7/8	SiC	saprolite	Blocky/ Polyhedral	really poors and mm
140-200	2.5Y 7/2 E with 7/8 E 8/1	SiC	saprolite	Blocky/ Polyhedral	no

Table 8 Summary of parameters detected in the field for BPR2.

Depth [m]	Colour	Texture from field survey	Skeleton [%]	Structure	Roots
0-15	2.5Y 6/3	SiL	<5	Granular and Polyhedral	yes, mm
15-25	2.5Y 6/3	SiL	<10	Granular and Polyhedral	yes, mm
25-43	2.5Y 7/2 and 10YR/1 9.5/	SiL	<10	Blocky/ Polyhedral	yes, abundant mm and cm
43-64	2.5Y 6/3	SiL	<10	Blocky/ Polyhedral	yes, abundant mm and cm
64-83	2.5Y 6/3	SiL	<5	Blocky/ Polyhedral	yes, abundant mm and cm
83-113	2.5Y 6/3	SiCL	<5	Blocky/ Polyhedral	poor cm e mm
113-150	2.5Y 6/2	SiCL	<2	Blocky/ Polyhedral	poor cm e mm
150-200	2.5Y 6/2 and 6/8	SiC	<2	Blocky/ Polyhedral	no

Creta (CRT)

In this study site two soil profiles were dug in the upper part and in the lower part of the slope and called CRT1 and CRT2 respectively.

Fig. 29 a) Location of profiles, b) Soil profile in CRT1 and c) soil profile in CRT2.

For both CRT1 and CRT2 the field grain size analysis done in the field resulted very homogeneous and fine (Silty clay) without skeleton percentage. The dominant structure of the soil is polyhedrical with abundant roots in the first's layers of soil. Finally, the colour of each horizon was estimated using the Munsell soil colour chart. The upper mentioned results are reported in the table below.

Table 9 Summary of parameters detected in the field for CRT1.

Depth [m]	Colour	Texture from field survey	Skeleton [%]	Structure	Roots
0/10	10YR4/4	Si	0	Blocky/ Polyhedral	yes, dense and mm
10/25	10YR5/6	Si	0	Blocky/ Polyhedral	yes, poor

25/35	10YR6/6	Si	0	Blocky/ Polyhedral	yes, poor
35/80	10YR5/4	Si	0	Blocky/ Polyhedral	yes, really poor
80/150 (fine scavo)	10YR5/3	Si	0	Blocky/ Polyhedral	yes, really poor

Table 10 Summary of parameters detected in the field for CRT2.

Depth [m]	Colour	Texture from field survey	Skeleton [%]	Structure	Roots
0/10	10YR4/4	Si	0	Blocky/ Polyhedral	yes, dense and mm
10/25	10YR4/3	Si	0	Blocky/ Polyhedral	yes, poor
25/60	10YR5/4	Si	0	Blocky/ Polyhedral	yes, poor
60/100	10YR5/3	Si	0	Blocky/ Polyhedral	yes, really poor
100/150	10YR5/6	Si	0	Blocky/ Polyhedral	yes, really poor

Vicobarone (VCB)

In this study site two soil profiles were dug in the upper part and in the lower part of the slope and called VCB2 and VCB1 respectively.

Fig. 30 a) Location of profiles, b) Soil profile in VCB1 and c) soil profile in VCB2.

For both VCB1 and VCB2 the field grain size analysis done in the field resulted very fine and homogeneous (Silty clay and Clay) with a variable percentage of skeleton. The dominant structure of the soil is polyhedrical with abundant roots in the first's layers of soil. Finally, the colour of each horizon was estimated using the Munsell soil colour chart. The upper mentioned results are reported in the table below.

Table 11 Summary of parameters detected in the field for VCB1.

Depth [m]	Colour	Texture from field survey	Skeleton [%]	Structure	Roots
0/15	2.5Y 4/3	SiC	<2	Blocky/ Polyhedral	yes, dense and mm
15/40	2.5Y 4/3 E 6/6	C	<3	Blocky/ Polyhedral	yes, dense and mm and cm
40/70	2.5Y 5/3 and 5/5 and 6/4	C	<4	Blocky/ Polyhedral	yes, poors and mm
70/100	2.5Y 6/2 and 6/4	C	/	Blocky/ Polyhedral	yes, mm
100/160	2.5Y 6/1 and 6/6	Weathered bedrock	/	Blocky/ Polyhedral	no

Table 12 Summary of parameters detected in the field for VCB2.

Depth [m]	Colour	Texture from field survey	Skeleton [%]	Structure	Roots
0/10	2.5Y 4/2	SiC	1	Blocky/ Polyhedral	yes, dense and mm
10/50	2.5Y 4/3 and 5/4 and 6/6	C	5	Blocky/ Polyhedral	yes, dense and mm and cm
50/65	2.5Y 6/3 and 6/6	SiC	10	Blocky/ Polyhedral	yes, poors and mm
65/90	2.5Y 5/6 and 6/4	SaC	20	Blocky/ Polyhedral	yes, poors and mm
90/160	2.5Y 5/4 and 7/4	Weathered bedrock WB	/	Blocky/ Polyhedral	no

Genepreto (GNP)

In this study site two soil profiles were dug in the upper part and in the lower part of the slope and called GNP1 and GNP2 respectively.

Fig. 31 a) Location of profiles, b) Soil profile of GNP1 and c) soil profile in GNP2.

For both GNP1 and GNP2 the field grain size analysis done in the field resulted homogeneous and fine (Clay, Silty clay and Silty Clay Loam) without skeleton percentage. The dominant structure of the soil is polyhedrical with abundant roots in the first's layers of soil. Finally, the colour of each horizon was estimated using the Munsell soil colour chart. The upper mentioned results are reported in the table below.

Table 13 Summary of parameters detected in the field for GNP1.

Depth [m]	Colour	Texture from field survey	Skeleton [%]	Structure	Roots
0/10	2.5Y 5/3	SiCL	<10	Polyhedral	yes, dense
10/30	2.5Y 6/3	SaCL	15/20	Polyhedral	yes, dense
30/50	2.5Y 5/4	C	20	Polyhedral	yes, dense
50/80	2.5Y 6/3	C	20	Polyhedral	yes
80/150	2.5Y 5/3		/	Polyhedral	yes

Table 14 Summary of parameters detected in the field for GNP2.

Depth [m]	Colour	Texture from field survey	Skeleton [%]	Structure	Roots
0/10	2.5Y 5/3	CL	20	Polyhedral	yes, poor
10/35	2.5Y 4/3	SiC	20	Polyhedral	yes, poor
35/145	2.5Y 4/3	C	20	Polyhedral	poor

Soil physical features

The soils of each demo farm were characterized in terms of physical properties, measuring the following parameters:

- soil texture, determining the weight percentage of sand, silt and clay;
- soil volumetric features, namely unit weight (γ), dry density (γ_d), porosity (ρ), void index (e), volumetric water content (θ), saturation degree (S_r).

Soil texture was determined for 68 sample, corresponding to each identified diagnostic horizon in each analyzed soil profile, using undisturbed samples of at least 1 kg collected in the trench pits. Soil texture of each analyzed layer was, then, classified according to United States Department of Agriculture (USDA) classification.
Table 15 lists the amount of sand, silt and clay measured for each analyzed soil horizon and the corresponding USDA classification. Fig. 32, 33, 34, 35, 36, 37 shows the distribution of soil samples on USDA triangle, while Fig. 38 shows the trends along depth of these amounts in the analyzed soil profiles of each demo farms.
The soil texture of the tested vineyards reflects the lithological features of the parent material. All the analyzed soil profiles present horizons with a predominant fine texture. The soils of SMV and VCB are clays, while the soils of the other demo farms are mostly loamy or with silty clay texture. SMV and VCB soils derived from interlayered flyshes and are characterized by a high amount in clay, typically higher than 55%, followed by a silt content higher than 23% and a sand content lower than 16%. GNP and CNV soils derived from calcareous marls and varicoloured clays, respectively. They are typically silty clays or loams with high amount in silt and clay, as testified by an amount in clay between 32.7 and 52.0%, followed by an amount in silt between 32.3 and 57.9% and by a sand content of 4.0-22.2%. BPR and CRT soils derived from sandy marls and quaternary alluvial deposits, respectively. They are characterized by a predominant silty fraction, which ranges between 38.6 and 56.2% and 46.5 and 65.1% in BPR and CRT, respectively. Instead, BPR soils are characterized averagely by a higher content in clayey fraction (22.3-46.9%) than CRT soils (17.9-30.5%). Also sand content is bigger in BPR than in CRT layers, even if it keeps averagely lower than 20% in both these soils.
Soil texture keeps quite constant along the depth in each soil profile, as stressed by average low values of standard error for each grain size class (<9.4% for sand, <7.3% for silt, <11.5% for clay). However, the layer in contact with the weathered bedrock, that constitutes the parent material of each soil profile, presents an increase in sand amount respect to the most superficial horizons. This increase is in the order of about 1-34% and is more evident in SMV, VCB, GNP and CRT soils.
Soil volumetric features were measured each 10 cm in depth along each soil profile, through undisturbed soil samples by means of the Drive-Cylinder Method, according to to American Society for Testing and Materials (ASTM) (1988) procedure (ASTM D2937). The total amount of tested samples were 149.
Table 16 lists the measured values of the soil volumetric features for each tested sample, while Fig. 39, 40, 41, 42, 43, 44 show the trends of these parameters along each reconstructed soil profile.
The soils characterized by the highest amounts in clay are also the ones with the least density and the highest porosity. Thus, SMV and VCB soils horizons have low values of γ and γ_d (averagely, 15.6-15.7 kN/m^3 and 11.3-11.6 kN/m^3 for γ and γ_d, respectively) and high values of ρ and e (averagely, 53.5-55.2% and 1.09-1.20 for ρ and e, respectively). The other soil profiles are characterized by higher density, as confimed by γ typically higher than 16 kN/m^3 and γ_d typically higher than 12.0 kN/m^3, and lower porosity, as testified by ρ typically lower than 54% and e typically lower than 1.
Soil volumetric features keep quite steady along the depth in each soil profile, as stressed by average low values of standard error of these different properties (<1 kN/m^3 for γ and γ_d, <3% for ρ, 0.08< for e). This situation is also evident comparing the values of two representative volumetric features of the soils (γ_d and ρ) measured in the first 0.2 m from ground level, which are the horizons most affected by tillage operations, and below this depth, in the layers less affected by the tillage operations carried out in the vineyards. The average differences in γ_d and in ρ measured in the first 0.2 m from ground level and below this depth are, in fact, of only 0.1 kN/m^3 and 0.2%, respectively (Fig. 45).
The trends of θ and of S_r measured during the execution of the soil profile are influenced by the period of samplings (end of spring) and by the amount of rainfall fallen in the previous periods. Thus, these trends can give only indications on some hydrological behaviors in the tested demo farm, which have to be monitored more in details through the field sensors installed in each tested vineyard.
In all the analyzed soil profiles, water content in the first 0.3 m from ground is higher than in the layers located below in depth, in correspondence of the sampling period. θ and S_r are averagely 0.02-0.10 m^3/m^3 and 5-30% higher in the first 0.3 m from ground level, respectively. However, in some soil profiles, an increase in saturation degree close to 100% testified conditions of complete saturation in correspondence of sampling period. This condition was detected from 1.2 m from ground in SMV1, from 0.6 m from ground in GNP1, from 0.8 m from ground in CRT1.

ID	Sample	(Sand) g/kg	(Silt) g/kg	(Clay) g/kg
1	SMV1 - 0/10	79	311	610
2	SMV1 - 10/25	85	273	642
3	SMV1 - 25/50	93	276	631
4	SMV1 - 50/90	80	236	684
5	SMV1 - 90-160	154	278	568
1	SMV2 - 0/10	114	308	578
2	SMV2 - 10/30	100	294	606
3	SMV2 - 35/65	94	285	621
4	SMV2 - 65/95	275	390	335

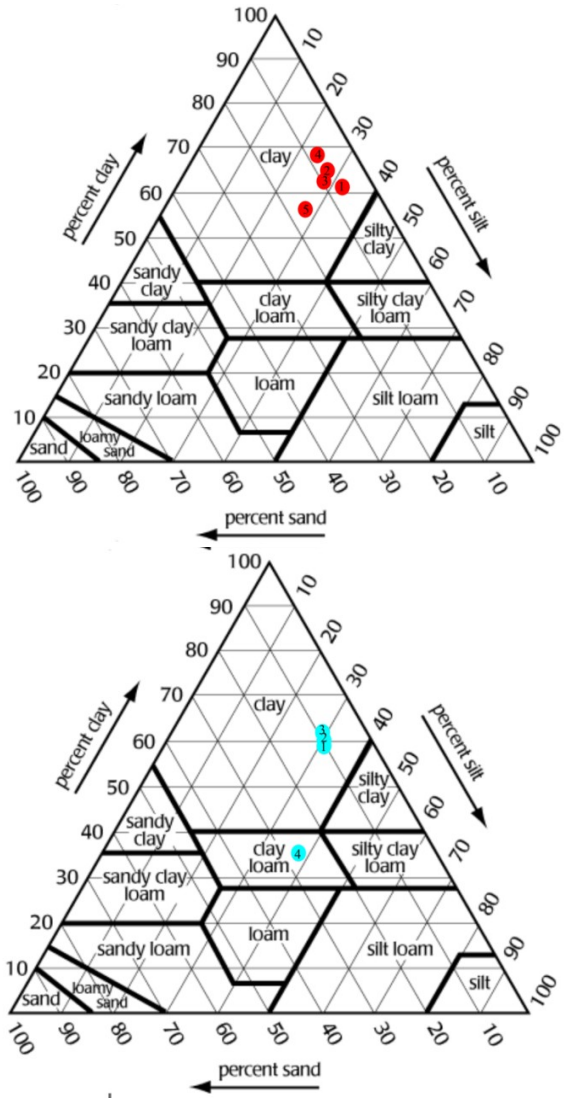

Fig. 32 Grain size analysis of SMV1 and SMV2.

ID	Sample description	(Sand) g/kg	(Silt) g/kg	(Clay) g/kg
1	CRT1 - 0/10	103	650	247
2	CRT1 - 10/25	75	639	286
3	CRT1 - 25/35	71	624	305
4	CRT1 - 35/80	84	651	265
5	CRT1 - 80/150	126	582	292
1	CRT2 - 0/10	89	614	297
2	CRT2 - 10/25	264	465	271
3	CRT2 - 25/60	150	551	299
4	CRT2 - 60/100	109	598	293
5	CRT2 - 100/150	313	508	179

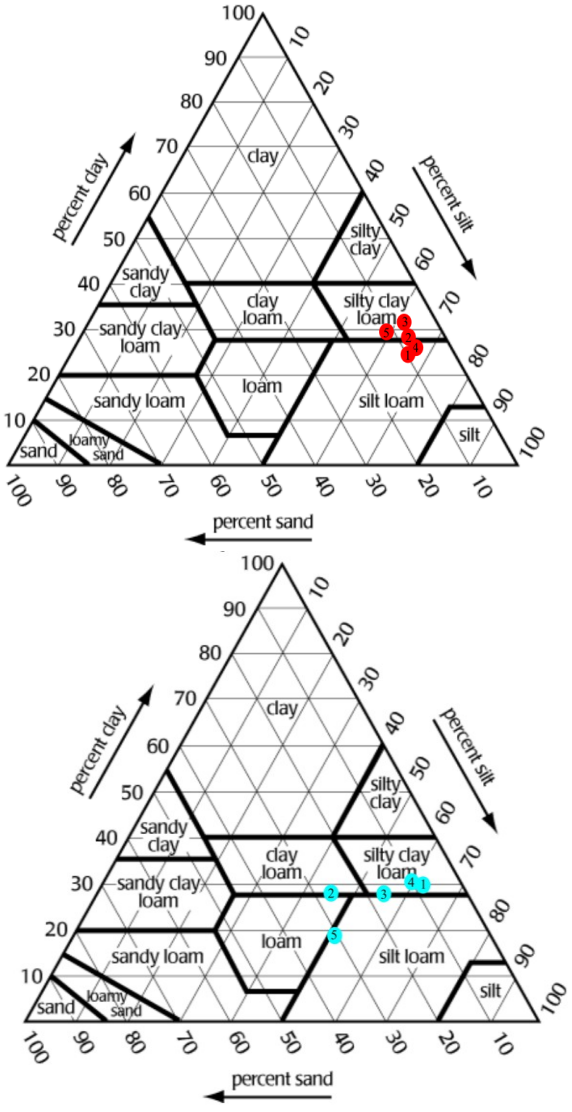

Fig. 33 Grain size analysis of CRT1 and CRT2.

ID	Sample	(Sand) g/kg	(Silt) g/kg	(Clay) g/kg
1	CNV1 - 0/15	222	386	392
2	CNV1 - 15/80	199	353	448
3	CNV1 - 80/130	212	421	367
4	CNV1 - 130/150	55	638	307
1	CNV2 - 0/15	31	476	493
2	CNV2 - 15/35	174	399	427
3	CNV2 - 35/65	40	440	520
4	CNV2 - 65/90	51	539	410
5	CNV2 - 90/150	64	579	357

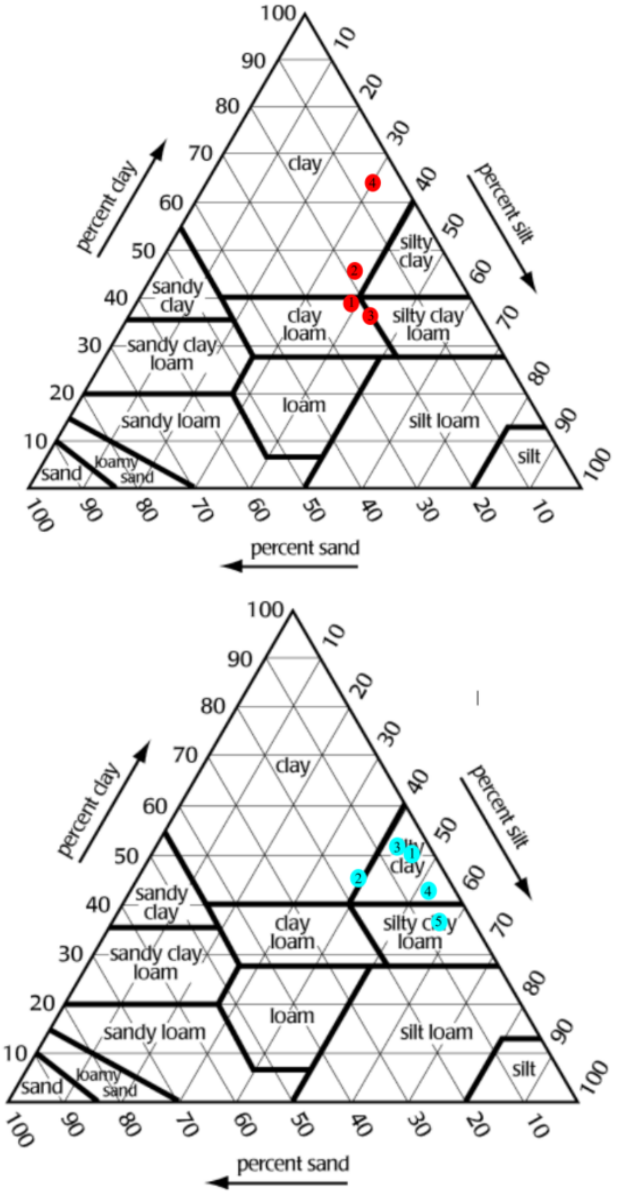

Fig. 34 Grain size analysis of CNV1 and CNV2.

ID	Sample	(Sand) g/kg	(Silt) g/kg	(Clay) g/kg
1	BPR1 - 0/17	144	526	330
2	BPR1 - 17/28	83	510	407
3	BPR1 - 28/50	249	386	365
4	BPR1 - 50/75	107	469	424
5	BPR1 - 75/110	94	439	467
6	BPR1 - 110/150	110	421	469
7	BPR1 - 140/200	250	387	363
1	40 DI TRANSIZIONE - 40	286	438	276
2	60 DI TRANSIZIONE - 60	98	502	400
1	BPR2 - 0/15	279	406	315
2	BPR2 - 15/25	373	404	223
3	BPR2 - 25/43	117	508	375
4	BPR2 - 43/64	185	515	300
5	BPR2 - 64/83	104	539	357
6	BPR2 - 83/113	41	562	397
7	BPR2 - 113/115	10	530	460
8	BPR2 - 150/200	45	505	450

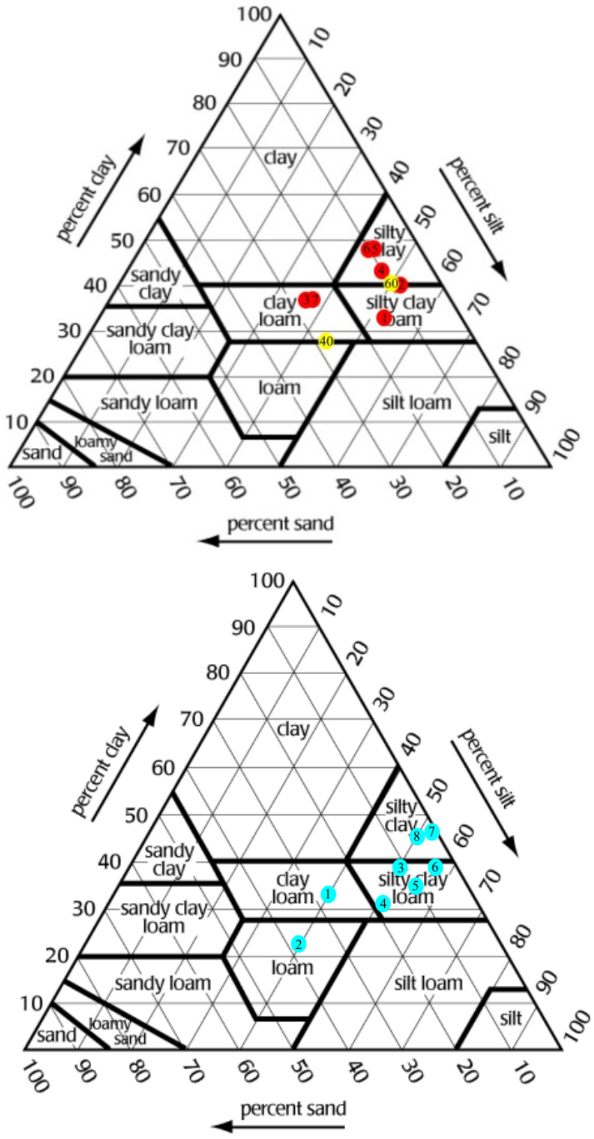

Fig. 35 Grain size analysis of BPR1 and BPR2.

ID	Sample description	(Sand) g/kg	(Silt) g/kg	(Clay) g/kg
1	VCB1 - 0/15	95	276	629
2	VCB1 - 15/40	90	273	637
3	VCB1 - 40/70	103	340	557
4	VCB1 - 70/100	327	263	410
5	VCB1 - 100/160	494	241	265
1	VCB2 - 0/10	53	311	636
2	VCB2 - 10/50	156	228	616
3	VCB2 - 50/65	464	271	265
4	VCB2 - 65/90	193	384	423
5	VCB2 - 90/160	247	382	371

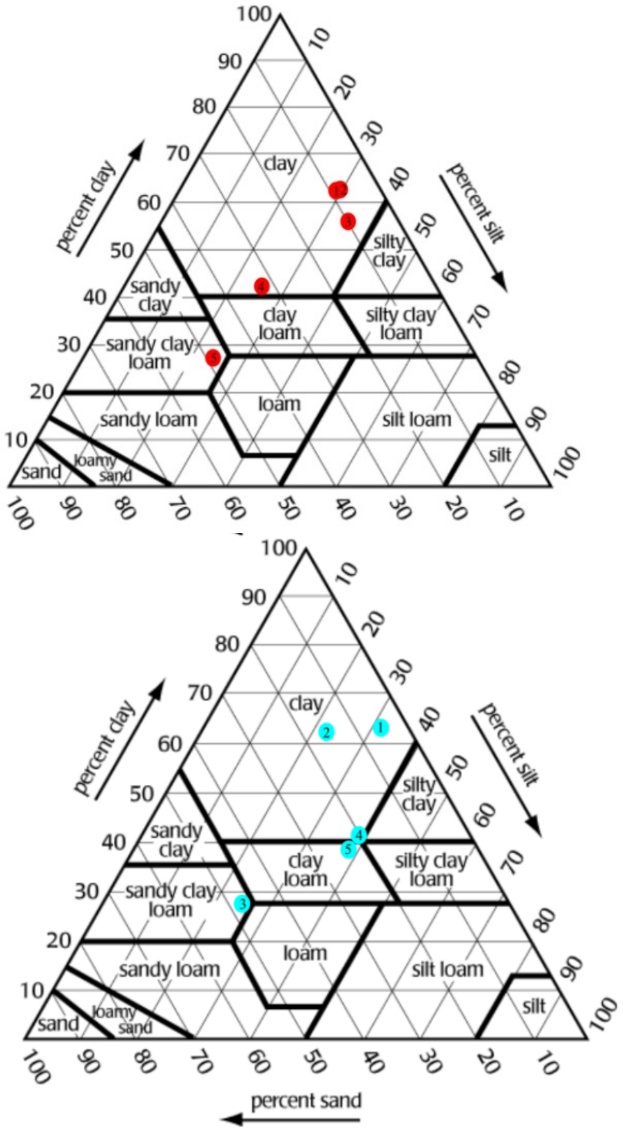

Fig. 36 Grain size analysis of VCB1 and VCB2.

ID	Sample description	(Sand) g/kg	(Silt) g/kg	(Clay) g/kg
1	GNP1 - 0/10	100	464	436
2	GNP1 - 0/20	195	357	448
3	GNP1 - 20/30	80	439	481
4	GNP1 - 30/40	162	396	442
5	GNP1 - 40/50	112	463	425
6	GNP1 - 50/80	199	406	395
7	GNP1 - 80/160	542	205	253
1	GNP1 - 0/10	154	450	396
2	GNP1 - 10/30	282	391	327
3	GNP1 - 30/50	177	366	457
4	GNP1 - 50/80	346	323	331
5	GNP1 - 80/160	524	234	242
1	GNP2 - 0/10	187	380	433
2	GNP2 - 10/35	160	324	516
3	GNP2 - 35/145	172	311	517

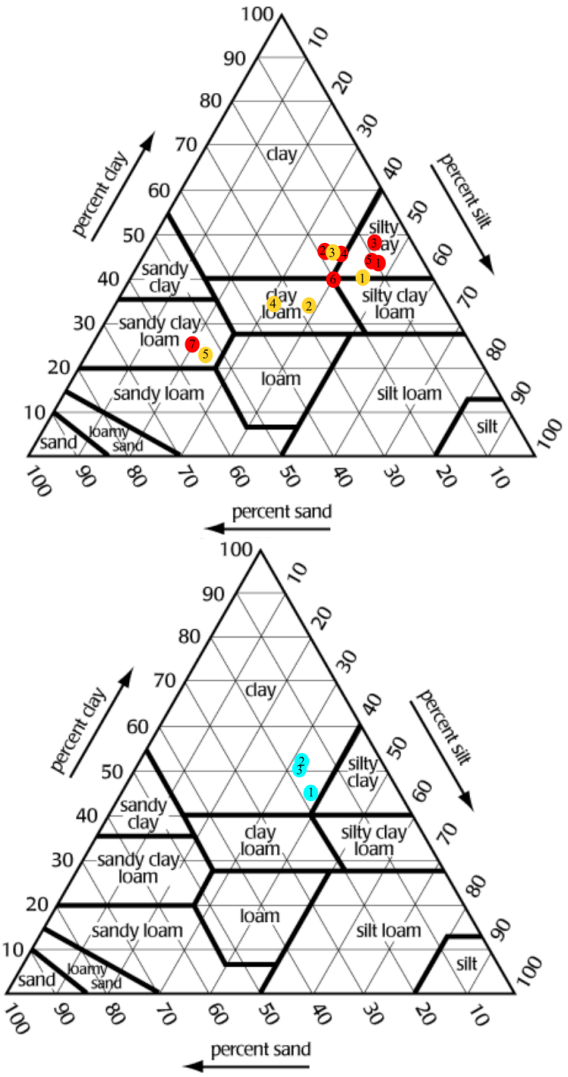

Fig. 37 Grain size analysis of GNP1 and GNP2.

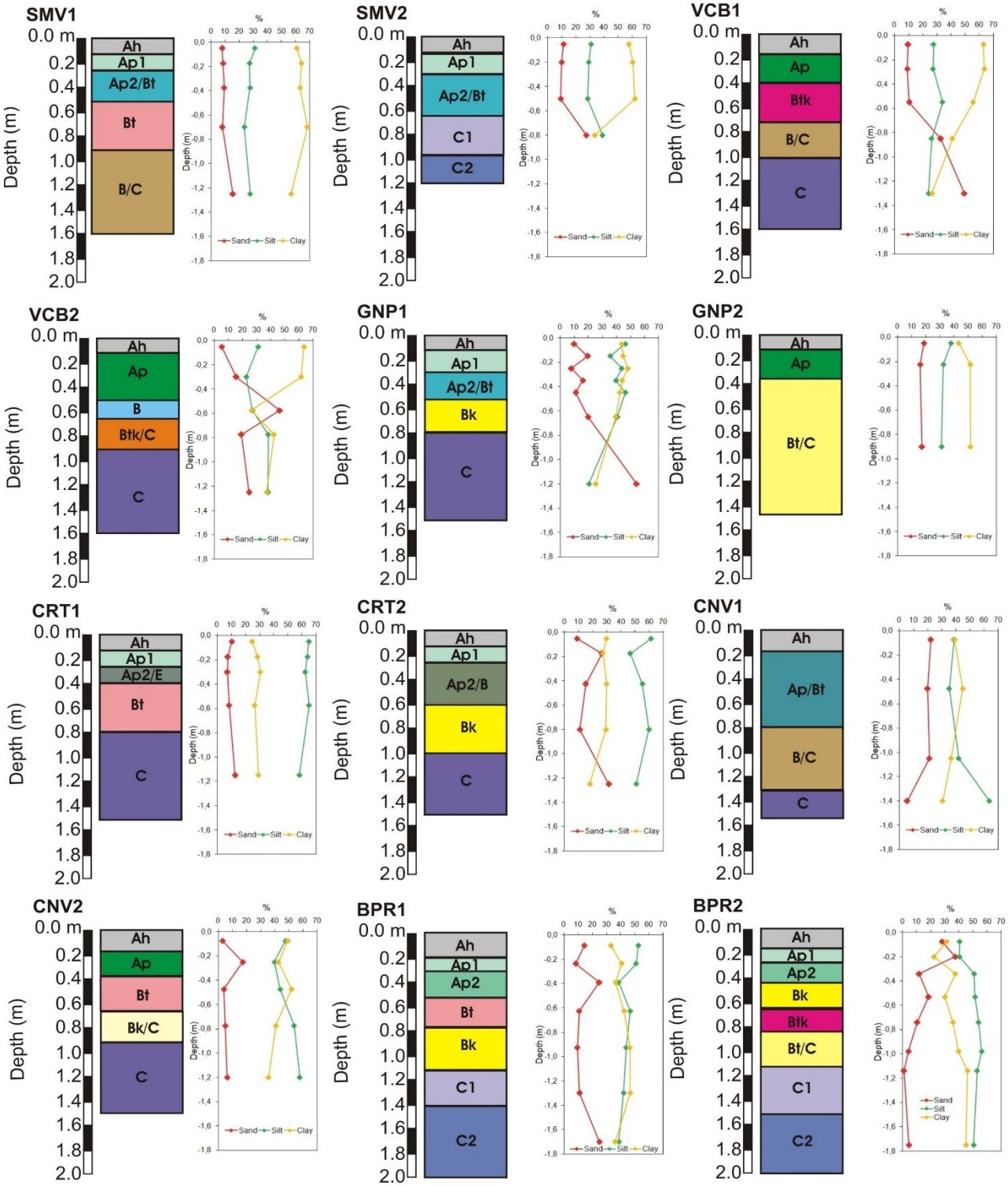

Fig. 38 Trends in depth of the grain size (sand, silt and clay amounts) for the soils of the different demo farms.

Table 15. Grain size distribution of the soils of the different demo farms. Sand) sand amount, Silt) silt amount, Clay) clay amount.

Demo farm	Soil profile	Depth (m)	Sand (%)	Silt (%)	Clay (%)	USDA classification
SMV	SMV1	0-0.10	7.9	31.1	61.0	Clay
	SMV1	0.10-0.25	8.5	27.3	64.2	Clay
	SMV1	0.25-0.50	9.3	27.6	63.1	Clay
	SMV1	0.50-0.90	8.0	23.6	68.4	Clay
	SMV1	0.90-1.60	15.4	27.8	56.8	Clay
	SMV2	0-0.10	11.4	30.8	57.8	Clay
	SMV2	0.10-0.30	10.0	29.4	60.6	Clay
	SMV2	0.35-0.65	9.4	28.5	62.1	Clay
	SMV2	0.65-0.95	27.5	39.0	33.5	Clay loam
VCB	VCB1	0-0.15	9.5	27.6	62.9	Clay
	VCB1	0.15-0.40	9.0	27.3	63.7	Clay
	VCB1	0.40-0.70	10.3	34.0	55.7	Clay
	VCB1	0.70-1.00	32.7	26.3	41.0	Clay
	VCB1	1.00-1.60	49.4	24.1	26.5	Sandy clay loam
	VCB2	0-0.10	5.3	31.1	63.6	Clay
	VCB2	0.10-0.50	15.6	22.8	61.6	Clay
	VCB2	0.50-0.65	46.4	27.1	26.5	Sandy clay loam
	VCB2	0.65-0.90	19.3	38.4	42.3	Clay
	VCB2	0.90-1.60	24.7	38.2	37.1	Clay loam
GNP	GNP1	0-0.10	10.0	46.4	43.6	Silty clay
	GNP1	0.10-0.20	19.5	35.7	44.8	Clay
	GNP1	0.20-0.30	8.0	43.9	48.1	Silty clay
	GNP1	0.30-0.40	16.2	39.6	44.2	Silty clay
	GNP1	0.40-0.50	11.2	46.3	42.5	Silty clay
	GNP1	0.50-0.80	19.9	40.6	39.5	Silty clay
	GNP1	0.80-1.60	54.2	20.5	25.3	Sandy clay loam
	GNP1	0-0.10	15.4	45.0	39.6	Silty clay
	GNP1	0.10-0.30	28.2	39.1	32.7	Clay loam
	GNP1	0.30-0.50	17.7	36.6	45.7	Clay
	GNP1	0.50-0.80	34.6	32.3	33.1	Clay loam
	GNP1	0.80-1.60	52.4	23.4	24.2	Sandy clay loam
	GNP2	0-0.10	18.7	38.0	43.3	Clay
	GNP2	0.10-0.35	16.0	32.4	51.6	Clay
	GNP2	0.35-1.45	17.2	31.1	51.7	Clay
CRT	CRT1	0-0.10	10.3	65.0	24.7	Silt loam
	CRT1	0.10-0.25	7.5	63.9	28.6	Silty clay loam

	CRT1	0.25-0.35	7.1	62.4	30.5	Silty clay loam
	CRT1	0.35-0.80	8.4	65.1	26.5	Silt loam
	CRT1	0.80-1.50	12.6	58.2	29.2	Silty clay loam
	CRT2	0-0.10	8.9	61.4	29.7	Silt clay loam
	CRT2	0.10-0.25	26.4	46.5	27.1	Clay loam
	CRT2	0.25-0.60	15.0	55.1	29.9	Silt clay loam
	CRT2	0.60-1.00	10.9	59.8	29.3	Silt clay loam
	CRT2	1.00-1.50	31.3	50.8	17.9	Silt loam
CNV	CNV1	0-0.15	22.2	38.6	39.2	Clay loam
	CNV1	0.15-0.80	19.9	35.3	44.8	Clay
	CNV1	0.80-1.30	21.2	42.1	36.7	Clay loam
	CNV1	1.30-1.50	5.5	63.8	30.7	Silty clay loam
	CNV2	0-0.15	3.1	47.6	49.3	Silty clay
	CNV2	0.15-0.35	17.4	39.9	42.7	Silty clay
	CNV2	0.35-0.65	4.0	44.0	52.0	Silty clay
	CNV2	0.65-0.90	5.1	53.9	41.0	Silty clay
	CNV2	0.90-1.50	6.4	57.9	35.7	Silty clay loam
BPR	BPR1	0-0.17	14.4	52.6	33.0	Silty clay loam
	BPR1	0.17-0.28	8.3	51.0	40.7	Silty clay loam
	BPR1	0.28-0.50	24.9	38.6	36.5	Clay loam
	BPR1	0.50-0.75	10.7	46.9	42.4	Silty clay
	BPR1	0.75-1.10	9.4	43.9	46.7	Silty clay
	BPR1	1.10-1.50	11.0	42.1	46.9	Silty clay
	BPR1	1.40-2.00	25.0	38.7	36.3	Clay loam
	BPR2	0-0.15	27.9	40.6	31.5	Clay loam
	BPR2	0.15-0.25	37.3	40.4	22.3	Loam
	BPR2	0.25-0.43	11.7	50.8	37.5	Silty clay loam
	BPR2	0.43-0.64	18.5	51.5	30.0	Silty clay loam
	BPR2	0.64-0.83	10.4	53.9	35.7	Silty clay loam
	BPR2	0.83-1.13	4.1	56.2	39.7	Silty clay loam
	BPR2	1.13-1.50.	1.0	53.0	46.0	Silty clay
	BPR2	1.50-2.00	4.5	50.5	45.0	Silty clay

Table 16 Volumetric features of the soils of the different demo farms. γ) unit weight, γd) dry density, e) void index, ρ) porosity, Sr) saturation degree, θ) water content.

Demo farm	Soil profile	Depth (m)	γ (kN/m^3)	γ_d (kN/m^3)	e (-)	ρ (%)	S_r (%)	θ (m^3/m^3)
SMV	SMV1	-0.1	17.4	13.0	0.93	48.1	91.28	0.44
	SMV1	-0.2	13.5	10.2	1.45	59.1	56.04	0.33
	SMV1	-0.3	16.7	12.2	1.04	51.1	87.65	0.45
	SMV1	-0.4	16.8	12.4	1.02	50.5	88.02	0.44
	SMV1	-0.5	15.3	10.9	1.30	56.5	77.99	0.44
	SMV1	-0.6	16.6	11.7	1.13	53.0	92.07	0.49

	SMV1	-0.7	16.1	11.4	1.20	54.6	86.73	0.47
	SMV1	-0.8	17.0	12.0	1.08	51.9	94.77	0.49
	SMV1	-0.9	16.2	11.3	1.22	54.9	89.42	0.49
	SMV1	-1	15.1	10.5	1.38	57.9	78.48	0.45
	SMV1	-1.1	17.0	12.1	1.06	51.5	94.98	0.49
	SMV1	-1.2	17.4	12.1	1.07	51.6	102.36	0.53
	SMV1	-1.3	17.3	12.0	1.09	52.2	101.83	0.53
	SMV1	-1.4	16.5	11.1	1.24	55.4	96.52	0.53
	SMV1	-1.5	16.7	11.7	1.13	53.0	94.02	0.50
	SMV1	-1.6	16.2	11.5	1.17	53.9	87.21	0.47
	SMV2	-0.1	15.1	11.6	1.16	53.8	65.57	0.35
	SMV2	-0.2	15.3	12.0	1.09	52.2	64.95	0.34
	SMV2	-0.3	16.3	12.6	0.99	49.7	74.51	0.37
	SMV2	-0.4	13.7	10.6	1.36	57.7	53.90	0.31
	SMV2	-0.5	13.9	10.7	1.33	57.2	55.02	0.31
	SMV2	-0.6	13.3	10.0	1.50	60.0	54.38	0.33
	SMV2	-0.7	13.2	10.2	1.46	59.4	51.57	0.31
	SMV2	-0.8	13.8	10.1	1.48	59.6	62.51	0.37
VCB	VCB1	-0.1	16.5	11.7	1.14	53.3	91.00	0.48
	VCB1	-0.2	17.7	13.0	0.92	48.0	97.43	0.47
	VCB1	-0.3	17.1	12.6	0.98	49.6	90.22	0.45
	VCB1	-0.4	15.4	11.5	1.18	54.2	72.71	0.39
	VCB1	-0.5	16.0	11.9	1.10	52.3	77.60	0.41
	VCB1	-0.6	16.1	12.0	1.09	52.0	78.11	0.41
	VCB1	-0.7	15.8	11.6	1.16	53.6	77.51	0.42
	VCB1	-0.8	16.3	11.8	1.12	52.9	85.52	0.45
	VCB1	-0.9	16.9	12.6	0.99	49.7	86.58	0.43
	VCB1	-1	16.5	12.3	1.04	50.9	83.53	0.43
	VCB1	-1.1	16.3	12.5	0.99	49.8	74.61	0.37
	VCB1	-1.2	16.9	12.6	0.98	49.5	86.68	0.43
	VCB1	-1.3	16.7	12.5	1.00	50.0	83.34	0.42
	VCB1	-1.4	17.2	13.4	0.86	46.2	82.10	0.38
	VCB1	-1.5	16.8	12.6	0.98	49.6	84.56	0.42
	VCB2	-0.1	15.5	11.2	1.23	55.2	78.11	0.43
	VCB2	-0.2	18.8	14.2	0.76	43.1	106.08	0.46
	VCB2	-0.3	17.1	13.0	0.92	48.0	84.71	0.41
	VCB2	-0.4	16.0	11.9	1.10	52.5	77.74	0.41
	VCB2	-0.5	14.5	11.3	1.21	54.8	58.74	0.32
	VCB2	-0.6	15.1	12.4	1.02	50.5	53.09	0.27
	VCB2	-0.7	15.2	11.9	1.10	52.3	63.37	0.33
	VCB2	-0.8	14.7	11.5	1.17	53.8	58.69	0.32

	VCB2	-0.9	14.7	11.9	1.10	52.4	52.57	0.28
	VCB2	-1	15.1	11.8	1.12	52.8	62.14	0.33
	VCB2	-1.1	14.5	11.2	1.24	55.3	59.58	0.33
	VCB2	-1.2	15.1	12.1	1.06	51.4	57.82	0.30
	VCB2	-1.3	12.7	9.7	1.58	61.2	48.48	0.30
	VCB2	-1.4	15.1	11.9	1.10	52.4	61.41	0.32
	VCB2	-1.5	14.0	10.9	1.29	56.4	55.65	0.31
	VCB2	-1.6	14.6	11.3	1.21	54.7	59.28	0.32
GNP	GNP1	-0.1	18.5	15.1	0.66	39.8	86.88	0.35
	GNP1	-0.2	18.0	14.5	0.72	41.8	82.42	0.34
	GNP1	-0.3	18.7	15.5	0.61	38.0	85.37	0.32
	GNP1	-0.4	18.8	15.5	0.61	37.9	86.06	0.33
	GNP1	-0.5	18.1	14.7	0.70	41.1	83.05	0.34
	GNP1	-0.6	18.7	14.8	0.69	40.7	95.67	0.39
	GNP1	-0.7	18.9	15.2	0.65	39.2	95.50	0.37
	GNP1	-0.8	17.1	12.5	1.00	50.0	91.27	0.46
	GNP1	-0.9	17.0	12.5	1.00	49.9	90.59	0.45
	GNP2	-0.1	18.2	14.7	0.71	40.9	78.46	0.47
	GNP2	-0.2	18.0	14.5	0.72	41.8	77.59	0.47
	GNP2	-0.3	18.5	15.2	0.64	39.1	86.73	0.52
	GNP2	-0.4	18.5	15.2	0.64	39.1	69.57	0.41
	GNP2	-0.5	18.1	14.7	0.70	41.1	61.03	0.37
	GNP2	-0.6	18.7	14.8	0.69	40.7	58.71	0.35
	GNP2	-0.7	18.9	15.2	0.65	39.2	58.89	0.35
	GNP2	-0.8	18.7	14.8	0.69	40.7	56.25	0.34
	GNP2	-0.9	18.9	15.2	0.65	39.2	56.08	0.33
	GNP2	-1	18.2	15.6	0.73	42.3	46.81	0.31
	GNP2	-1.1	18.5	15.4	0.71	40.3	47.89	0.30
	GNP2	-1.2	18.7	15.3	0.72	41.0	43.17	0.27
CRT	CRT1	-0.1	18.9	15.7	0.60	37.4	86.13	0.32
	CRT1	-0.2	19.1	15.5	0.62	38.1	96.35	0.37
	CRT1	-0.3	19.1	15.6	0.61	37.8	94.25	0.36
	CRT1	-0.4	19.3	15.5	0.62	38.2	101.36	0.39
	CRT1	-0.5	19.5	15.9	0.58	36.6	99.13	0.36
	CRT1	-0.6	19.2	15.2	0.64	39.2	102.32	0.40
	CRT1	-0.7	19.2	15.5	0.62	38.2	98.20	0.37
	CRT1	-0.8	19.2	15.3	0.64	38.9	100.40	0.39
	CRT1	-0.9	19.4	15.4	0.63	38.6	104.50	0.40
	CRT1	-1	19.7	15.7	0.72	41.8	95.79	0.40
	CRT1	-1.1	19.1	15.3	0.64	39.0	97.89	0.38
	CRT1	-1.2	19.8	16.1	0.61	38.1	97.52	0.37

	CRT1	-1.3	19.4	15.6	0.67	40.1	96.46	0.39
	CRT2	-0.1	16.3	13.2	0.89	47.1	64.62	0.30
	CRT2	-0.2	16.7	13.6	0.84	45.8	68.28	0.31
	CRT2	-0.3	16.2	13.2	0.90	47.4	64.38	0.31
	CRT2	-0.4	16.2	13.1	0.90	47.4	65.17	0.31
	CRT2	-0.5	16.2	13.1	0.91	47.6	65.66	0.31
	CRT2	-0.6	16.3	13.2	0.90	47.3	66.72	0.32
	CRT2	-0.7	16.6	13.5	0.86	46.1	67.73	0.31
	CRT2	-0.8	16.7	13.5	0.85	46.0	69.49	0.32
	CRT2	-0.9	16.5	13.3	0.88	46.8	69.22	0.32
	CRT2	-1	17.9	15.1	0.65	39.4	68.66	0.27
	CRT2	-1.1	17.2	14.2	0.76	43.0	68.08	0.29
	CRT2	-1.2	16.9	13.9	0.80	44.4	66.65	0.30
CNV	CNV1	-0.1	16.5	13.8	0.99	49.7	54.05	0.27
	CNV1	-0.2	17.2	13.8	1.00	49.9	68.70	0.34
	CNV1	-0.3	18.9	15.3	0.80	44.5	81.36	0.36
	CNV1	-0.4	17.4	14.1	0.95	48.6	66.73	0.32
	CNV1	-0.5	17.9	14.6	0.89	47.1	70.98	0.33
	CNV1	-0.6	16.9	13.3	1.06	51.5	68.46	0.35
	CNV1	-0.7	18.7	15.0	0.84	45.6	81.21	0.37
	CNV1	-0.8	16.9	13.1	1.09	52.2	72.19	0.38
	CNV1	-0.9	18.8	15.1	0.82	45.1	82.92	0.37
	CNV1	-1	18.9	15.2	0.81	44.9	83.53	0.37
	CNV1	-1.1	16.9	14.0	0.96	49.0	58.34	0.29
	CNV1	-1.2	16.1	13.3	1.07	51.8	54.86	0.28
	CNV1	-1.3	16.2	13.2	1.08	51.8	57.74	0.30
	CNV1	-1.4	15.1	11.9	1.31	56.7	55.97	0.32
	CNV1	-1.5	16.8	14.2	0.94	48.4	54.74	0.26
	CNV2	-0.1	17.9	14.9	0.84	45.7	65.98	0.30
	CNV2	-0.2	14.5	11.6	1.37	57.8	50.21	0.29
	CNV2	-0.3	16.6	13.7	1.01	50.2	58.02	0.29
	CNV2	-0.4	15.4	12.5	1.21	54.7	53.46	0.29
	CNV2	-0.5	14.4	11.4	1.41	58.6	50.60	0.30
	CNV2	-0.6	15.8	12.8	1.15	53.6	56.12	0.30
	CNV2	-0.7	16.3	13.5	1.04	50.9	55.96	0.28
	CNV2	-0.8	16.4	13.5	1.04	51.0	58.23	0.30
	CNV2	-0.9	16.6	14.0	0.97	49.3	54.40	0.27
	CNV2	-1	17.3	14.7	0.87	46.4	55.27	0.26
	CNV2	-1.1	17.0	14.6	0.89	47.0	50.55	0.24
	CNV2	-1.2	16.8	14.2	0.94	48.4	54.97	0.27
	CNV2	-1.3	17.2	15.0	0.83	45.5	48.12	0.22

	CNV2	-1.4	17.5	15.4	0.79	44.0	48.58	0.21
	CNV2	-1.5	17.1	14.7	0.87	46.5	52.15	0.24
BPR	BPR1	-0.1	15.8	14.5	0.89	47.2	27.61	0.13
	BPR1	-0.2	15.5	13.0	1.11	52.7	46.87	0.25
	BPR1	-0.3	16.9	14.2	0.93	48.2	56.11	0.27
	BPR1	-0.4	16.0	13.2	1.08	51.8	52.83	0.27
	BPR1	-0.5	15.0	12.6	1.19	54.3	44.23	0.24
	BPR1	-0.6	14.7	12.1	1.28	56.1	46.59	0.26
	BPR1	-0.7	16.5	13.6	1.02	50.5	56.75	0.29
	BPR1	-0.8	18.6	15.2	0.81	44.7	75.63	0.34
	BPR1	-0.9	18.7	15.3	0.80	44.4	77.82	0.35
	BPR1	-1	18.9	15.4	0.79	44.0	79.72	0.35
	BPR1	-1.1	19.2	15.7	0.76	43.0	82.92	0.36
	BPR2	-0.1	15.1	12.6	1.18	54.2	45.72	0.25
	BPR2	-0.2	15.0	12.6	1.19	54.3	45.33	0.25
	BPR2	-0.3	15.2	12.7	1.17	53.9	47.56	0.26
	BPR2	-0.4	14.9	13.6	1.03	50.7	26.53	0.13
	BPR2	-0.5	18.6	16.1	0.71	41.4	60.90	0.25
	BPR2	-0.6	14.0	11.5	1.40	58.4	44.39	0.26
	BPR2	-0.8	15.3	12.6	1.19	54.3	50.23	0.27

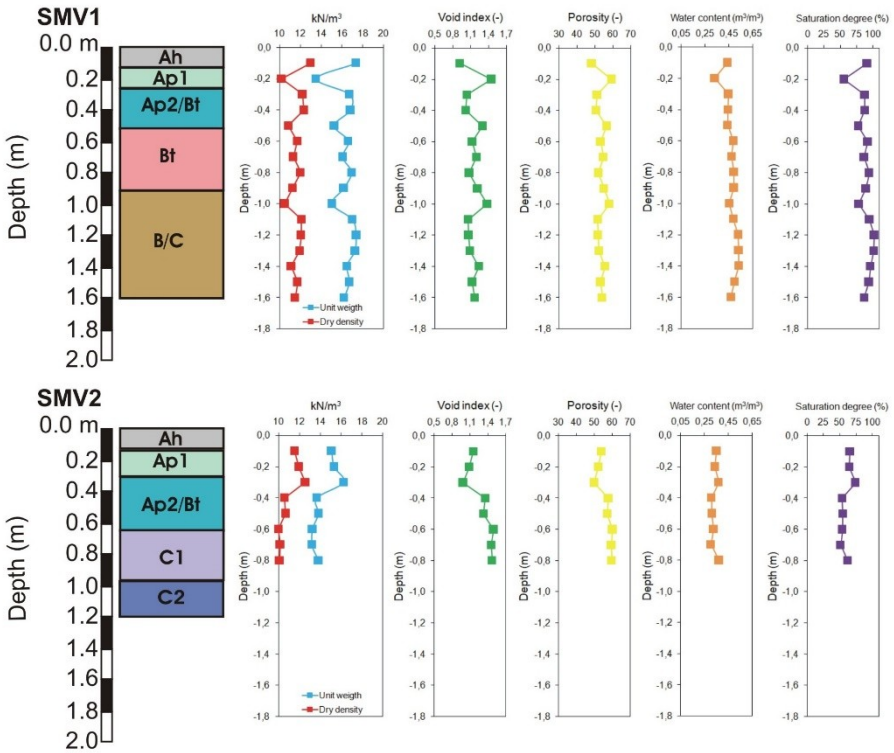

Fig. 39 Trends in depth of the volumetric features (unit weight, dry density, void index, porosity, water content, saturation degree) for the soils of SMV demo farm.

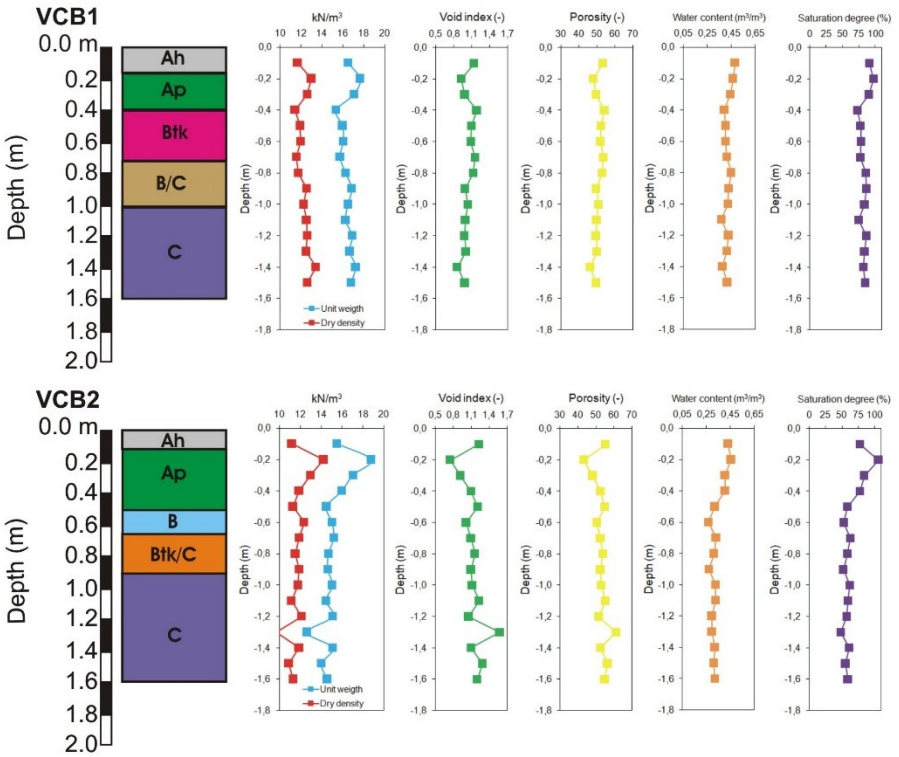

Fig. 40 Trends in depth of the volumetric features (unit weight, dry density, void index, porosity, water content, saturation degree) for the soils of VCB demo farm.

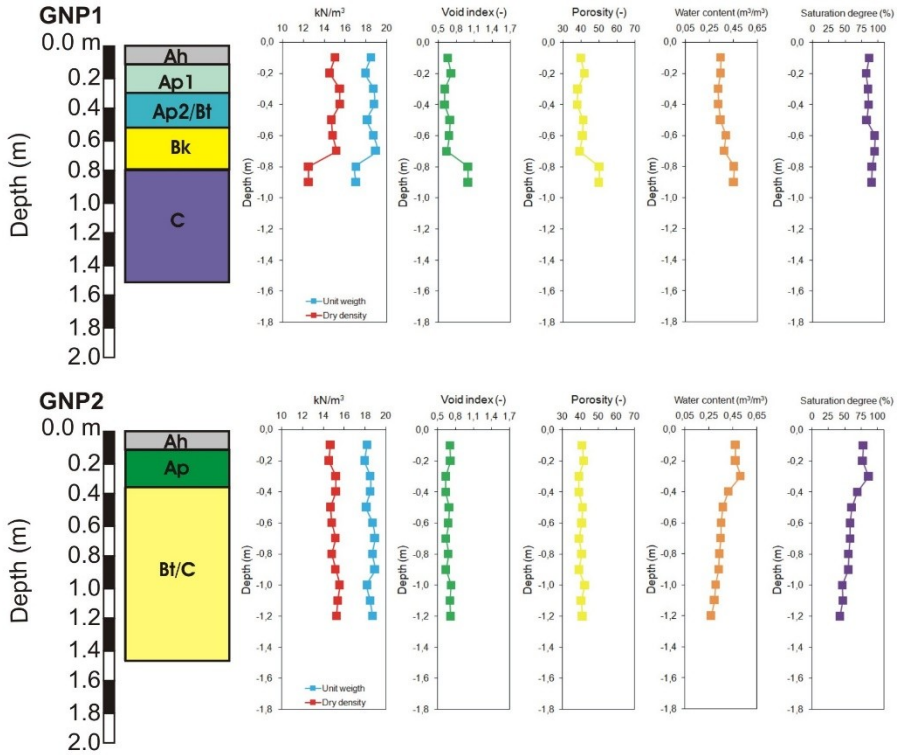

Fig. 41 Trends in depth of the volumetric features (unit weight, dry density, void index, porosity, water content, saturation degree) for the soils of GNP demo farm.

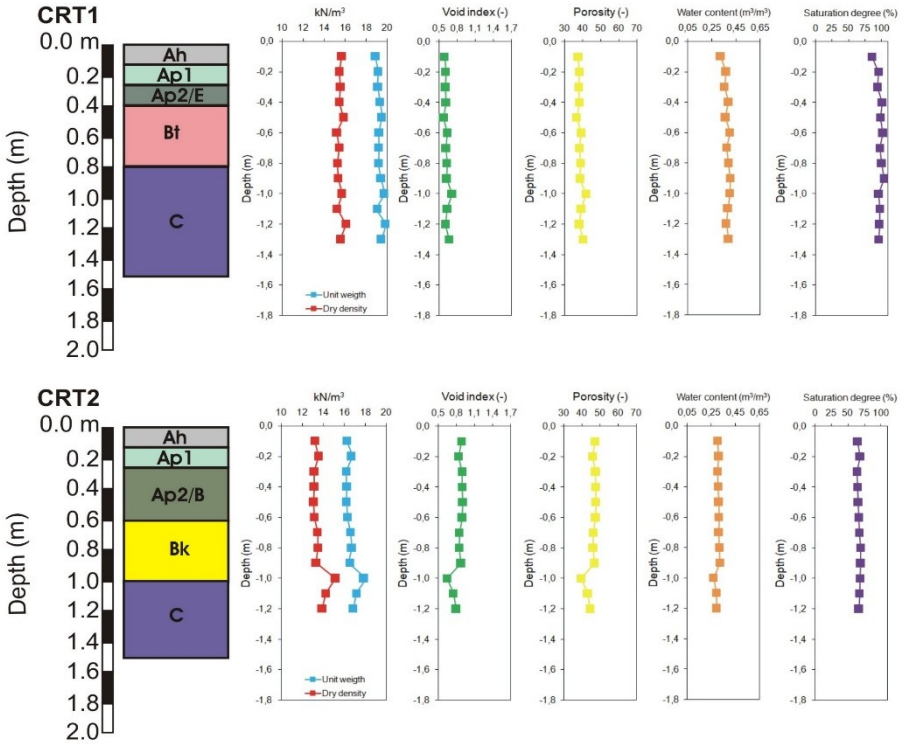

Fig. 42 Trends in depth of the volumetric features (unit weight, dry density, void index, porosity, water content, saturation degree) for the soils of CRT demo farm.

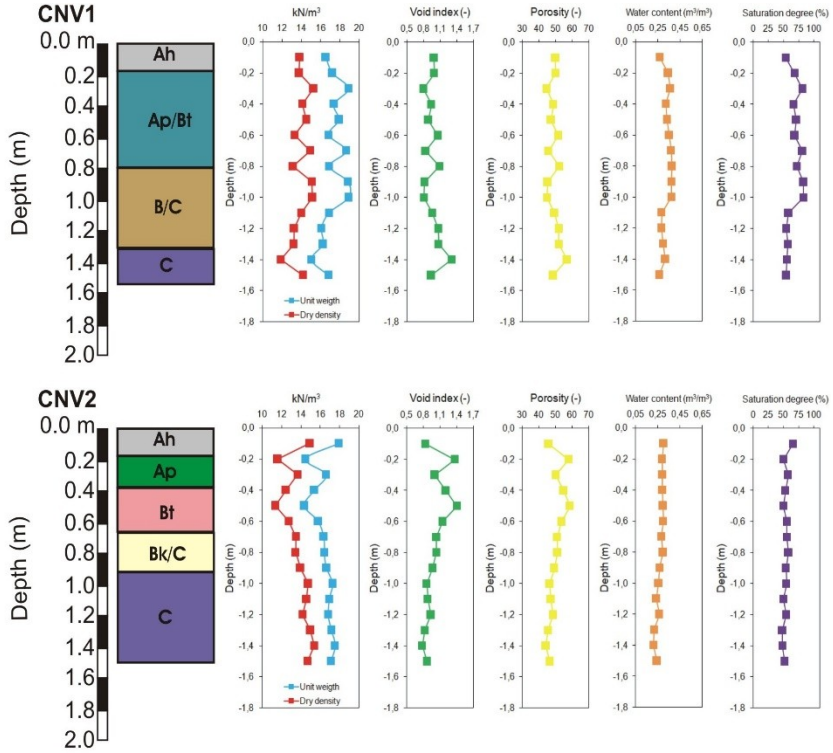

Fig. 43 Trends in depth of the volumetric features (unit weight, dry density, void index, porosity, water content, saturation degree) for the soils of CNV demo farm.

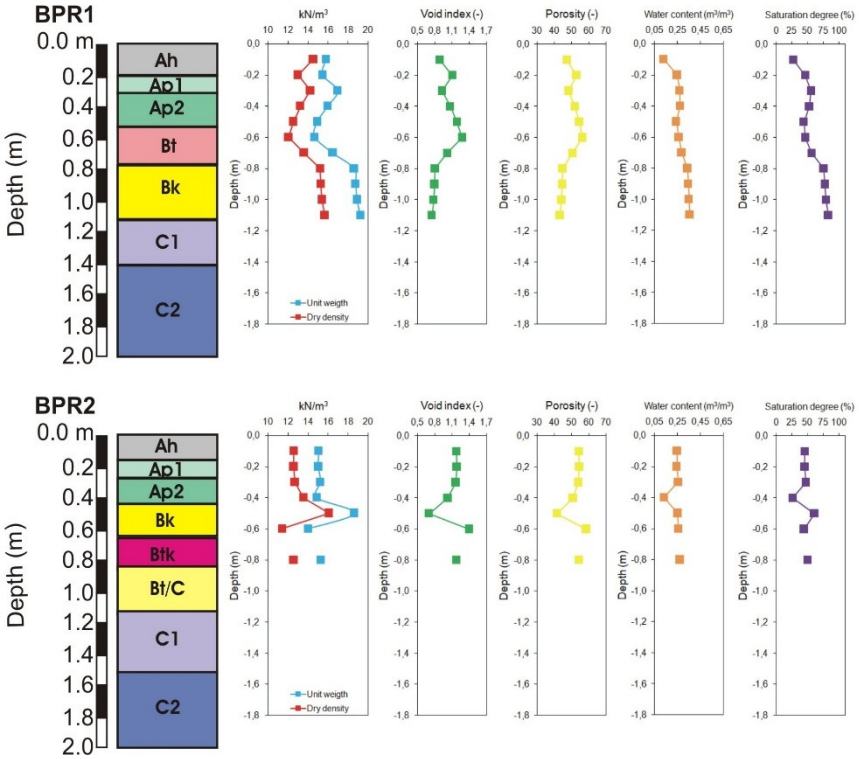

Fig. 44 Trends in depth of the volumetric features (unit weight, dry density, void index, porosity, water content, saturation degree) for the soils of BPR demo farm.

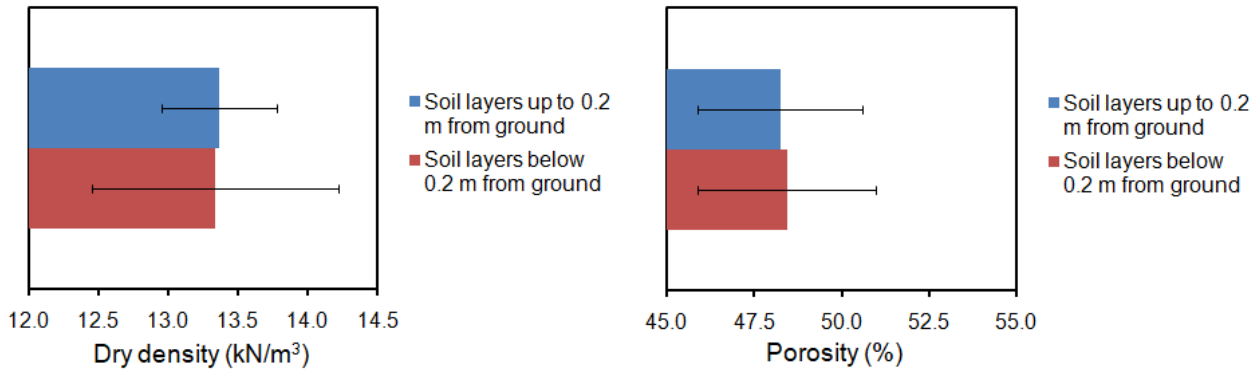

Fig. 45 Mean and standard error of dry density and porosity for the soils of the different demo farms, considering the measures in the first 0.2 m from ground level and the measures in the layers below this depth.

Soil hydrological features

The soils of each demo farm were characterized in terms of hydrological properties, measuring the water retention curve (WRC) parameters.
A representative WRC was measured for the soil of each demo farm, for a total number of 8 samples. WRCs were reconstructed through laboratory test, using an evaporimetric technique (Hyprop, Meter, Munich, Germany) on undisturbed samples collected below the most superficial layers. Measured WRC pairs were then fitted through Van Genuchten's (1980) model, in order to retrieve the soil hydrological properties of each tested soil: saturated water content (θ_s), residual water content (θ_r), fitting parameters of WRC equation (α and n).

The reconstructed WRCs are shown in Fig. 46, while the values of the parameters of Van Genuchten's fitting model of the WRCs are listed in Table x. Soil texture and porosity influenced the shape of the WRCs measured in each test-site. SMV and VCB demo farms, characterized by more porous soils, presents higher values of θ_s than the other demo-farms (0.48-0.57 m^3/m^3 respect to 0.40-0.46 m^3/m^3 for the other demo farms). Instead, θ_r values are similar for all the reconstructed WRCs (0.01-0.05 m^3/m^3). The fitting parameters of Van Genuchten's model allow to represent the retention properties of the tested soils. n parameter varies in a narrow range (1.25-1.53), while bigger differences are measured for α parameter. According to the values of this parameter, the soils of SMV, VCB and CNV are characterized by a higher capacity of water retention, as testified by values of αlower than 0.01 kPa (0.002-0.004 kPa). Instead, the soils of the other demo farms are characterized by a lower water retention capacity and by a higher ability to let water infiltrate in the soil profile, as testified by values of αhigher than 0.01 kPa (0.010-0.020 kPa). According to these results, SMV soils are the ones characterized by the highest water retention, while GNP soils are the ones which have the lowest water retention properties.

Table 17. Van Genuchten's (1980) model parameters of the WRCs reconstructed for the soils of the different demo farms. θ_s) saturated water content, θ_r) residual water content, α and n) fitting parameters of WRC equation.

Demo farm	Soil profile	Sampling depth (m)	θ_s (m^3/m^3)	θ_r (m^3/m^3)	α (kPa^{-1})	n (-)
SMV	SMV2	-0.2	0.57	0.05	0.002	1.25
VCB	VCB2	-0.3	0.48	0.02	0.003	1.25
GNP	GNP1	-0.5	0.42	0.01	0.010	1.35
GNP	GNP1	-0.7	0.40	0.01	0.020	1.38
CRT	CRT1	-0.5	0.45	0.01	0.012	1.45
CRT	CRT2	-0.6	0.46	0.01	0.015	1.38
CNV	CNV2	-0.5	0.45	0.03	0.004	1.25
BPR	BPR2	-0.5	0.43	0.01	0.012	1.53

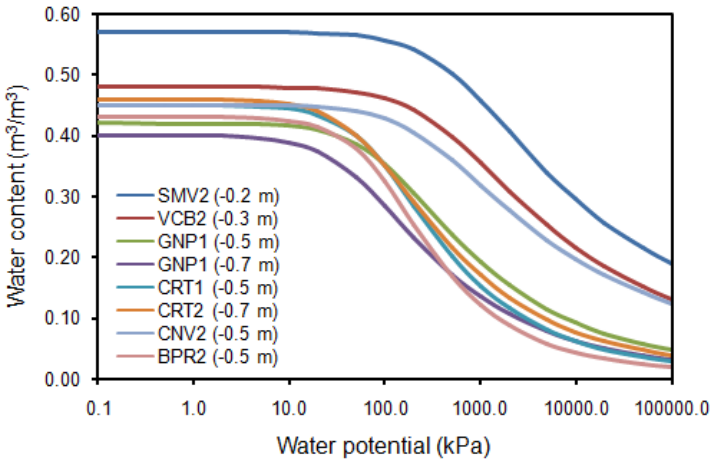

Fig. 46 Measured water retention curves (WRCs) of the soils of the different demo farms.

Laboratory analysis of soil physical and chemical characteristics

Subsequently each soil layers were fully characterised from a chemical point of view thought laboratory tests.
The following parameters were analysed in laboratory:

- pH
- Electric conductivity using 1:5 solution [dS.m-1]
- Cation exchange capacity [meq/100 g]

- Excangable calcium [meq/100 g]
- Exchangeable magnesium [meq/100 g]
- Exchangeable potassium [meq/100 g]
- Excangable sodium [meq/100 g]
- C/N ratio
- Total Nitrogen [g/kg]
- Active carbonate [g/kg]
- Total carbon [g/kg]
- Organic matter [g/kg]
- Assimiliable phosphorus (Olsen method) [mg/kg P]
- Total Base saturation TBS%

The parameters were plotted in value-depth diagramms as reported below (Fig. 47 to Fig. 58)

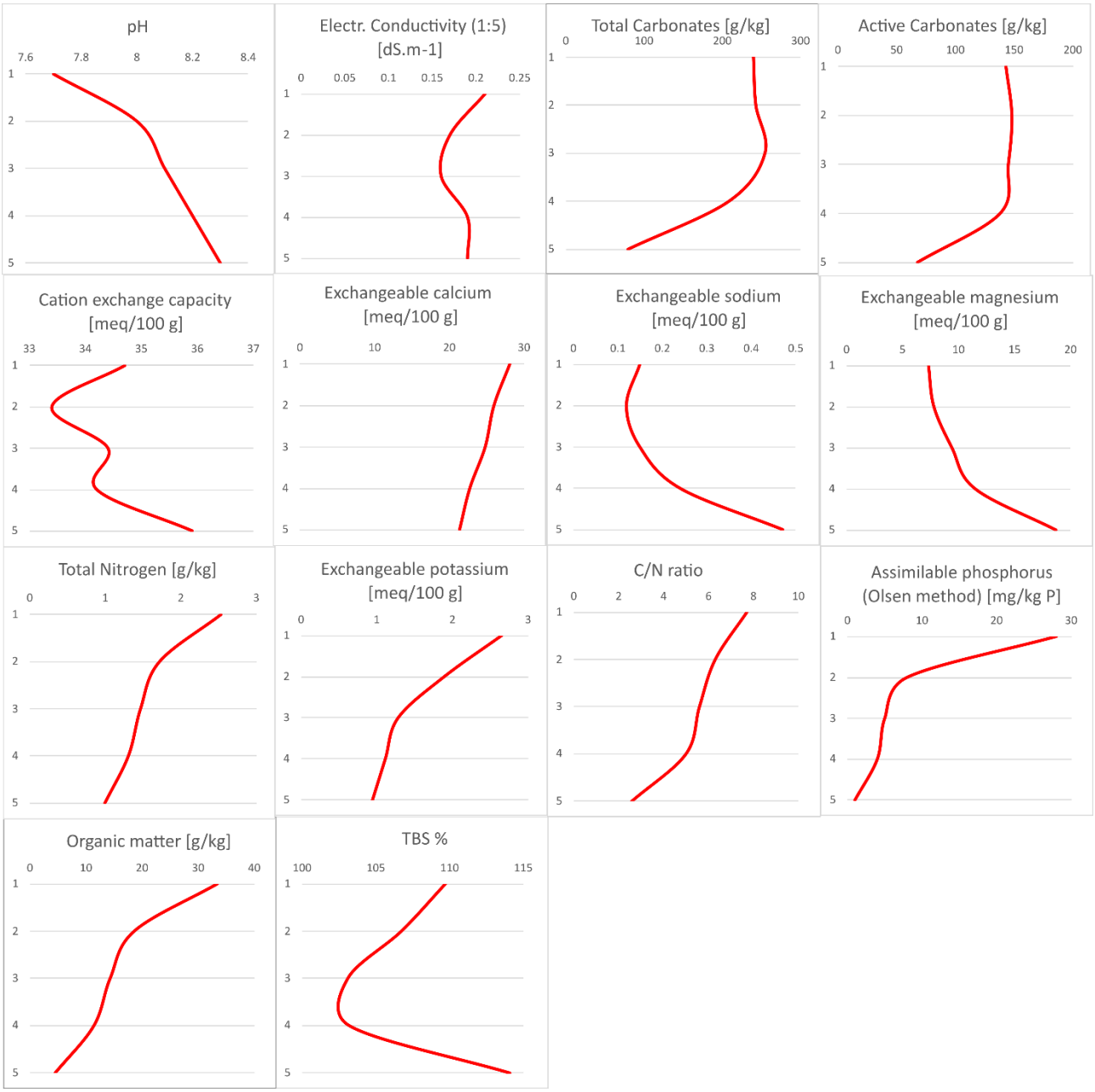

Fig. 47 Chemical parameters of SMV1. X axis represent soil id, Y axis represents the parameter value.

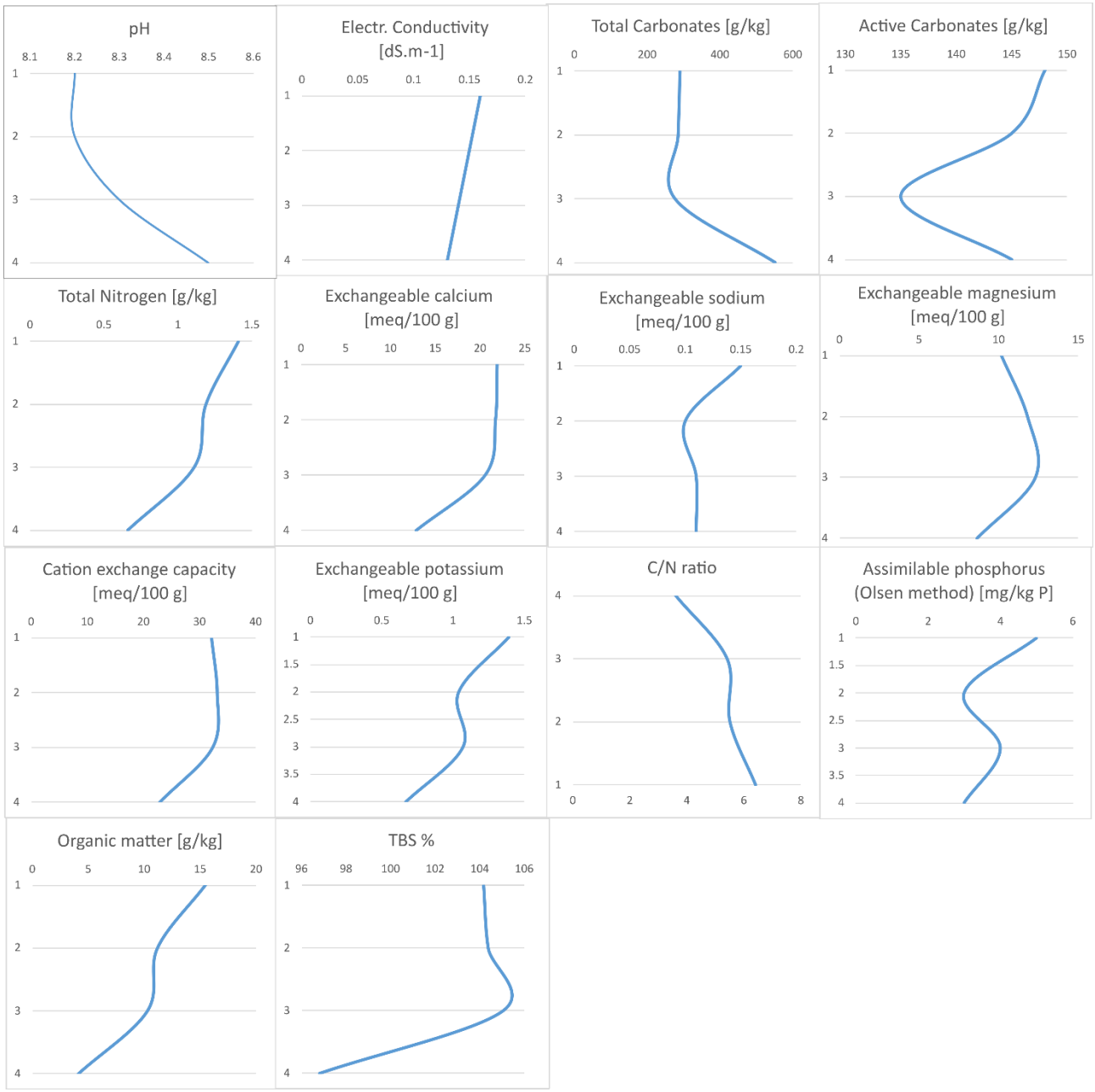

Fig. 48 Chemical parameters of SMV2. X axis represent parameter value Y axis represents the depth according to the horizon ID.

.

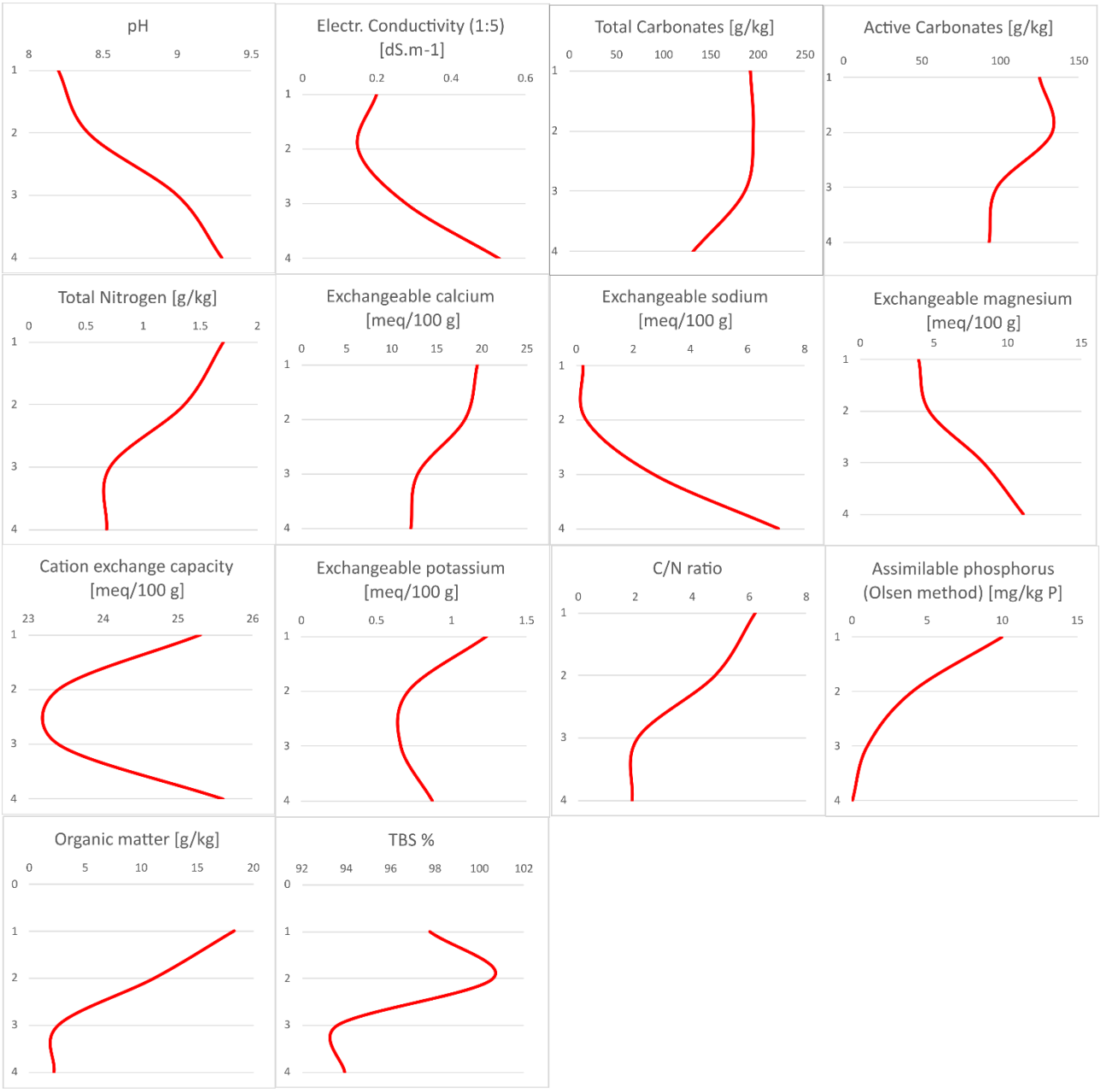

Fig. 49 Chemical parameters of CNV1. X asis represent parameters of CNV1. Y axis represent the soil depth according to the horizon ID.

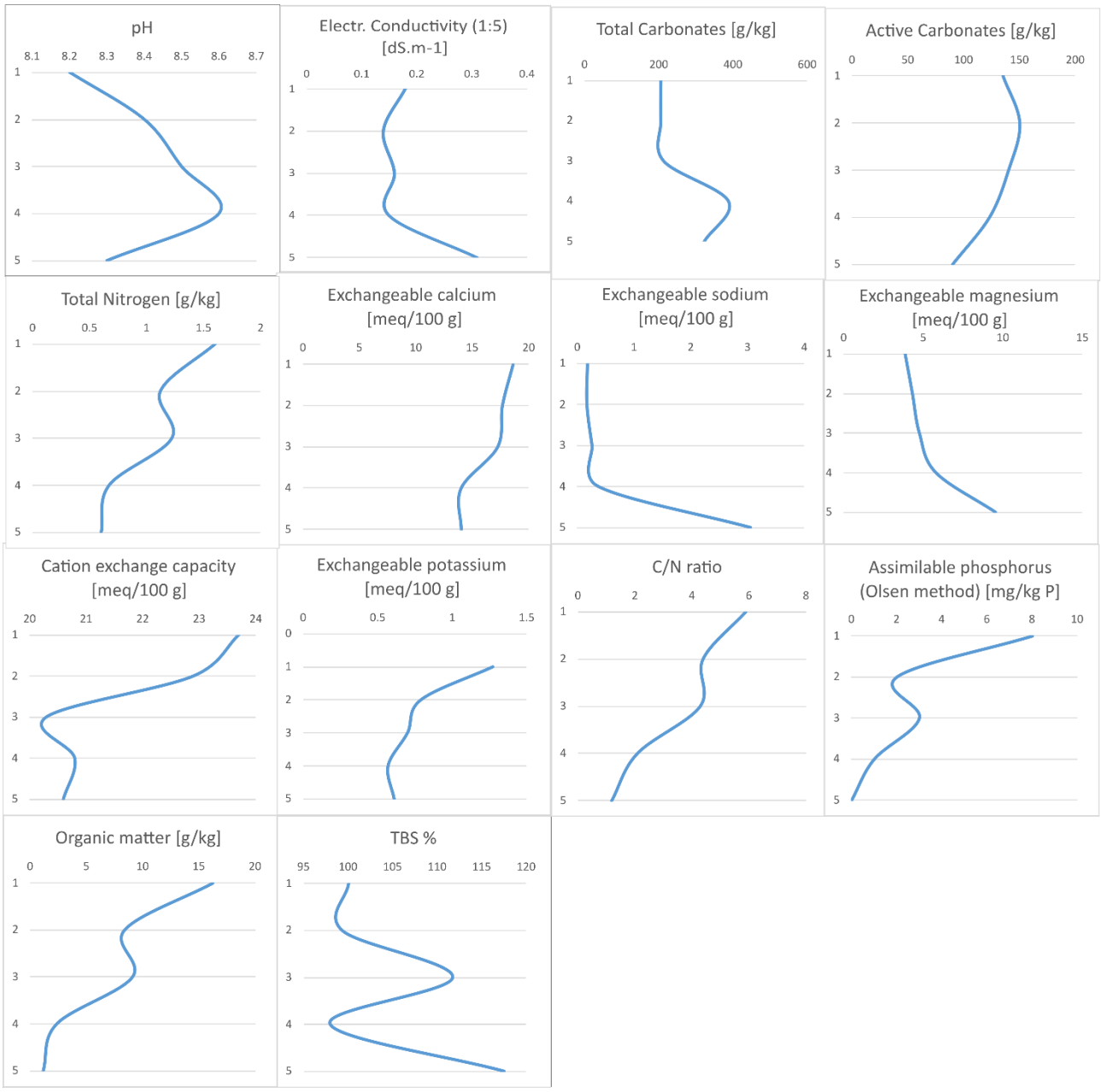

Fig. 50 Chemical parameters of CNV2. X asis represent soil id, Y axis represents the parameter value.

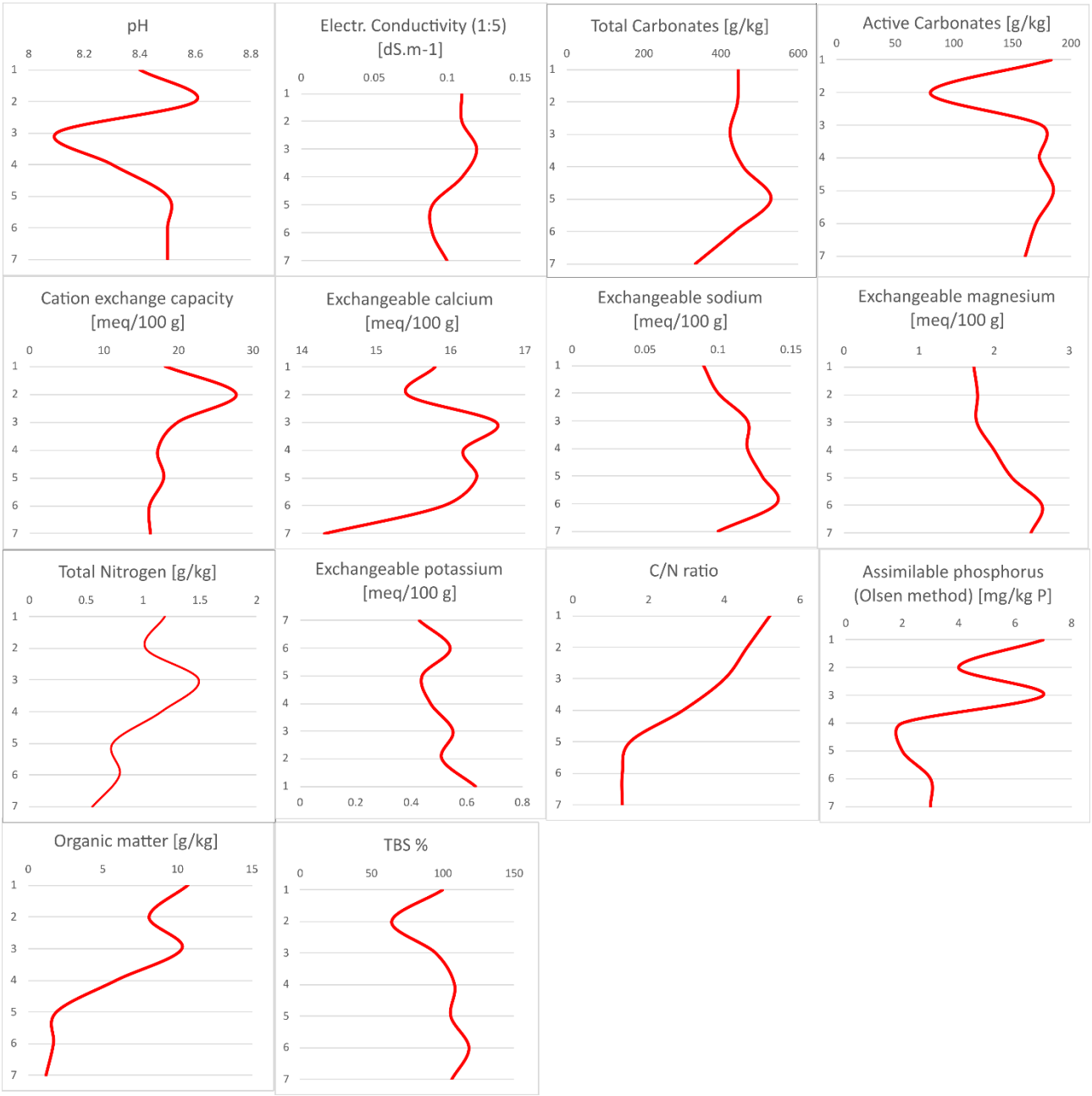

Fig.51 Chemical parameters of BPR1. X asis represent soil id, Y axis represents the parameter value.

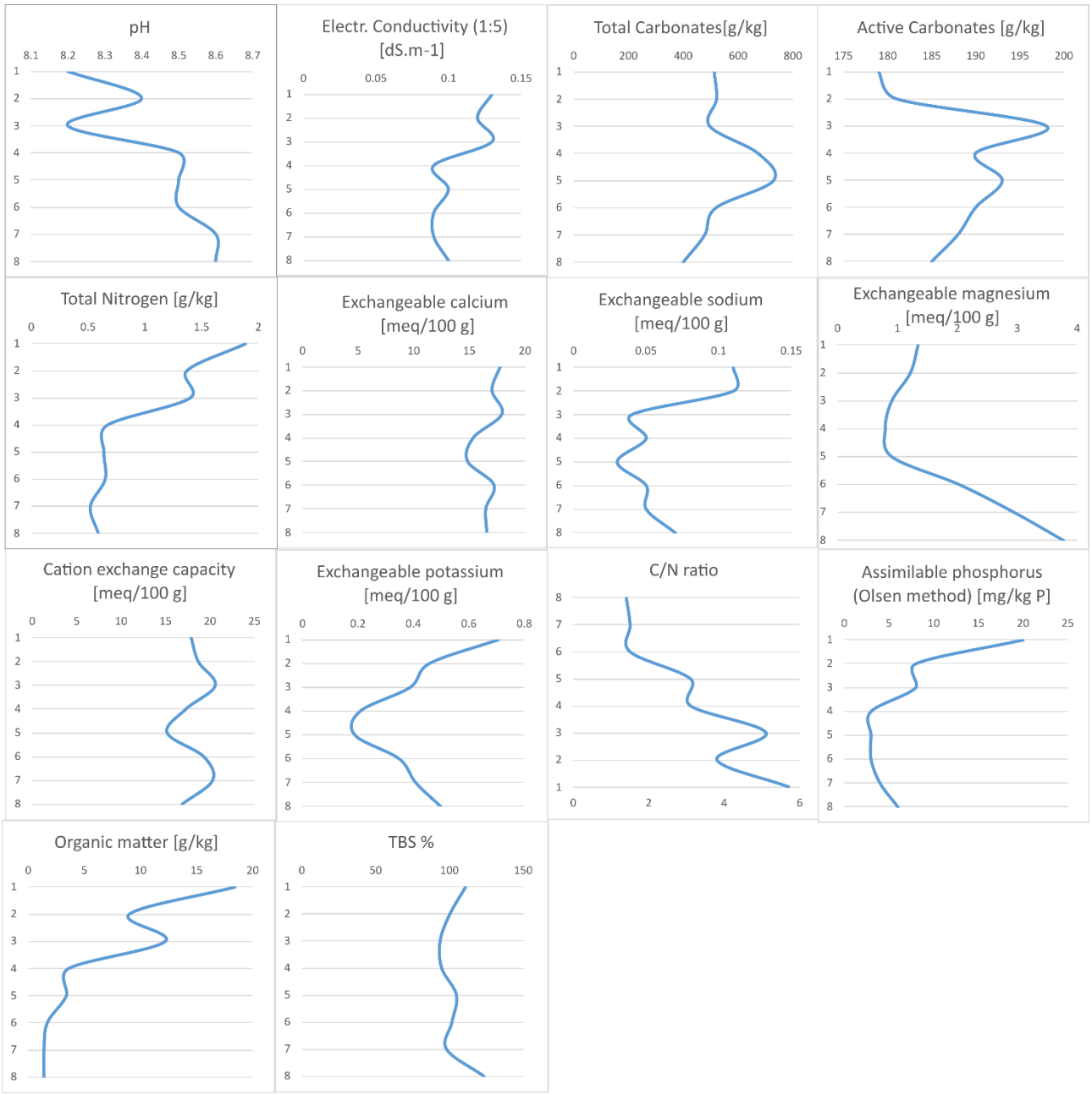

Fig.52 Chemical parameters of BPR2. X asis represent soil id, Y axis represents the parameter value.

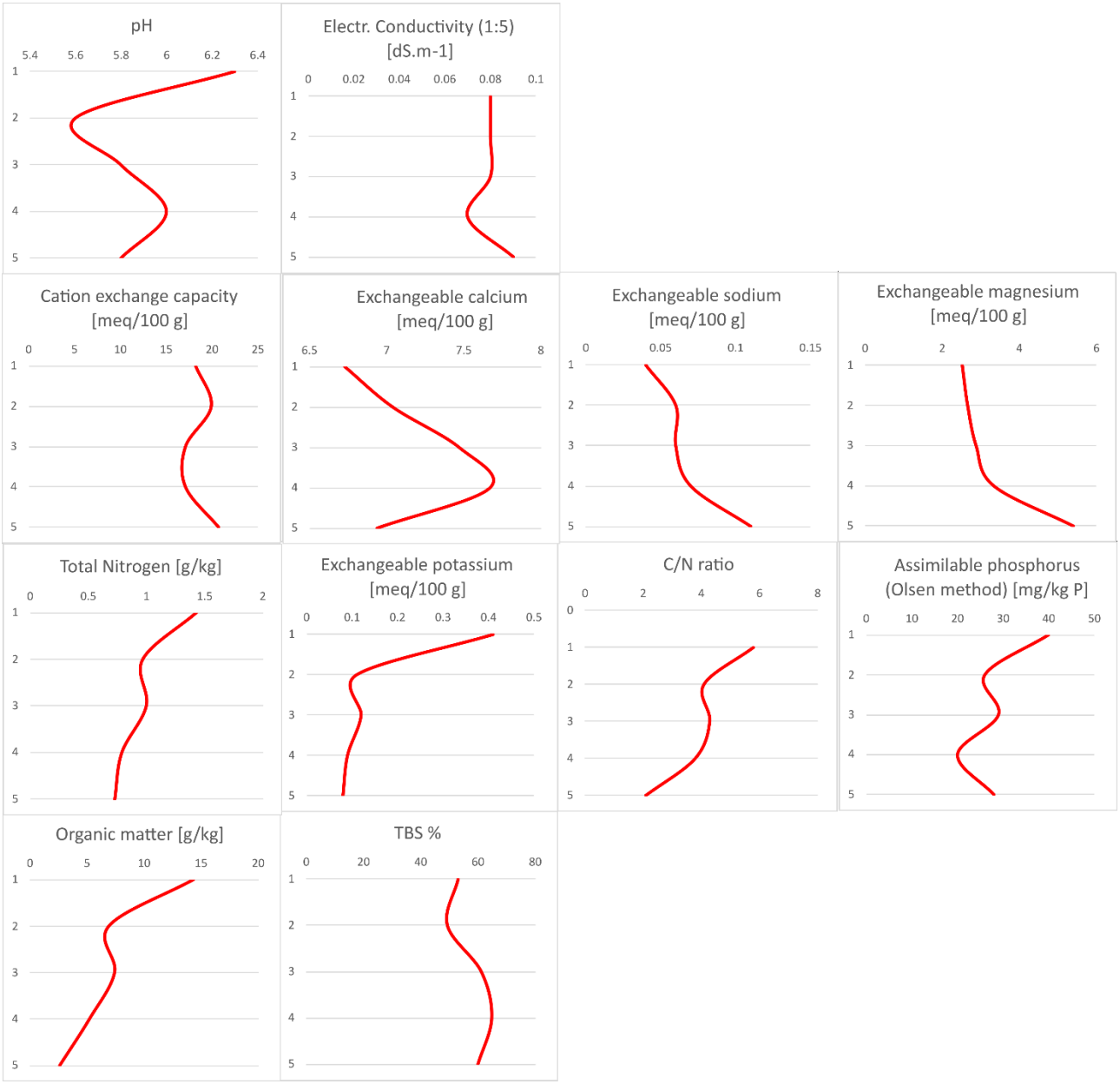

Fig. 53 Chemical parameters of CRT1. X asis represent soil id, Y axis represents the parameter value.

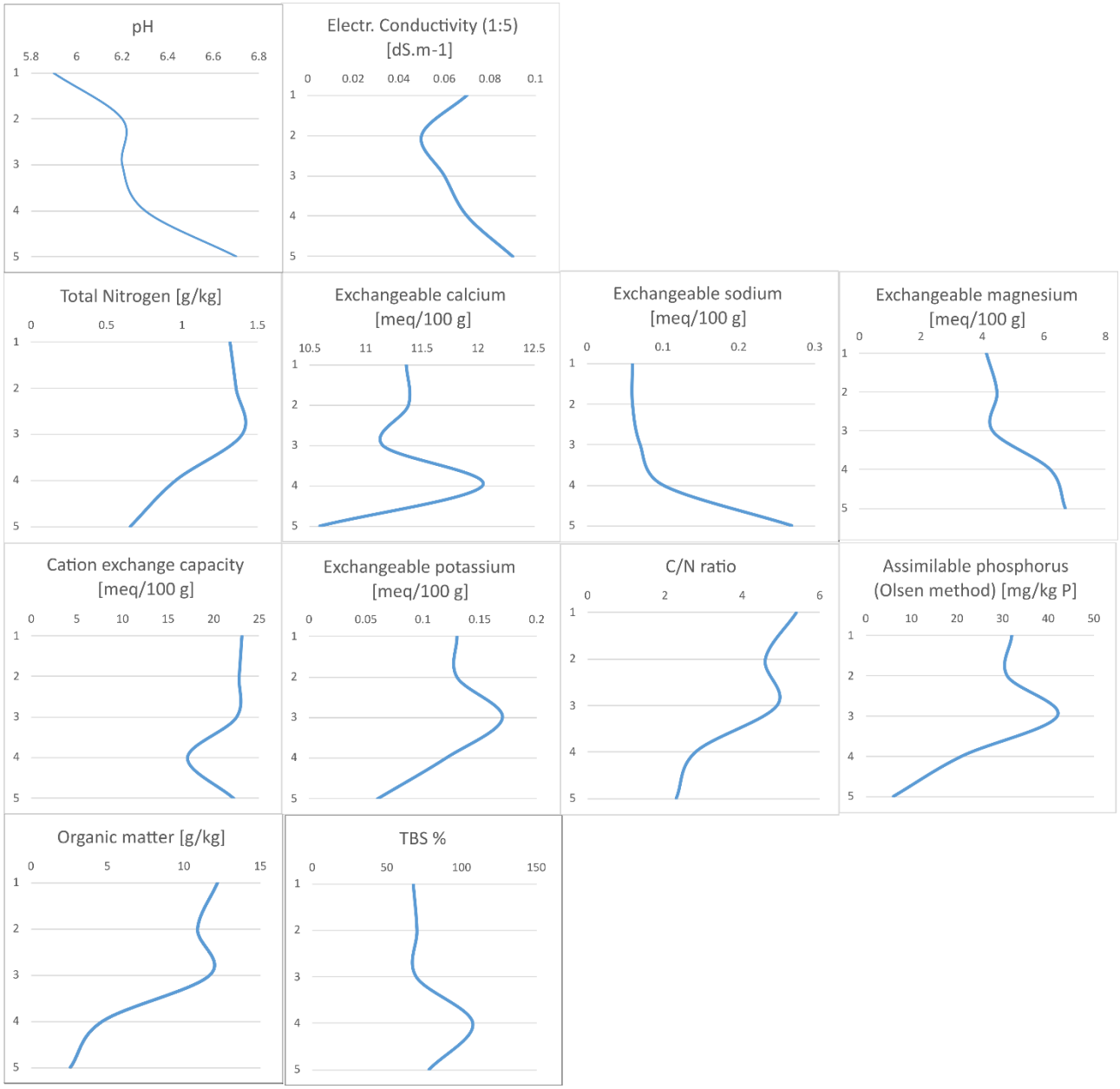

Fig. 54 Chemical parameters of CRT2. X asis represent soil id, Y axis represents the parameter value.

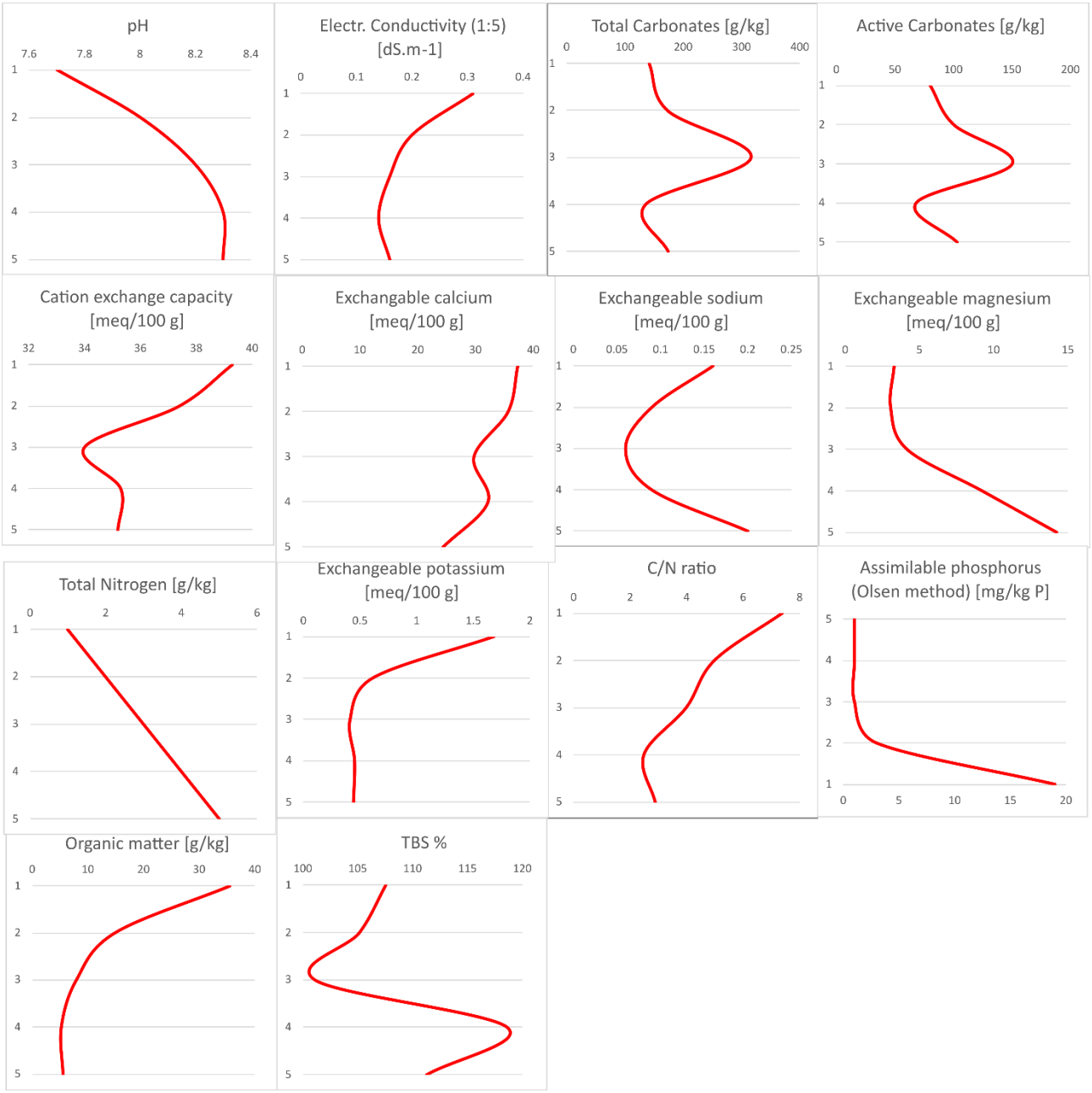

Fig. 55 Chemical parameters of VCB1. X asis represent soil id, Y axis represents the parameter value.

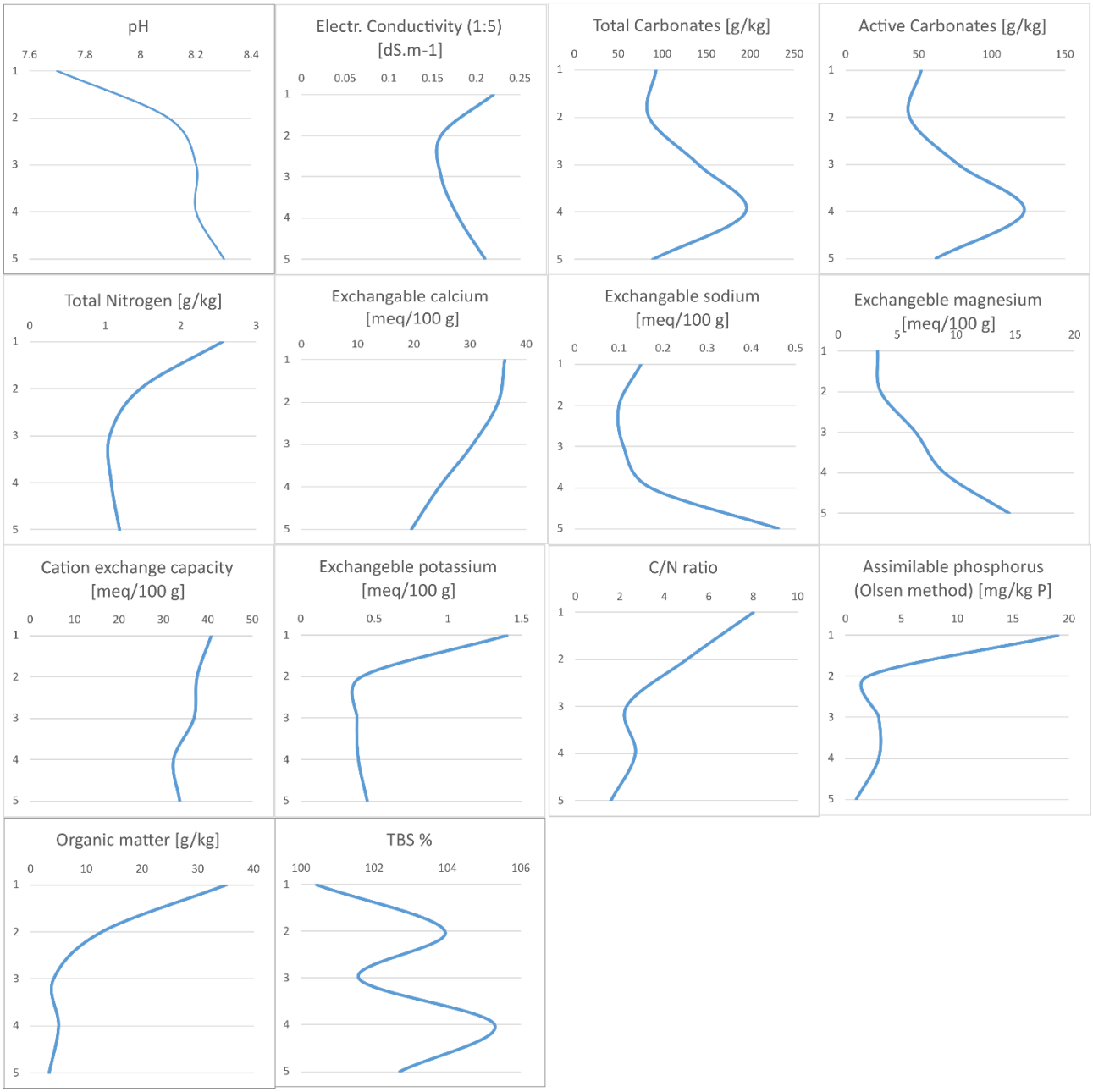

Fig. 56 Chemical parameters of VCB2. X asis represent soil id, Y axis represents the parameter value.

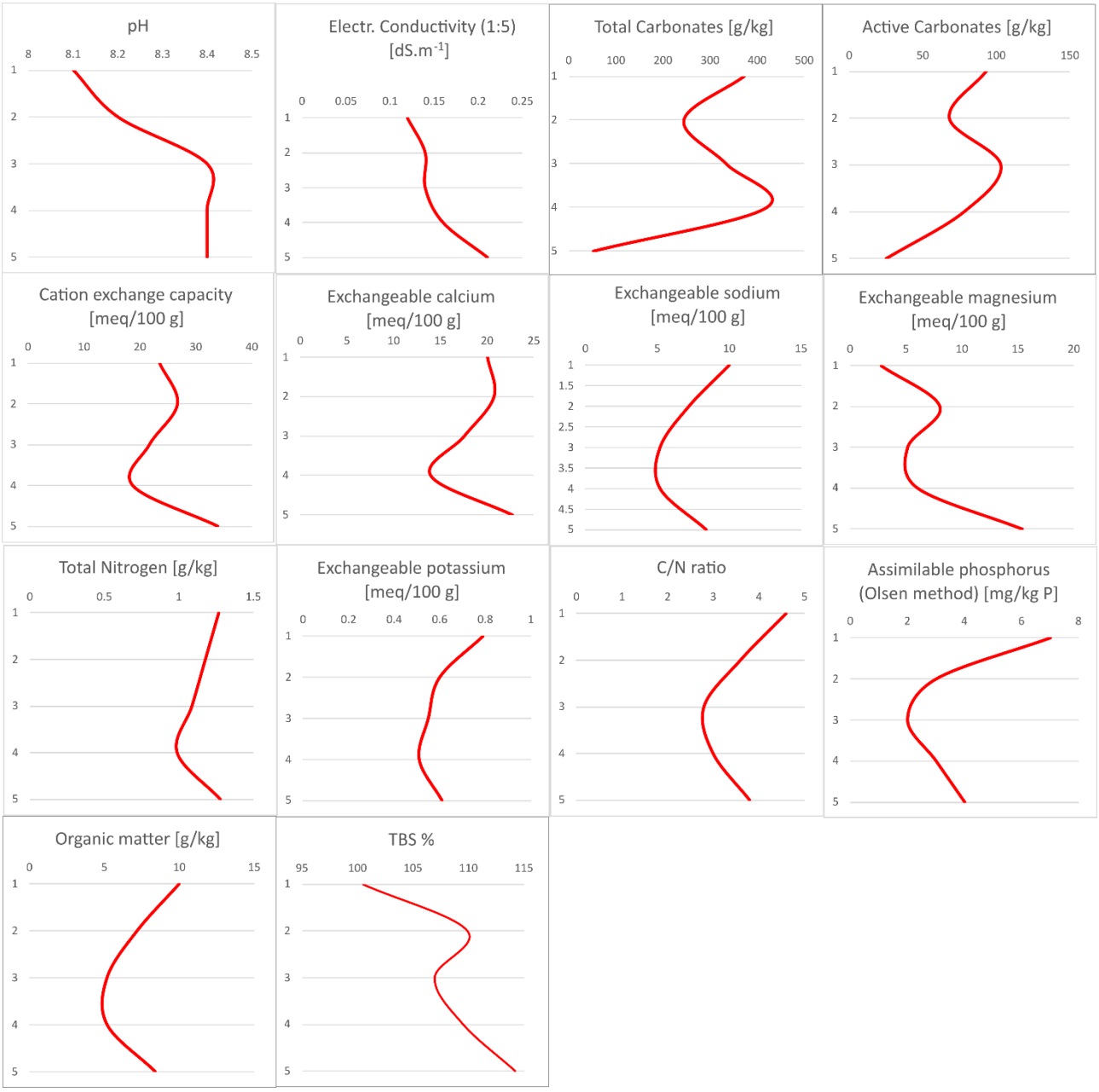

Fig. 57 Chemical parameters of GNP1. X asis represent soil id, Y axis represents the parameter value.

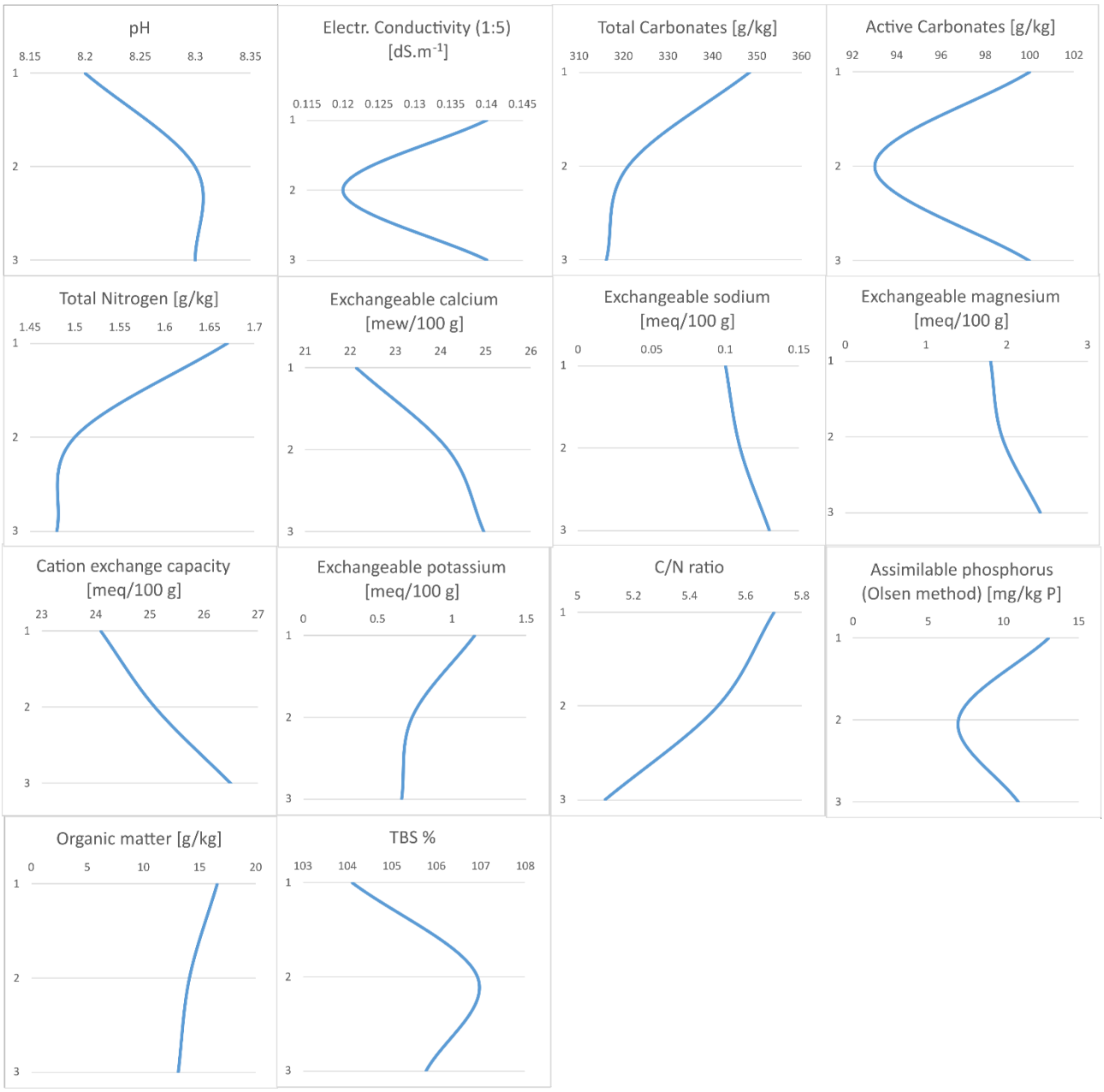

Fig. 58 Chemical parameters of GNP2. X asis represent soil id, Y axis represents the parameter value.

Field measurements of hydraulic conductivity

The purpose of this study is to understand the hydraulic conductivity of both topsoil and subsoil in the demonstrative vineyards. In each field the K-Sat measurements were conducted using a compact constant head permeameter (Amoozemeter; /Amoozegar, 1989) (Fig. 59) in the period July 2021. The saturated hydraulic conductivity on the topsoil (0-20cm) and subsequently in the subsoil (20-40) was measured in the interrow for each land use type characterizing the vineyard. The results characterize the hydraulic conductivity in the field and these measurements will be further used as input data in the hydrological modelling phase.

Fig. 59 Ksat measurements in the Demo-vineyards throught the Amoozemeter.

The results for SMV demo farm follow.

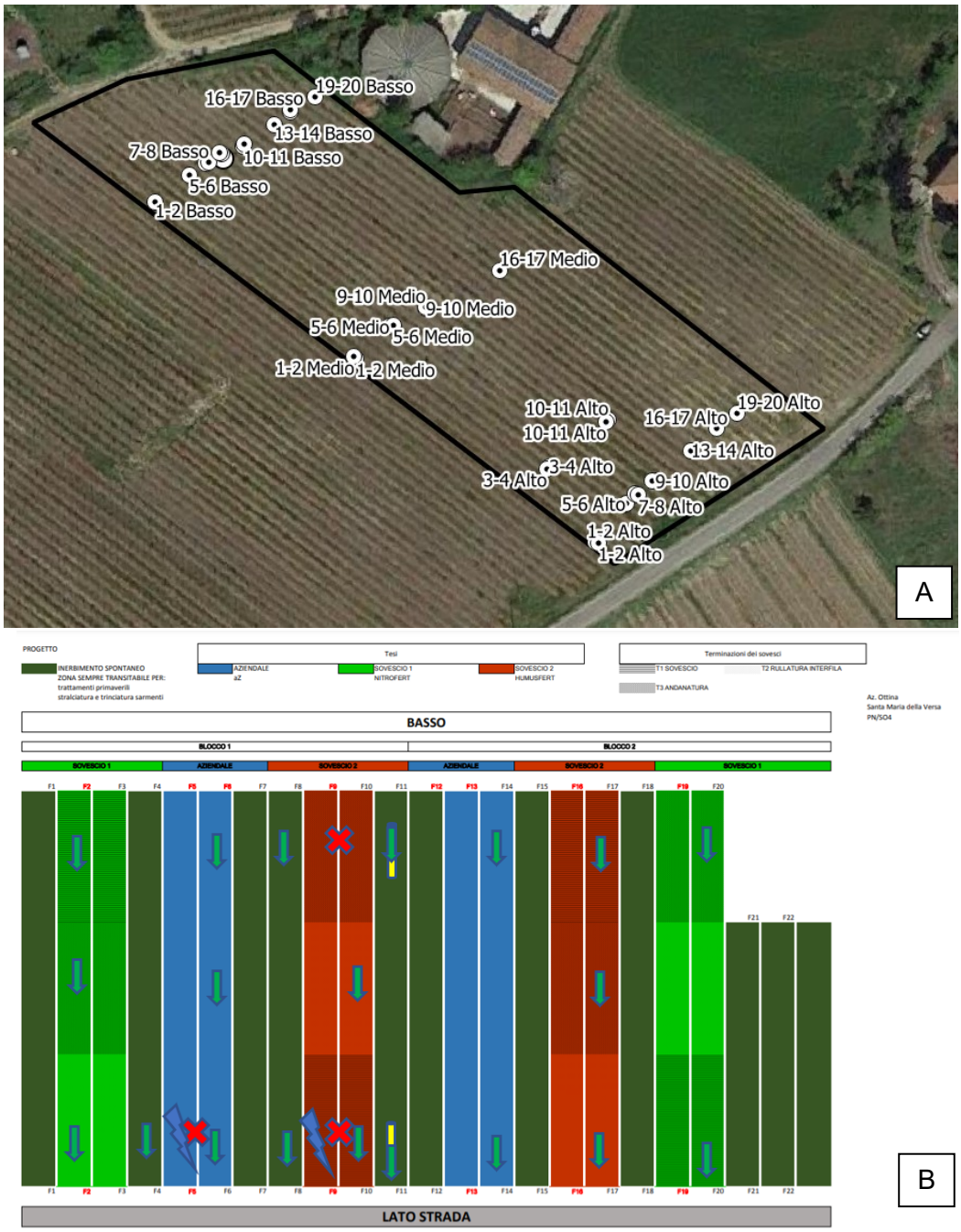

Fig. 60 A) Location of Ksat measurements in SMV and b) the green arrow represents the location of Ksat measurement reported on each land use treatment.

Table 18 Topsoil and subsoil Ksat values in SMV.

SMV	KSat [cm/h] Topsoil (0-20)	KSat [cm/h] Subsoil (20-40)
1-2 Basso	10.48	0.31
1-2 Medio	83.16	0.10
1-2 Alto	0.37	0.71

3-4 Alto	2.21	4.91
5-6 Basso	-	0.05
5-6 Medio	1.33	0.11
5-6 Alto	12.10	0.19
7-8 Basso	3.02	0.13
7-8 Alto	-	11.97
9-10 Basso	26.61	0.029
9-10 Medio	13.3	0.02
9-10 Alto	3.8	0.01
10-11 Basso	59.8	0.05
10-11 Alto	16.63	0.06
13-14 Basso	-	16.6
13-14 Alto	-	0.01
16-17 Basso	99.7	0.69
16-17 Medio	-	0.04
16-17 Alto	-	0.42
19-20 Basso	-	8.68
19-20 Alto	3.67	0.88

The results for CNV demo farm follow.

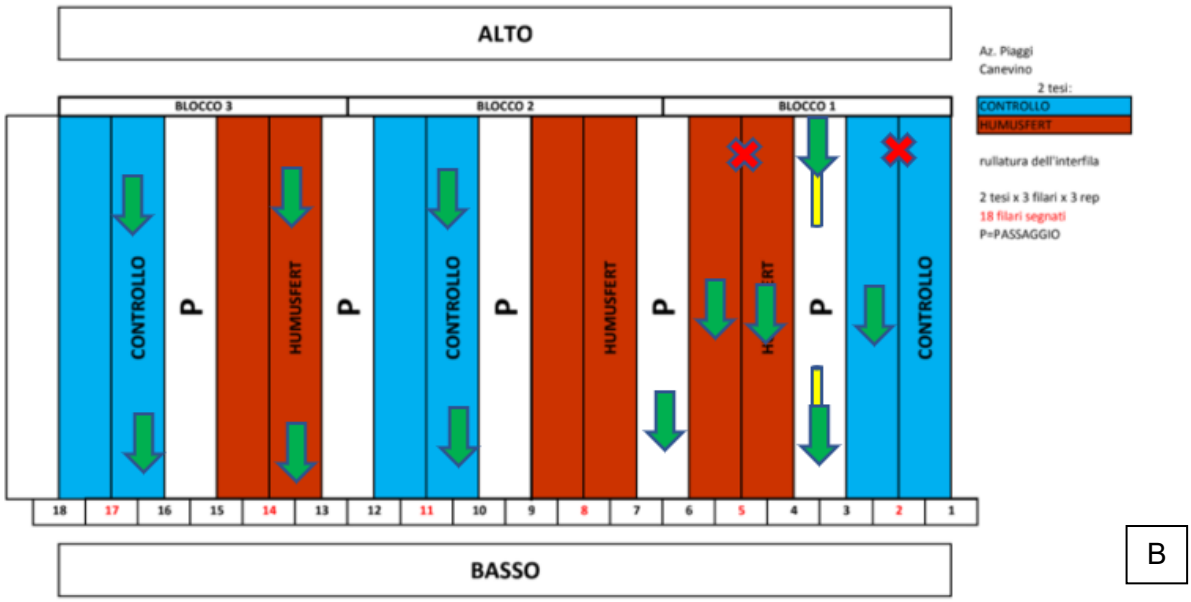

B

Fig. 61 A) Location of Ksat measurements in CNV and b) the green arrow represents the location of Ksat measurement reported on each land use treatment.

Table 19 Topsoil and subsoil Ksat values in CNV.

CNV	KSat [cm/h] Topsoil (0-20)	KSat [cm/h] Subsoil (20-40)
1-2 Stazione	1.64	2.53
3-4 Basso	2.78	1.64
3-4 Alto	0.97	1.92
4-5 Stazione	6.65	0.01
5-6 Stazione	8.31	0.28
6-7 Basso	5.06	0.29
10-11 Basso	0.23	0.11
10-11 Alto	0.04	0.03
13-14 Basso	13.30	0.15
13-14 Alto	0.31	13.97
16-17 Basso	2.53	2.21
16-17 Alto	2.21	0.93

In both SMV and CNV fields capillar soil craks were observed during the field measurements. In both fields soil cracks are persistent up to 50 cm on depth and affect Ksat measurements.

The results for CRT demo farm follow.

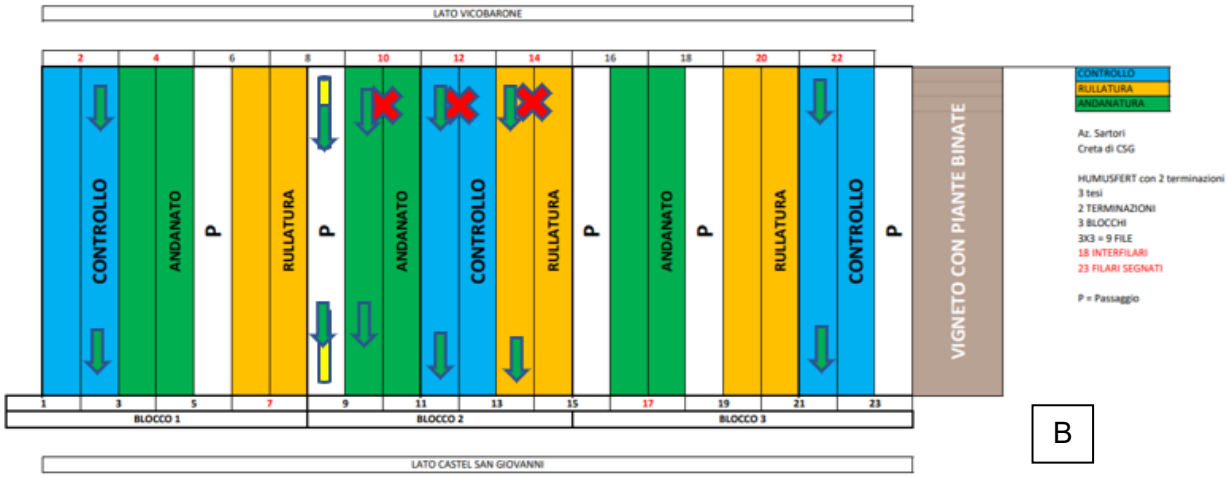

Fig. 62 A) Location of Ksat measurements in CRT and b) the green arrow represents the location of Ksat measurement reported on each land use treatment.

Table 20 Topsoil and subsoil Ksat values in CRT.

CRT	KSat [cm/h] Topsoil (0-20)	KSat [cm/h] Subsoil (20-40)
2-3 Basso	1.45	-

2-3 Alto	0.84	0.06
8-9 Basso	0.42	0.48
8-9 Alto	0.42	0.32
9-10 Basso	0.33	0.03
9-10 Alto	0.54	0.38
11-12 Basso	-	44
11-12 Alto	0.25	2.64
13-14 Basso	0.47	0.10
13-14 Alto	0.42	2.07
21-22 Basso	0.52	0.48
21-22 Alto	1.26	1.05

The results for BPR demo farm follow.

A

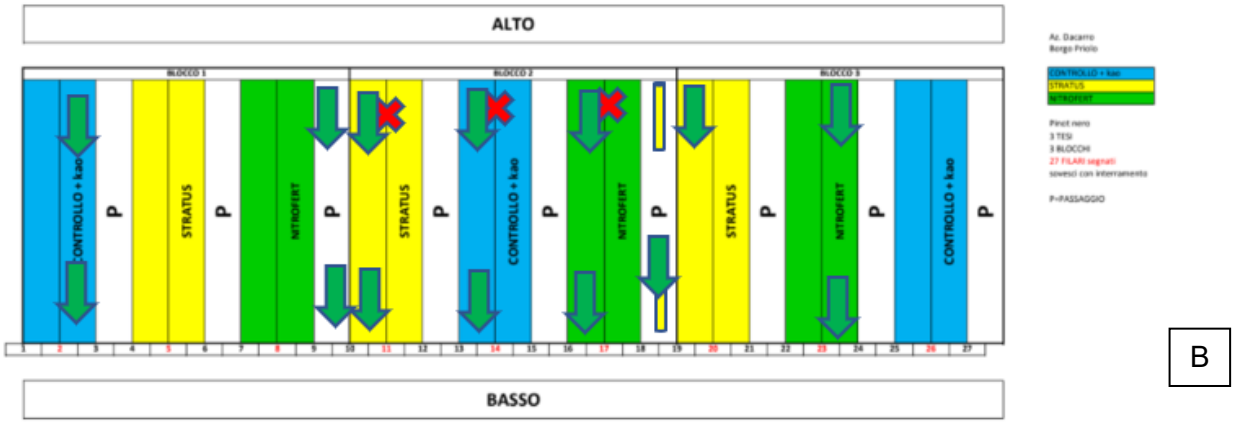

B

Fig. 63 A) Location of Ksat measurements in BPR and b) the green arrow represents the location of Ksat measurement reported on each land use treatment.

Table 21 Topsoil and subsoil Ksat values in BPR.

BPR	KSat [cm/h] Topsoil (0-20)	KSat [cm/h] Subsoil (20-40)
2-3 Basso	5.53	1.01
2-3 Alto	3.10	2.39
9-10 Basso	1.77	1.23
9-10 Alto	2.02	2.53
10-11 Basso	3.54	0.13
10-11 Alto	3.92	0.46
13-14 Basso	4.43	1.50
13-14 Alto	1.52	1.28
16-17 Basso	2.99	0.69
16-17 Alto	4.98	4.32
18-19 Basso	2.91	0.63
18-19 Alto	1.09	0.65
23-24 Basso	7.98	1.82
23-24 Alto	3.05	1.79

The results for VCB demo farm follow.

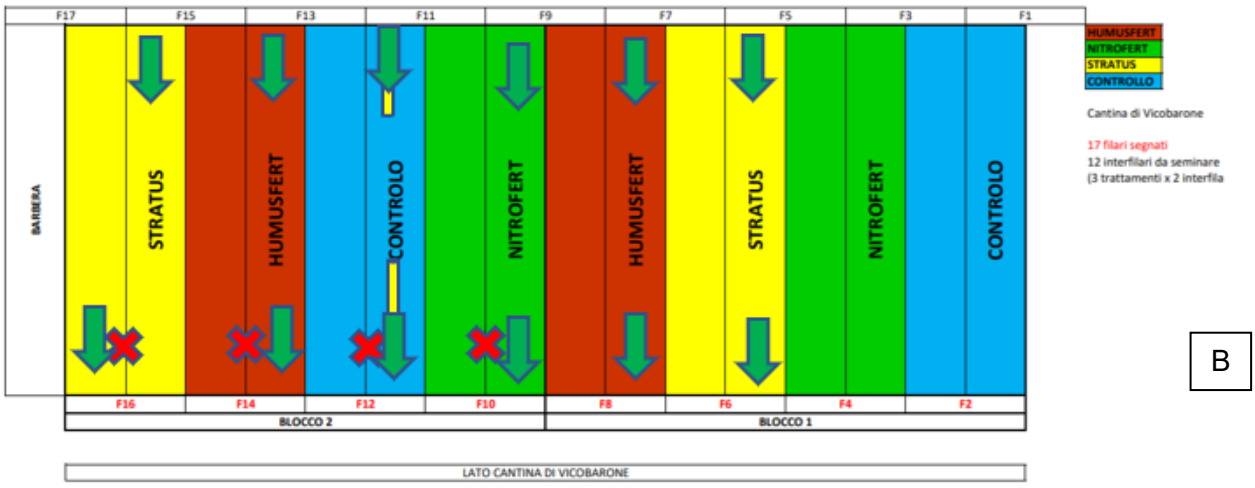

Fig. 64 A) Location of Ksat measurements in VCB and b) the green arrow represents the location of Ksat measurement reported on each land use treatment.

Table 22 Topsoil and subsoil Ksat values in VCB.

VCB	KSat [cm/h] Topsoil (0-20)	KSat [cm/h] Subsoil (20-40)
5-6 Basso	53.04	0.08
5-6 Alto	-	0.63

7-8 Basso	-	0.79
7-8 Alto	6.3	0.13
9-10 Basso	-	7.63
9-10 Alto	0.15	19.95
11-12 Basso	-	6.64
11-12 Alto	-	5.98
13-14 Basso	-	1.32
13-14 Alto	-	8.64
15-16 Basso	-	5.07
16-17 Alto	-	2.15

The results for GNP demo farm follow.

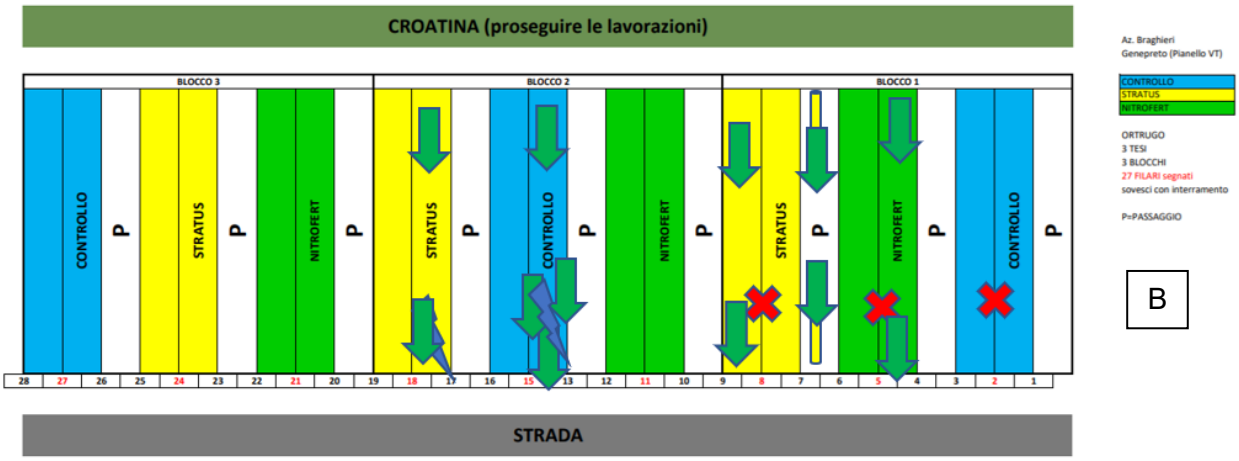

Fig. 65 A) Location of Ksat measurements in GNP and b) the green arrow represents the location of Ksat measurement reported on each land use treatment.

Table 23 Topsoil and subsoil Ksat values in GNP.

GNP	KSat [cm/h] Topsoil (0-20)	KSat [cm/h] Subsoil (20-40)
4-5 Basso	6.98	33.45
4-5 Alto	4.98	6.05
6-7 Basso	16.22	-
6-7 Alto	8.64	5.32
8-9 Basso	3.04	0.34
8-9 Alto	12.67	7.68
14-15 Basso	2.79	0.44
14-15 Alto	6.65	4.03
14-15 R.	5.32	2.03
14-15 R.P.	0.23	0
17-18 Basso	10.65	0.91
17-18 Alto	3.32	24.21

Installation and verification of the good functioning of integrated weather and hydrological monitoring stations

In each demo farm, a set of monitoring tools were installed to measure in time the trends of the main meteorological (rainfall, air temperature, air humidity, atmospheric pressure, wind speed and direction, solar radiation) and soil hydrological (soil water content, soil electrical conductivity, soil temperature) parameters. The aim of this monitoring is to evaluate the effect induced by different management on hydrological behaviors in the soil, in particular relating to the dynamics in soil water content in different seasons.
The monitoring stations were installed in the period April-May 2021. In each demo farm, the probes for the measure of the meteorological parameters were installed in correspondence of a station, which is connected by remote with different monitoring points of the soil hydrological parameters installed in the tested vineyard. The number of monitoring points in each demo farm is equal to the number of management types implemented in that demo farm (Table 24).
For each demo farm, the monitoring tool is composed in the following way:

- the meterological station (MeteoSense 4.0, Netsens, Sesto Fiorentino, Italy), composed by: a rain gauge (measure of rainfall amount), a thermo-igrometer (measure of air temperature and humidity, dew point and leaf wetness), a barometer (measure of atmospheric pressure), a radiometer (measure of solar radiation), an anemometer (measure of wind speed and direction). In correspondence of this station, an acquisition system and a receiving system are present to collect the data from the meteorological probes and from the connected monitoring probes of the hydrological parameters installed in soil;
- a set of monitoring points, installed in each management of each demo farm, constituted by a probe (Drill & Drop 90 cm, Sentek Sensor Technologies, Stepney, Australia) able to measure soil water content, soil temperature and soil salinity each 10 cm in depth, from 0.1 to 0.9 m from ground level. The accuracy of this probe for the water content measure is of 0.03%, while its range of measure is of 1-100%. For each monitoring point, a datalogger is present to store the data and to send them to the receiving system.

The monitoring data are available and can be downloaded by remote, through the web-cloud LiveData interface (Netsens, Sesto Fiorentino, Italy). The temporal resolution of the measure can be set equal to minutes or more. In this case, a 15-minutes temporal resolution of the measures was set. All the sensors are powered by a power supplì with a photovoltaic panel.
A flow chart of this monitoring system is provided in Fig. 66.

Table 24 Number of monitoring points of soil hydrological parameters and starting date of the monitoring in each demo farm.

Demo farm	Number of monitoring points of soil hydrological parameters	Starting date of the monitoring
SMV	4	2021/04/15
VCB	4	2021/05/07
GNP	3	2021/04/06
CRT	3	2021/04/06
CNV	2	2021/05/07
BPR	3	2021/05/13

The phases of the installation of a monitoring system in a demo farm for soil hydrological parameters are reported in Fig. 67. Monitoring points were installed in different soil within the same vineyard, to highlight possible differences in hydrological dynamics related to the soil management. The probe was installed under the rows, between two plants, in a hole enough large to allow the installation of the sensor. After the installation of the probe, the hole was recovered and filled with the same soil materials, to allow the contact between the soil and the sensors.
Field measures were validated, comparing measurements at different depth and in different vineyards with the values of water content obtained from undisturbed samples taken at the same moment and depth (Fig. 68). The correspondence between field and laboratory measures is generally good, as testified by a high value of R^2 (0.85) and a low value of the Mean Absolute Error (MAE of 5.1%) considering all the tests (Table 25). Water content measured by the field sensors installed in CRT, VCB and SMV demo farms have a better correspondence with the values measured in laboratory (MAE lower than 5% and R^2 of 0.87-0.89). Instead, water content measured by the field sensors installed in CNV demo farm has the lowest correspondence with the values measured in laboratory (MAE of 7.9% and R^2 of 0.78). The results of

these analyses confirm the reliability of the field measures of the soil hydrological parameters, carried on in the different test-sites, and can furnish indications for a better calibration of the field monitored soil water content trends.

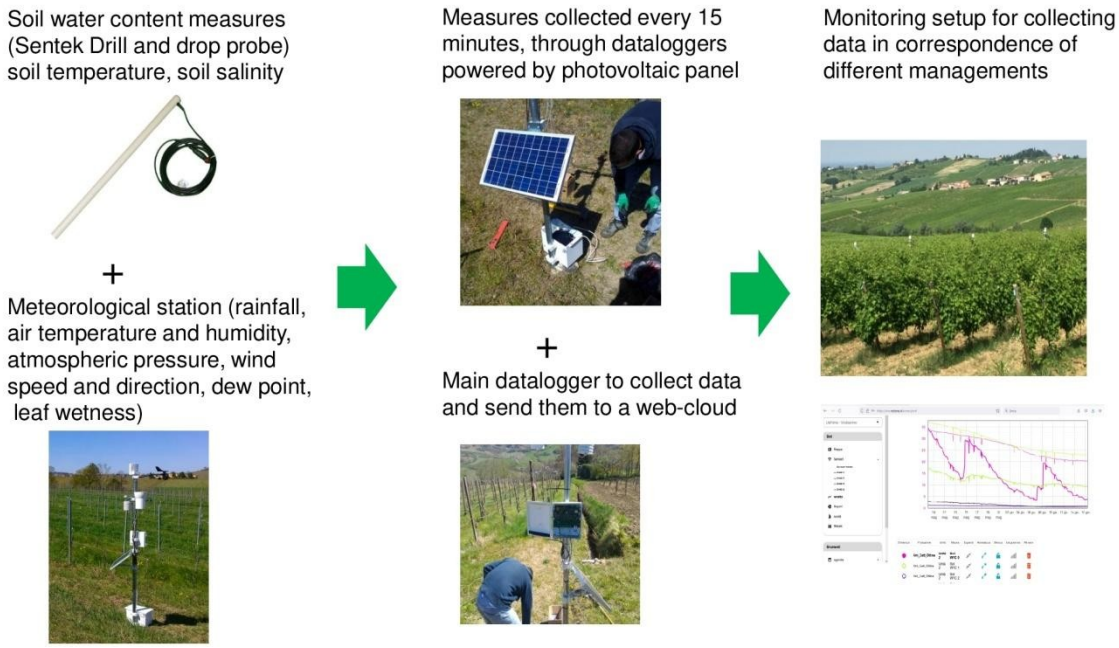

Fig. 66 Flowchart of the monitoring system in a demo farm.

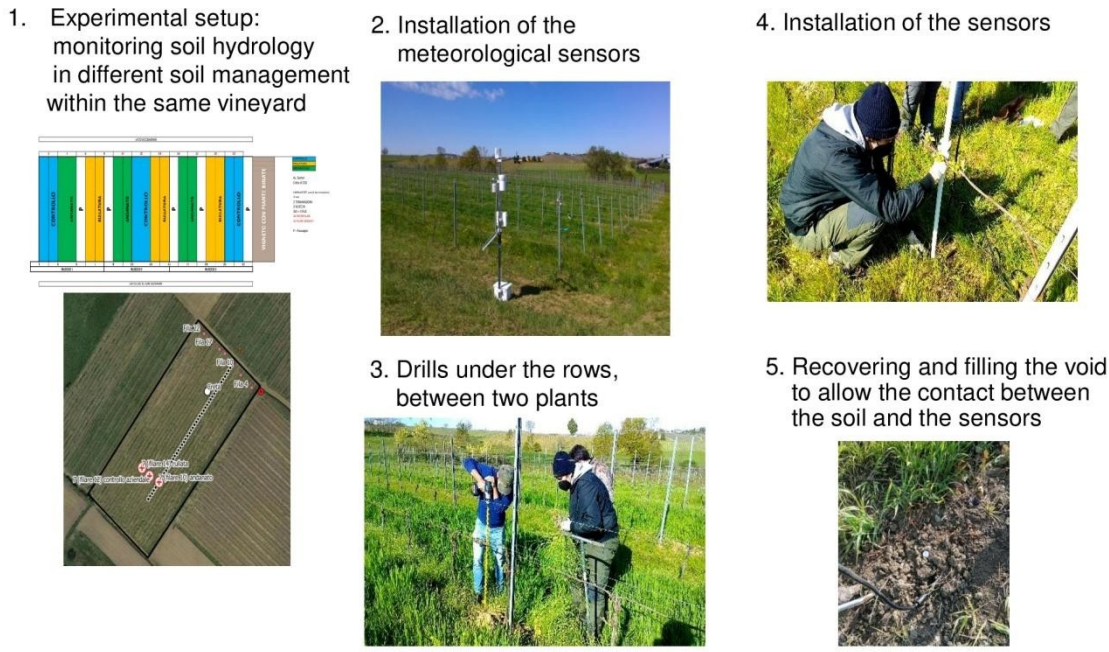

Fig. 67 Phases of installation of the monitoring system in a demo farm.

A semi-automatic procedure, written in R language, was also developed to show and to help in the interpretation of the hydrological trends in soil at different depths and for different treatments, in relation to prolonged dry periods, high temperatures, prolonged rainy periods, intense rainfall events.
The analyses of the monitored trends are obviously preliminary, since the monitored time span is of only 5-6 months and covers only end of spring and summer months. These analyses have to be improved, considering a more prolonged

monitored time span (e.g. all the seasons throughout a year) and comparing the trends of different monitoring points to highlight possible effects of soil management.

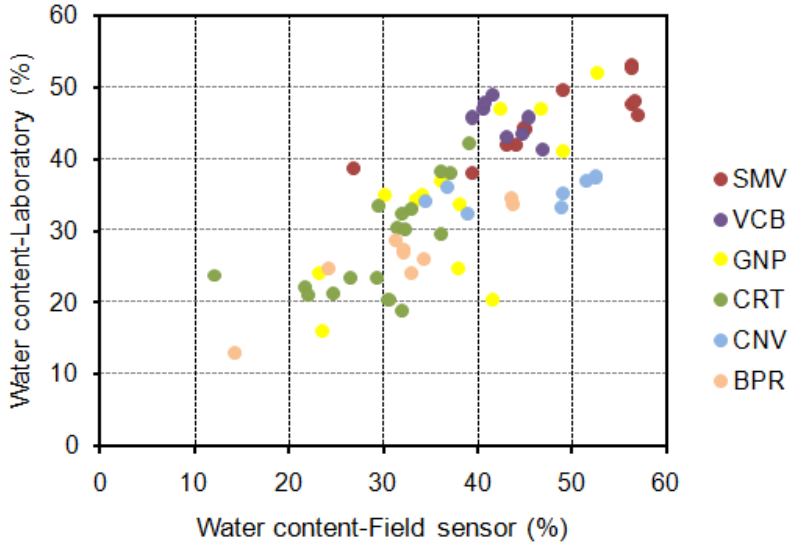

Fig. 68 Comparison between field and laboratory measured soil water content in different demo farm.

Table 25 Main statistics of the comparison between field and laboratory measured soil water content in different demo farm.

Demo farm	Number of tests	R^2 (-)	MAE (%)
SMV	12	0.87	4.7
VCB	8	0.89	4.3
GNP	13	0.78	5.2
CRT	17	0.87	4.2
CNV	8	0.78	7.9
BPR	8	0.86	4.7
All	66	0.85	5.1

However, some indications can be deduced from the analyses of this first months of monitoring:

- fast response of soil levels in the first 0.3-0.5 m from ground level after summer thunderstorms, as testified by a fast increase in soil water content of these layers;
- the lowest values of soil water content are measured in the first 0.5 m from ground level during prolonged dry and hot periods, due to a strong evapotranspiration involving these layers;
- soil water content changes are more limited in the deepest soil levels, generally below 0.5 m from ground level, testified by steady trends of by a small decrease in soil water content during prolonged dry and hot periods. At these depths, the highest values of soil water content are generally measured in each monitoring point.

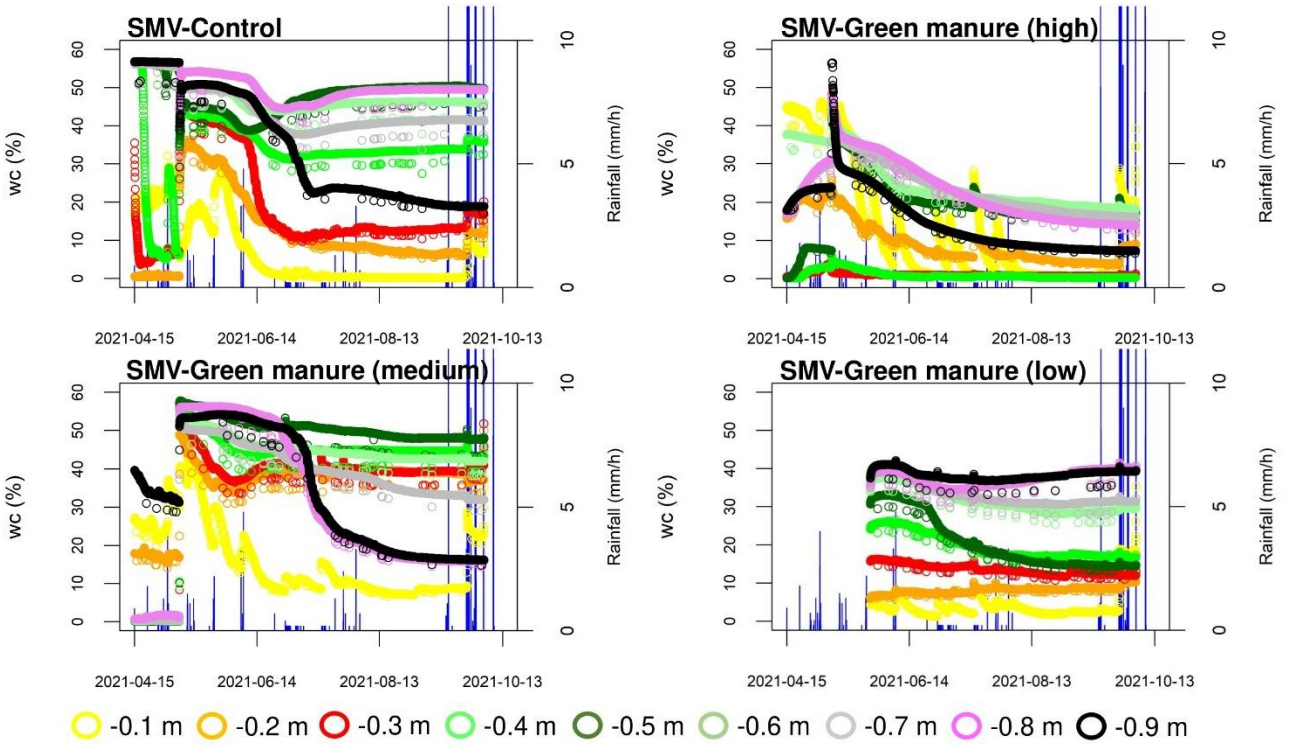

Fig. 69 Soil water content trends at different depths in the measuring points of SMV demo farm (last measure 2021/10/13).

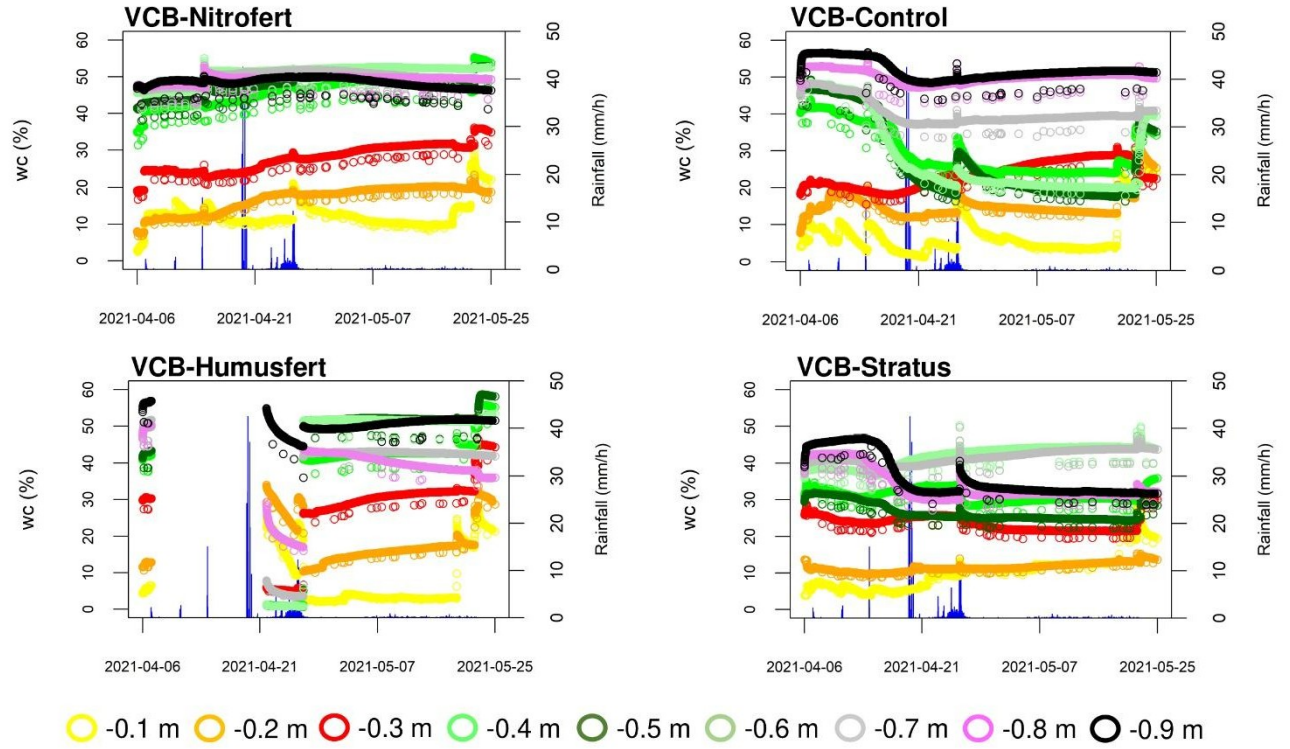

Fig. 70 Soil water content trends at different depths in the measuring points of VCB demo farm (last measure 2021/10/13).

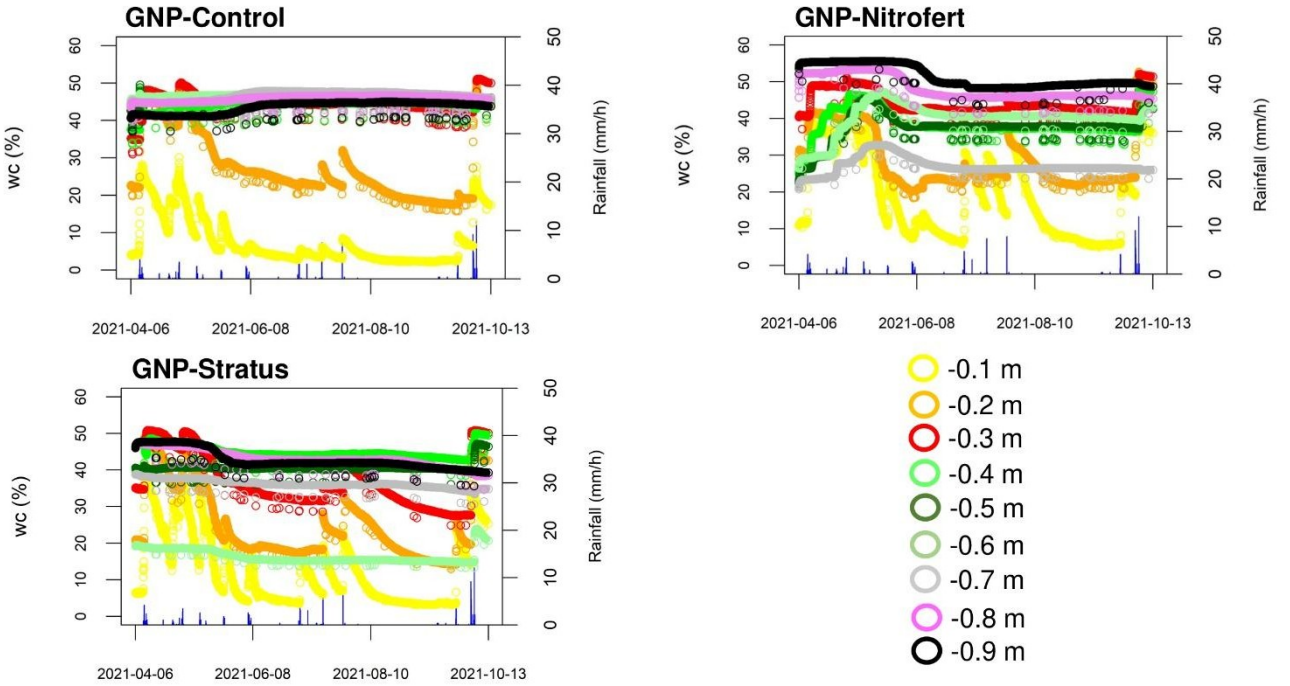

Fig. 71 Soil water content trends at different depths in the measuring points of GNP demo farm (last measure 2021/10/13).

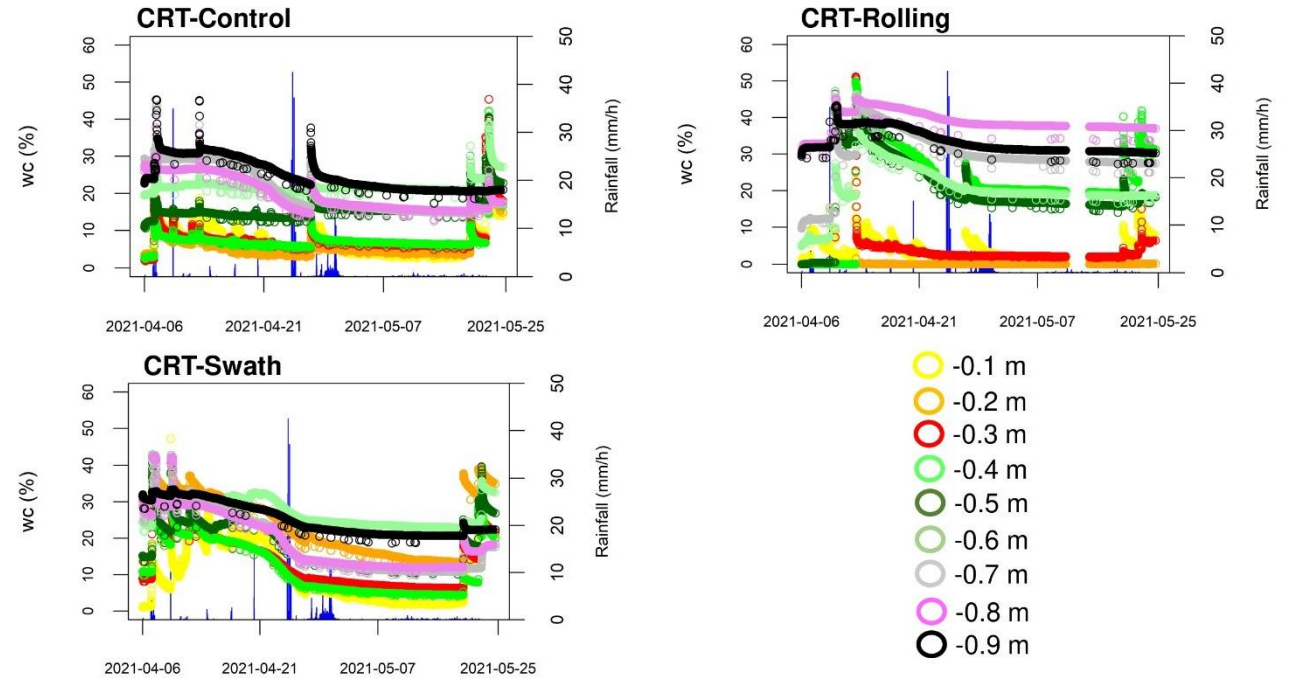

Fig. 72 Soil water content trends at different depths in the measuring points of CRT demo farm (last measure 2021/10/13).

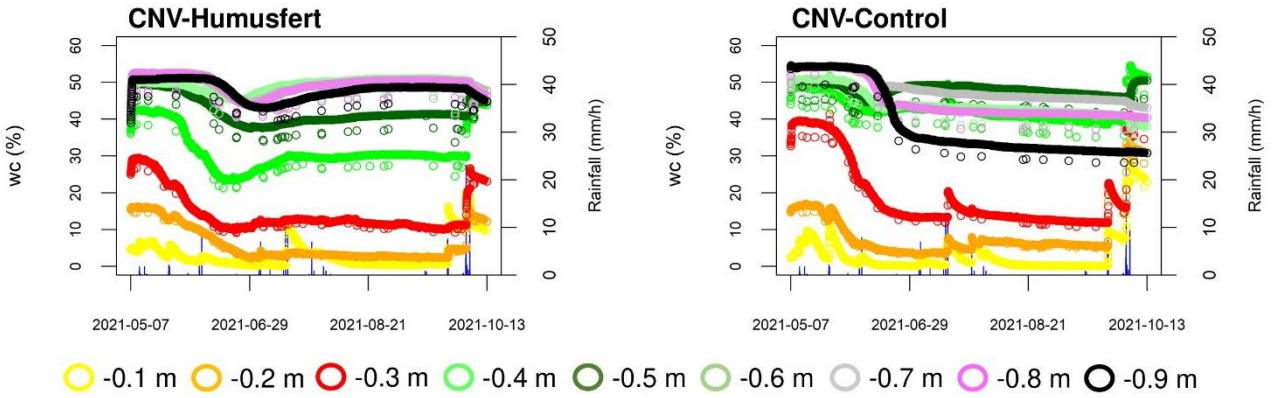

Fig. 73 Soil water content trends at different depths in the measuring points of CNV demo farm (last measure 2021/10/13).

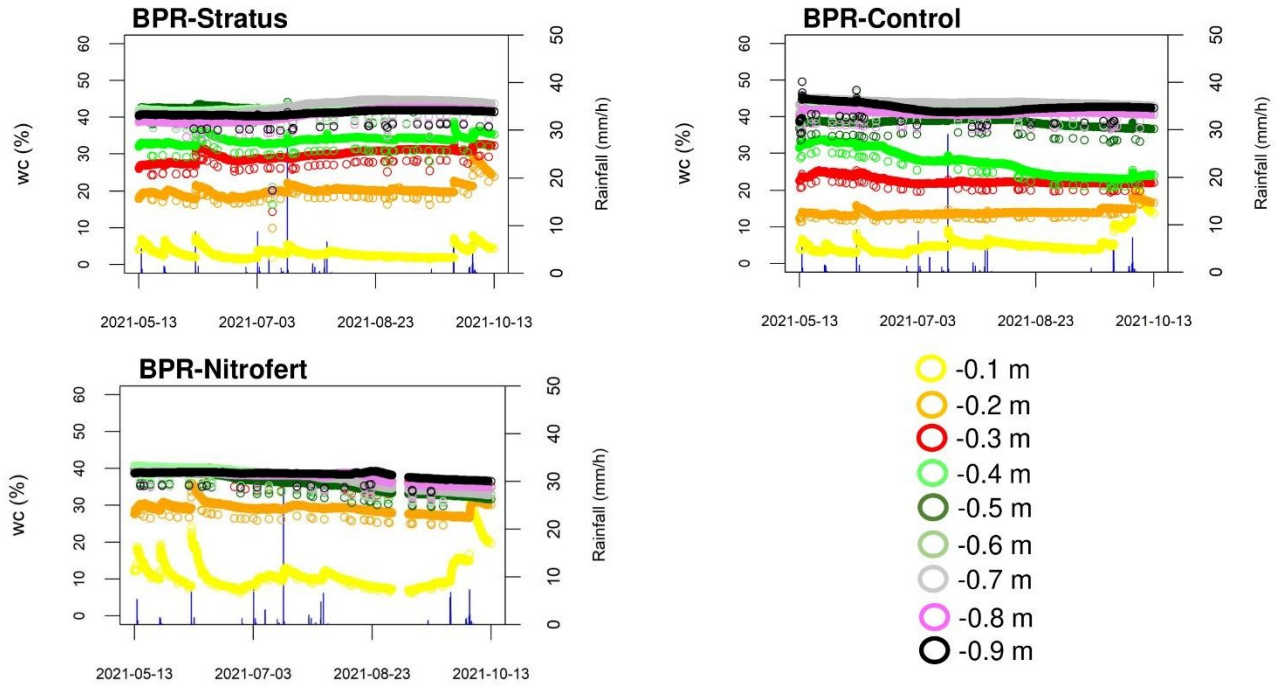

Fig. 74 Soil water content trends at different depths in the measuring points of BPR demo farm (last measure 2021/10/13).

References

Amoozegar, A. (1989). Comparison of the Glover solution and simultaneous-equations approach for measuring hydraulic conductivity. Soil Science Society of America Journal 53, 1362–1367.
Brady, C.B., Weil, R.R. (2002). The nature and properties of soils. 13. Prentice Hall, NJ, USA.
Cremaschi, M., Rodolfi, G. (1991). Il suolo. La Nuova Italia Scientifica, Rome, Italy.
Dazzi, C. (2013): Fondamenti di pedologia. La penseur, Italy.
ERSAL (2001). I suoli dell'Oltrepo Pavese. Milan, Italy.
Finke, P.A. (2012). On digital soil assessment with models and the Pedometrics agenda. Geoderma 171, 3-15.
Havlin, J.L . (2005): Encyclopedia of Soils in the Environment 2005. Pages 10-19
Hillel, D. (1998): Environmental Soil Physics. Academic Press, San Diego, USA.
ISPRA (2018). Landslides and floods in Italy: hazard and risk indicators — Summary Report 2018. Technical report. The Institute for Environmental Protection and Research, Rome, Italy.
IUSS Working Group WRB (2014). World Reference Base for Soil Resources (2014). Update 2015. FAO, Rome, Italy 2015, ISBN 978-92-5-108369-7.
Meisina, C., Zucca, F., Fossati, D., Ceriani, M., Allievi, J. (2006). Ground deformation monitoring by using the permanent scatterers technique: The example of the Oltrepo Pavese (Lombardia, Italy). Engineering Geology 88, 240–259.
Regione Emilia Romagna 1994. Carta dei suoli dell'Emilia Romagna scala 1:50000. Bologna, Italy.
Regione Emilia Romagna 1996. Carta geologica dell'Emilia Romagna scala 1:50000. Bologna, Italy.
Servizio Geologico d'Italia (2005). Carta Geologica d'Italia alla scala 1:50.000, Foglio 179 Ponte dell'Olio. Rome, Italy.
Servizio Geologico d'Italia (2014). Carta Geologica d'Italia alla scala 1:50.000, Foglio 178 Voghera. Rome, Italy.
Soil Survey Staff (2014). Keys to Soil Taxonomy. 12th edition. Natural Resources Conservation Service. U.S. Department of Agriculture. Washington D.C., USA.
Van Genuchten, M. T. (1980). A closed-form equation for predicting the hydraulic conductivity of unsaturated soils. Soil Science Society of America Journal 44, 892–898.
Zech, W., Schad, P., Hintermaier-Erhard, G. (2014). Böden der Welt. 2. Auflage. Springer-Spektrum, Heidelbeg, Germany.